SANDRA MIKUCKYTĖ

INVESTIGATION OF BIOMECHANICAL SPINE BEHAVIOUR UNDER VARIOUS LOADINGS AND DEVELOPMENT OF SPINE REHABILITATION METHODS

DOCTORAL DISSERTATION

Kaunas
2020

KAUNAS UNIVERSITY OF TECHNOLOGY

SANDRA MIKUCKYTĖ

INVESTIGATION OF BIOMECHANICAL SPINE BEHAVIOUR UNDER VARIOUS LOADINGS AND DEVELOPMENT OF SPINE REHABILITATION METHODS

Doctoral Dissertation
Technology Sciences, Mechanical Engineering (T 009)

2020, Kaunas

This doctoral dissertation was prepared at Kaunas University of Technology, Institute of Mechatronics during the period of 2015–2019.

Scientific Supervisor:

Prof. Dr. Habil. Vytautas Ostaševičius (Kaunas University of Techology, Technology Sciences, Mechanical Engineering, T 009).

Doctoral dissertation has been published in:
http://ktu.edu

Editor:

dr. Armandas Rumšas (Publishing Office “Technologija”)

KAUNO TECHNOLOGIJOS UNIVERSITETAS

SANDRA MIKUCKYTĖ

ŽMOGAUS STUBURO BIOMECHANINIO ATSAKO Į ĮVAIRIAS APKROVAS TYRIMAS IR STUBURO REABILITACIJOS METODŲ KŪRIMAS

Daktaro disertacija
Technologijos mokslai, Mechanikos inžinerija (T009)

2020, Kaunas

Disertacija rengta 2015–2019 metais Kauno technologijos universiteto Mechatronikos institute.

Mokslinis vadovas:

Prof. habil. dr. Vytautas Ostaševičius (Kauno technologijos universitetas, technologijos mokslai, mechanikos inžinerija, T 009).

Interneto svetainės, kurioje skelbiama disertacija, adresas:
http://ktu.edu

Redagavo:

dr. Armandas Rumšas (leidykla “Technologija”)

CONTENTS

NOMENCLATURE

∇p	Pressure gradient vector
C	Elasticity matrix under drained conditions
c	Energy dissipation
c_e	External salt concentration
c_F	Fixed charge density
$\mathrm{CTDI_{vol}}$	Computed tomography dose index
DLP	Dose-length product
e	Voids ratio
E	Young's modulus
F	Deformation gradient tensor
G	Shear modulus
I	Tensor identity
I_1	First strain invariant
J	Determinant of deformation gradient tensor
K	Bulk modulus
k	Stiffness
K_d	Bulk modulus of drained porous matrix
M	Empirical constant of poroelastic material
MVIC	Maximum voluntary isometric contraction
n_0	Initial fluid volume fraction
p_f	Fluid pore pressure
p_m	Total mean pressure
q	Fluid flux
R	Universal gas constant
T	Absolute temperature
W	Strain energy density of drained matrix
x	Displacement
α_B	Biot-Willis coefficient
γ_i, γ_e	Activity coefficients
ε	Strain
ϵ_p	Porosity
ε_{vol}	Volumetric strain
ξ	Damping ratio
κ	Permeability
μ	Dynamic viscosity
ν	Poisson's ratio
ρ	Density
ρ_d	Drained density of porous material
σ	Cauchy stress tensor
ϕ	Tissue porosity
φ_e, φ_i	External/internal osmotic coefficients
χ_f	Compressibility

INTRODUCTION

Relevance of the topic

The human spine is a complex structure which carries the weight of the upper body, helps maintaining the upright posture, allows moving, amortises loadings, and protects the spinal cord. Any changes in this structure could lead to discomfort, loss of function, or pain. Musculoskeletal problems are one the most frequent causes of severe long-term pain and years lived with disability in most parts of the world as well as in Lithuania. For example, the global prevalence of low back pain increased by 17.3% between 2005 and 2015 [1]. Low back pain is related with changes in the lumbar spine and is prevalent in all age groups starting from the teen years and reaching its peak in the middle-aged population [2], however, it is more common among females than males [3]. The fact that low back pain is the leading cause of disabilities in the middle-age group, or, in other words, in the working age group, means that it also has a significant negative socioeconomic impact not only on the individuals but also on society.

Low back pain can be caused by various known and unknown disorders. One of the more common causes of low back pain is intervertebral disc degeneration. Although the exact cause of disc degeneration is still unknown, aging, genetic and biological factors may be regarded as significant players. Besides, the spine may be considered as a mechanical system, and intervertebral disc degeneration may be related with the history of mechanical loading. Due to this reason, mechanical measures may also be implemented in order to preserve or improve the condition of the human spine. For example, mechanical influence may be used to improve insufficient nutrition of intervertebral discs by increasing the diffusion of nutrients, or to strengthen the paraspinal muscles which are also important to the health of the lumbar spine as they stabilise the spinal column. Current studies represent various aspects of the spine research: from the cellular level studies to *in vivo* studies of the effectiveness of various exercise programmes or invasive procedures. The influence of various mechanical loads on the lumbar spine is also researched; however, due to different research methods or procedures, some contradictory results have been obtained, and there still is lack of knowledge regarding which types of spinal loadings, as well as which loading magnitudes and frequencies are harmful and which may be used as a foundation of new and effective measures for the improvement of the spine condition and the reduction of the prevalence of low back pain and other spinal disorders.

Given the increasing statistics of lumbar spine disorders and the fact that invasive lumbar spine treatment methods are less cost-effective, and some of them could lead to future degeneration of the nearby segments of the surgery site, noninvasive, easy and safe to use research-based measures for the prevention and rehabilitation of the lumbar spine are still in high demand.

Research Aim and Objectives

The aim of this research is to numerically and experimentally investigate the biomechanical behaviour of the human lumbar spine and to propose noninvasive measures for lumbar spine prevention and rehabilitation. In order to achieve this aim, the following objectives are formulated:

1. To conduct a comprehensive literature review on human lumbar spine biomechanical behaviour and contemporary methods of lumbar spine prevention and rehabilitation.
2. To develop numerical models of human spine intervertebral disc and lumbar spine that would allow investigating the biomechanical behaviour of the lumbar spine under various loadings.
3. To identify the equipment and methods for experimental investigation of the biomechanical behaviour of the lumbar spine by incorporating mechanical and medical measures.
4. To experimentally investigate the influence of cyclic and short-term dynamic loading on spine segments.
5. To develop innovative equipment for the improvement of lumbar spine prevention and rehabilitation and to conduct an experimental study that would evaluate its effectiveness.

Research Methods

Both theoretical and experimental studies were conducted in this research. The theoretical study was accomplished by using the numerical method; *COMSOL Multiphysics* (*COMSOL Inc*.) software was used for finite element modelling of the spine. The geometry of the models as well as the design of the spinal actuator prototype was accomplished with *SolidWorks* (*Dassault Systèmes SolidWorks Corp*.) software.

The majority of the experimental studies were performed at the Institute of Mechatronics at Kaunas University of Technology. The response to an impact load of the spinal section was measured with a non-contact laser displacement sensor unit *LK-82G* (*Keyence Inc*.) and oscilloscope *Picoscope 3424* (*Picotech LTD*). The investigation of the spine cyclic loading was carried out with a linear-torsion static and fatigue testing machine *Instron ElectroPuls E10000T* (*Instron Corp*.). Muscle activity was measured with a wireless telemetric EMG system *TeleMyo DTS 2400R G2* (*Noraxon USA Inc*.) and recorded and primarily processed with *Noraxon MR 3.8* software.

The computed tomography of the specimens was carried out at the Hospital of Lithuanian University of Health Sciences with *LightSpeed VCT* (*GE Healthcare Inc*.) computed tomography system. Image processing was performed with *MATLAB* (*The MathWorks Inc*.) and *Sante DICOM Viewer 3D Pro* (*SanteSoft LTD*) software.

Scientific Novelty

1. An experimental setup that combines mechanical testing measures and computed tomography and allows to visually and numerically evaluate changes in spinal specimens has been developed.
2. A finite element model of the lumbar intervertebral disc has been created, and fluid flow velocity within the intervertebral disc due to the different loads has been calculated; also, a poroelastic finite element model of the lumbar spine has been used to evaluate the distribution of loading within the lumbar spine.
3. A unique prototype of training equipment has been developed, and an experimental study presenting the effectiveness of the exercise performed with this equipment has been conducted.

Defended Dissertation Statements

1. The developed finite element models of the intervertebral disc and the lumbar spine allow researching the influence of various loads and their distribution within the lumbar spine, as well as to model various grades of intervertebral disc degeneration by changing the material properties of the model.
2. Previous cyclic loading has an impact on how the spine reacts to short-term dynamic loading, and previous higher frequency cyclic loading may lead to a smaller reduction of the intervertebral disc height.
3. The developed spinal actuator prototype has an original design, allows facilitating the performance of the active lateral bending exercise, and it affects the user with passive lateral bending moves.
4. The results of the study of effectiveness of the spinal actuator validate the statement that the exercise of lateral bending constrained in the frontal plane targets lumbar multifidus muscles more intensively than the ordinary lateral bending exercise in the supine position. Furthermore, abdominal hollowing additionally increases the activity of trunk muscles during the lateral bending exercise.

Practical Value

1. The developed finite element model is useful for the investigation of the influence of various loadings on the lumbar spine, and this data may be used for developing non-invasive spine prevention and rehabilitation methods.
2. A recommendation is provided that the lateral bending exercise is more effective on the deep layer back muscles when performed strictly in the frontal plane, and a prototype of training equipment aimed to facilitate this exercise is developed and patented.

Research Approbation and Publications

The results of this dissertation have been published in 5 scientific papers: 2 in journals with the impact factor indexed in the *Web of Science* database and 3 in conference proceedings. Furthermore, a Lithuanian patent for the invention of spine

training equipment has been obtained and an application for another one has been submitted.

Some of the research results were obtained by implementing a project funded by the Research Council of Lithuania, project No. SEN-10/2015.

The results have also been presented at 7 scientific conferences:

1. 6th Lithuanian Academy of Sciences Conference of Young Scientists *Fizinių ir technologijos mokslų tarpdalykiniai tyrimai* 2016 (Vilnius, Lithuania);
2. 21st International Scientific Conference *Mechanika 2016* (Kaunas, Lithuania);
3. *12th Annual International Conference on Kinesiology and Exercise Sciences 2016* (Athens, Greece);
4. 22nd International Scientific Conference *Mechanika 2017* (Biržtonas, Lithuania);
5. *29th International Conference on Vibroengineering 2017* (Vilnius, Lithuania);
6. 23rd International Scientific Conference *Mechanika 2018* (Druskininkai, Lithuania);
7. 24th International Scientific Conference *Mechanika 2019* (Kaunas, Lithuania).

Structure of the Dissertation

The dissertation consists of introduction, four sections, conclusions, a list of 103 references, a list of the author's publications and one annex. The volume of the dissertation is 97 pages, 13 numbered formulas, 86 figures, and 10 tables.

The first section reviews the general knowledge of the anatomy of the lumbar spine, intervertebral disc nutrition and common spine disorders. A summary of the influence of various mechanical loadings on the lumbar spine is also presented and exercise therapy and spine rehabilitation equipment is overviewed before the formulation of the aim and objectives of the dissertation.

The second section presents mathematical models of the intervertebral disc and the lumbar spine. The intervertebral disc model is used to calculate the fluid flow velocity within the intervertebral disc as well as other parameters, while the lumbar spine model allows evaluating the load distribution within the entire lumbar spine.

The third section presents experimental *in vitro* studies of porcine spine segments. Response to impact loading and stiffness of the porcine spine segment is measured. Computed tomography is used to evaluate the influence of cyclic loading on spine segments, and changes of the response of porcine spine segments to short-term dynamic loading due to previous cyclic loading are investigated.

The fourth section presents the developed and patented training equipment for the prevention of function decline and for the rehabilitation of the lumbar spine. Also, the results of the *in vivo* study of the effectiveness of this training equipment on strengthening deep layer back muscles are presented.

In the Conclusions section, summarised conclusions drawn from theoretical and experimental studies are presented.

1. LITERATURE REVIEW OF LUMBAR SPINE ANATOMY, LOADING AND TREATMENT

1.1. Anatomy of the lumbar spine

The human spine is composed of 33 vertebrae divided into five anatomical regions: the cervical spine of 7 vertebrae, the thoracic spine of 12 vertebrae, the lumbar spine of 5 vertebrae, the sacrum of 5 vertebrae, and the coccyx of 4 vertebrae (Fig. 1.1). In the sagittal plane, the vertebral column is naturally curved, the inward cervical and lumbar curvatures are called *lordosis*, and the convex thoracic and sacrococcygeal curvatures are called *kyphosis*. These curvatures strengthen the vertebral column but could lead to higher shear stress values in the transition regions between the curves. Cervical, thoracic and lumbar vertebrae are separated by intervertebral discs, while vertebrae of sacrum and coccyx are fused together.

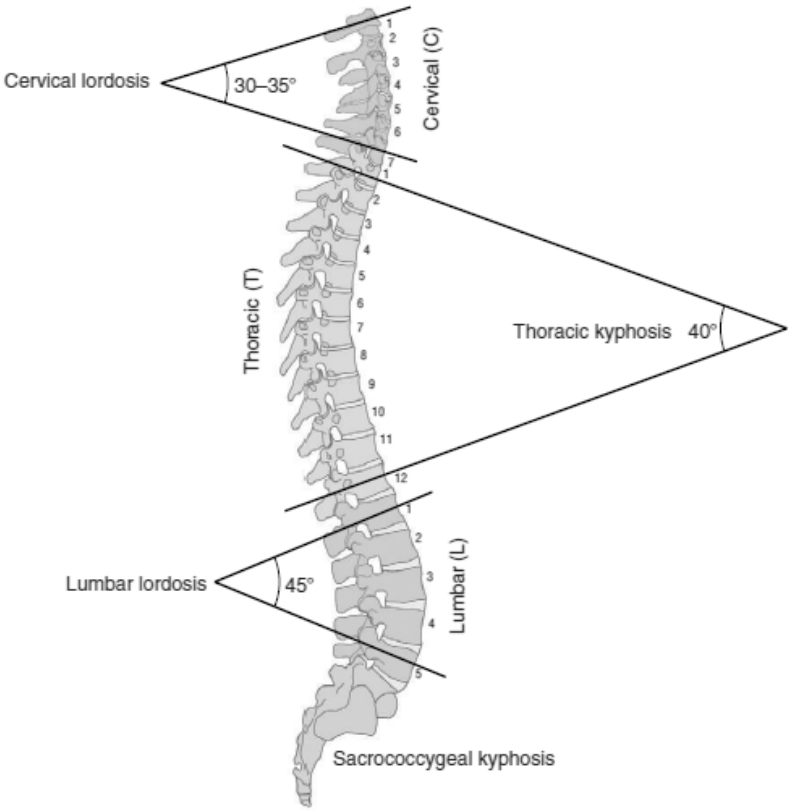

Fig. 1.1. Vertebral column and its normal sagittal plane curvatures [4]

Low back pain is usually associated with changes in the lumbar spine. Lumbar vertebrae are the biggest ones in the vertebral column as they have to bear the weight of the human head, arms and trunk. All the lumbar vertebrae can be divided into three functional regions: the vertebral body that bears most of the weight, the posterior elements that protect the spinal cord and perform as attachments to

muscles and ligaments, and pedicles that connect the vertebral body and posterior elements. Separate vertebrae are connected not only by intervertebral discs and articulating facet joints between articular processes of adjacent discs but also by anterior and posterior longitudinal ligaments, ligamentum flavum, supraspinous and interspinous ligaments (Fig. 1.2).

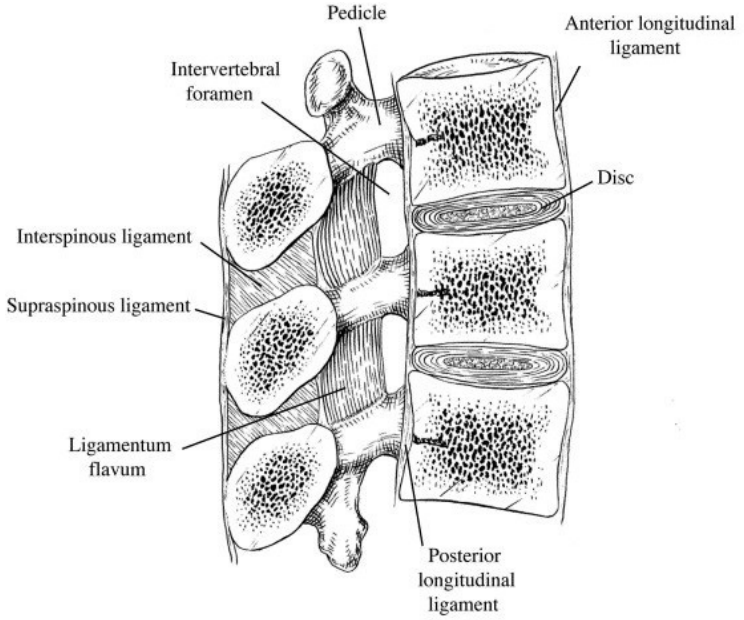

Fig. 1.2. Sagittal section of lumbar spine [5]

The intervertebral disc (Fig. 1.3) is a sophisticated structure that not only has to withstand the loads but also to deform and allow movements. The lumbar intervertebral disc consists of the central gel-like nucleus pulposus surrounded by 15 to 25 concentric lamellae of annulus fibrosus. Superior and inferior surfaces of the disc are covered by cartilaginous end plates.

70% to 90% of nucleus pulposus is water trapped between randomly arranged type II collagen and proteoglycans which, in response of hydrostatic pressure, are synthesised by rounded-shaped cells similar to those of articular cartilage. Biomechanically, the fluid nature of nucleus pulposus allows it to be deformed but not compressed and to transmit the acting loading in all directions [6].

Annulus fibrosus consists of 60% to 70% of water and has two distinct areas: outer annulus fibrosus and inner annulus fibrosus. The inner region is similar to nucleus pulposus and is composed of type II collagen and proteoglycans, while the outer region is highly structured and is mainly composed of type I collagen which, in response to deformation, is synthesised by elongated cells which are parallel to annulus fibrosus. Collagen fibers of annulus fibrosus are oriented at 60° to 70° from the vertical plane, their direction of inclination is opposite to the two neighbouring lamellae, which creates a cross-hatched structure. This configuration of annulus

fibers provides stability of the vertebral column and resistance to intervertebral distraction, shear and torsion [4, 7].

Cartilaginous end plates are up to 1 mm thick and fully cover the superior and inferior surfaces of nucleus pulposus but only partially cover the surfaces of annulus fibrosus. The surfaces of end plates that face the intervertebral disc mostly consist of fibrocartilage which directly and strongly binds to collagen within the annulus fibrosus, while the surfaces facing intervertebral bodies are composed of calcified cartilage that is weakly affixed to the bone. This end plate and bone interface is usually described as a weak link of the lumbar spine [4] because it tends to fracture under high and repetitive load [8].

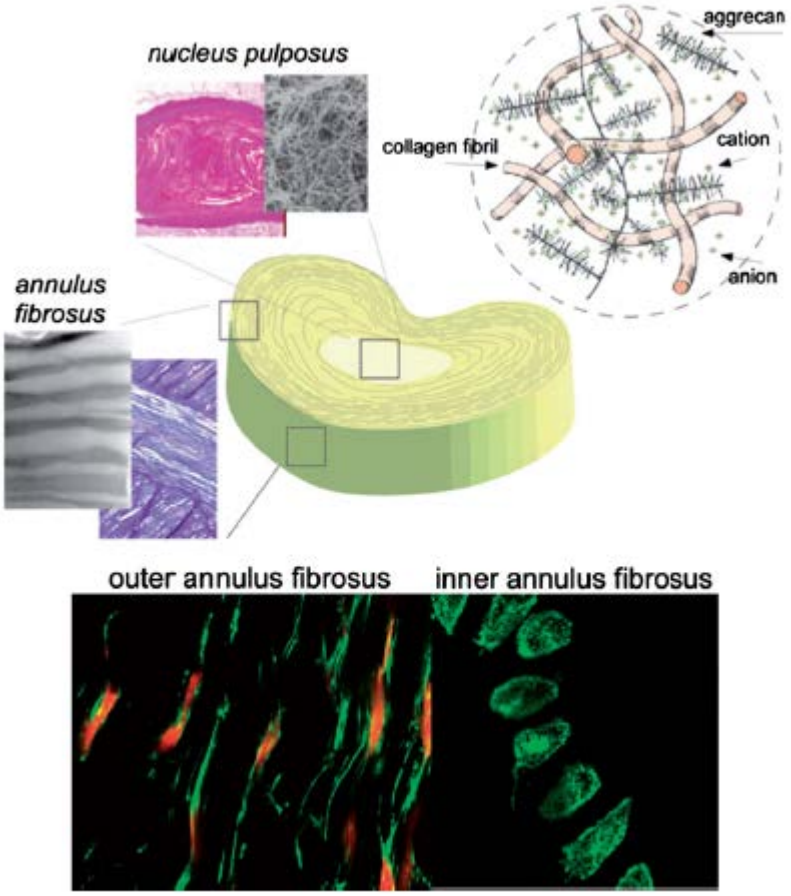

Fig. 1.3. Structure of the intervertebral disc. Inserts show a macroscopic view of annulus fibrosus, the structure of lamellae, a macroscopic view of gel-like nucleus pulposus and network of collagen fibers. The bottom inserts illustrate the shape of cells in outer and inner annulus fibrosus [9]

1.2. Nutrition of intervertebral disc

The intervertebral disc is considered the biggest avascular tissue in the human body, and only the outer layer of annulus fibrosus is supplied with nutrients by

capillaries from the tissues around the disc. Most of the nutrients are supplied by the vertebral capillaries that penetrate subchondral plates through the marrow pores and end at the boundary between the subchondral plates and the cartilaginous end plates (Fig. 1.4). Nutrients diffuse through cartilaginous end plates and a dense disc matrix to the disc cells, whereas metabolites move in the opposite direction [10]. The lowest amount of nutrients and the highest concentration of metabolites are in the center of the disc. The balance between the nutrient supply and consumption is delicate, and its disturbance could reduce the activity or viability of the cells which ensure the functionality of the disc matrix.

Cells obtain energy by glycolysis when glucose is oxidised into pyruvate, and adenosine triphosphate (ATP – a primary carrier of energy in the cell) is produced. Then, pyruvate may be oxidised with or without oxygen. Anaerobic oxidation produces only lactate, while aerobic oxidation leads to the production of an even higher amount of ATP than during glycolysis.

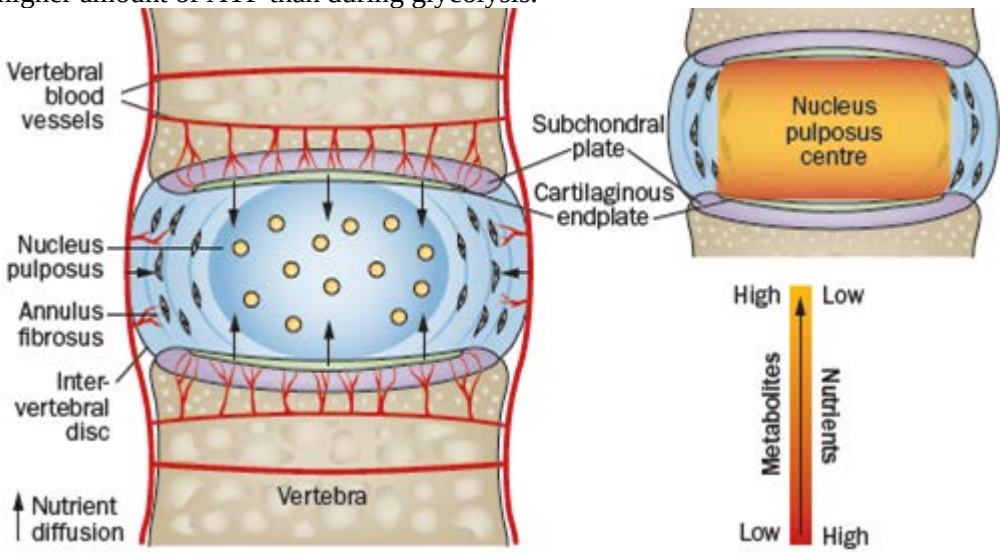

Fig. 1.4. Scheme of intervertebral disc nutrition and distribution of nutrients and metabolites within nucleus pulposus [10]

In vitro comparison of ovine discs under physiological loading submerged in media with sufficient and limited glucose concentration reveals that sufficient glucose concentration allows maintaining the cell viability up to 21 days, while insufficient concentration of glucose reduces the percentage of the viable cells by 56% in nucleus pulposus and 62% in annulus fibrosus after 7 days, but there are no significant differences between gene expressions or the newly synthesised aggrecan content under both conditions after 7 and 21 days [11], while the study of cartilaginous endplates tissues placed in diffusion chambers reveals that the diffusivity of cartilaginous endplates is related with biochemical composition of the tissue: cartilaginous endplates with poor diffusivity have greater amounts of collagen and aggrecan, more minerals and lower cross link maturity [12].

In silico studies reveal that the cell viability decreases with an increased distance from the supply source and emphasise the significant role of cartilaginous endplates for the solute transport and cell viability as mechanical deformations are not capable to preserve the cell viability when the nutrient flow through cartilaginous endplates is reduced [13, 14]. Cartilaginous endplates work as a gateway for nutrient transportation as the increased *in vitro* mechanical loading of the endplate tissue leads to the reduction of glucose and lactate diffusivity through the endplates and the assurance of the balance of the nutritional environment [15].

1.3. Spine disorders

Low back pain is classified by the duration, etiology, or therapy methods. Depending upon the duration of low back pain, it is called acute, subacute and chronic pain. Acute pain lasts up to 4 weeks, subacute pain lasts 4 to 12 weeks, and chronic pain lasts more than 12 weeks [16]. Furthermore, low back pain is classified as nociceptive – related to the damage of the non-neural tissue, or neuropathic – caused by a lesion of the somatosensory nervous system [17]. Nociceptive and neuropathic pain is defined as specific pain because it has a clear diagnosis contrary to nonspecific pain when the precise cause of the pain is unknown. Less than 15% of all the cases of low back pain are specific [18].

Low back pain could be caused by trauma, inflammation, tumours, degeneration, diseases of abdominal organs, and psychological reasons [19]. Trauma-related low back pain is caused by damaged muscles or fascia, intervertebral disc herniation or fractures of vertebral bodies that occur due to excessive and/or repetitive loading, for example, heavy lifting or fall, or osteoporosis. Pain related with ankylosing spondylitis – an inflammatory disease that primarily affects the spine and could cause fusion of vertebrae (Fig. 1.5) – usually improves with the activities and not the rest, and frequently occurs in the morning together with increased spinal stiffness. Low back pain can also be caused by malignant tumours metastasised to the lumbar spine, multiple myeloma, spinal cord cancer or various diseases of the liver, the pancreas, the uterus, etc. Psychological issues such as anxiety, depression, or catastrophising could also lead to low back pain.

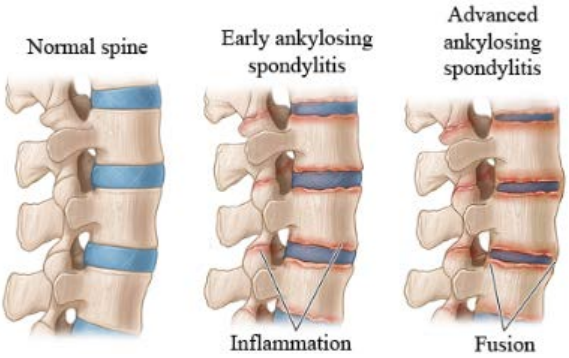

Fig. 1.5. Progression of ankylosing spondylitis: inflammation of vertebrae leads to fusion and immobility of spine segments [20]

Pain that is related with disorders of intervertebral discs is called discogenic pain. Intervertebral disc degeneration is known as a common cause of low back pain [21, 22]. The degenerative intervertebral disc disease is associated with a loss of proteoglycans that is followed by dehydration of nucleus pulposus, disorganization and tearing within annulus fibers (Fig. 1.6) that leads to a decrease of the disc height, reduced ability to bear loads, loss of stability, and pain.

Fig. 1.6. Picture of a normal disc (left) and a degenerated disc (right). The degenerated disc is denoted by dehydrated nucleus pulposus and disorganised annulus fibrosus [23]

The extent of disc degeneration can be evaluated by using one of the existing grading systems, for example, the Thompson grading system [24] which evaluates gross macroscopic changes of midsagittal sections of the lumbar intervertebral disc, the Pfirrmann grading system [25] that is based on the assessment of MRI scans (Fig. 1.7), or Boos classification [26] which evaluates the histological changes of the lumbar intervertebral disc. The intervertebral disc degeneration disease is no longer explained only by the aging and wear-and-tear theory but is understood as a complex disease with molecular and genetic changes. Adams and Roughley [27] summarised that disc degeneration is a process driven by the biochemical or cellular changes in the tissue weakened by various factors, such as genetic inheritance, when genetic defects may lead to structural or functional changes of specific collagens [28], an increase of degenerative enzymes, poor cell nutrition, exposure to vibrations, history of mechanical loadings and even smoking, which may reduce the content of disc proteoglycans and synthesis of new proteoglycans and collagen and increase the porosity of cartilaginous endplates [29].

While genetic defects cannot be escaped and smoking can be avoided quite easily, the relationship between the other factors is more complex. An initial factor of disk degeneration could be a limited nutrient supply due to the calcification of cartilaginous endplates or atherosclerosis of vertebral blood vessels followed by reduced cell viability, especially in the center of the disc where the first signs of disc degeneration are usually noticed [30]. The influence of mechanical loading on the disc nutrition is contradictory as there is some evidence that dynamic loading could improve the nutrient supply to the disc, but, on the other hand, it could cause fractions or calcification of the endplates, and disturb the nutrient supply.

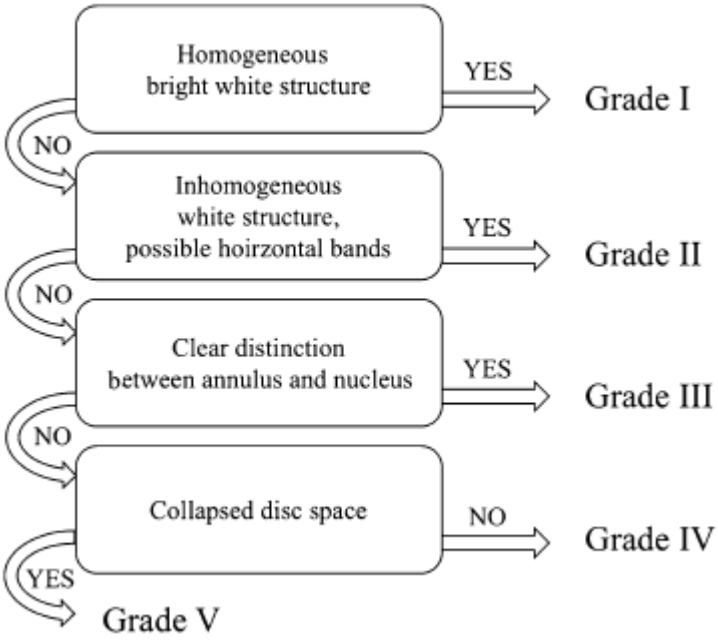

Fig. 1.7. Algorithm of Pfirrmann's intervertebral disc grading system based on evaluation of MRI scans [31]

1.4. Influence of mechanical loading on the lumbar spine

During the day, the spine is compressed by the weight of the upper body and any additional weight the person is carrying. Furthermore, the human spine allows movements in three anatomical planes (Fig. 1.8): the frontal plane divides the human body into the front and back sides, the sagittal plane divides the human body into the left and right sides, and the axial plane divides the human body into the upper and lower parts. Flexion and extension movements are performed in the sagittal spine, lateral bending movements are performed in the frontal plane, and torsional moves are performed in the horizontal or parallel to the horizontal planes.

The influence of spine kinematics on intervertebral discs has been widely researched *in silico*, *in vitro* and *in vivo*. Economic and ethical reasons as well as parameters that cannot be measured *in vitro* are the main reasons why *in silico* models are being used in the biomechanical research of the human spine, and efforts to create subject specific finite elements models for the calculation of stresses within intervertebral discs during flexion and extension by using magnetic resonance images and quantitative fluoroscopy have been proposed [32]. Due to the same economic and ethical reasons as well as availability, animal models are preferred to cadaveric spines. *In vivo* studies are mostly carried out when noninvasive procedures are sufficient to investigate the hypothesis.

In the following paragraphs, the results of relevant studies related with a range of motion, stresses, fluid flow, nutrition and other factors that could cause disc degeneration are presented and classified by the type of load.

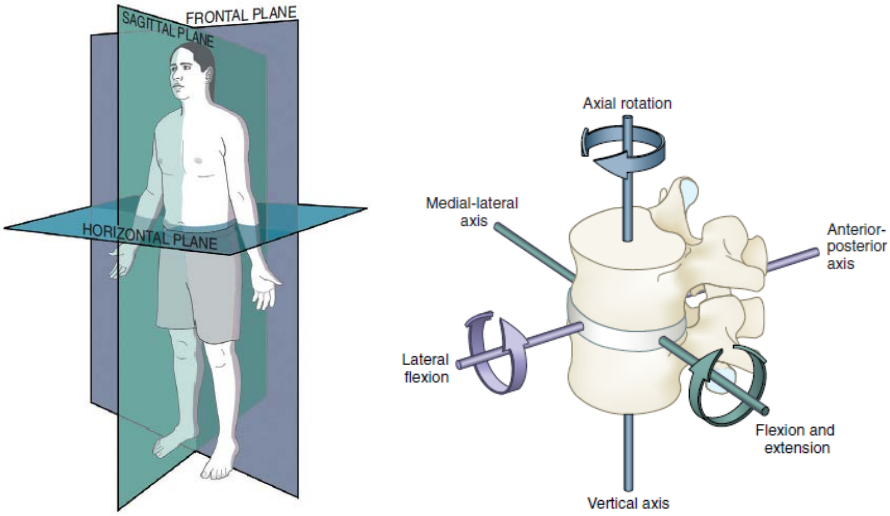

Fig. 1.8. Anatomical planes of the human body (left) and spinal movements (right) [4]

Compression and diurnal cycle loading

The fluid content in intervertebral discs varies during the day. The human spine shortens approximately by 1% of its height during the day and returns to its initial height during the night rest due to the inflow of fluid, although the time of rest is two times shorter than the loading period. It is said that the fluid flow is important for governing cell metabolism and could improve the transportation of nutrients. The results of the diurnal cycle loading (8 hours of rest and 16 hours of compressive loading) of the poroelastic and mass transport model revealed that the fluid flow velocities induced by daily activities do not increase the transportation of low weight solutes (a molecular weight of 400 Da), such as glucose, lactic acid and oxygen (Fig. 1.9), but increases the transportation of large solutes (a molecular weight of 40 kDa), especially during swelling [33].

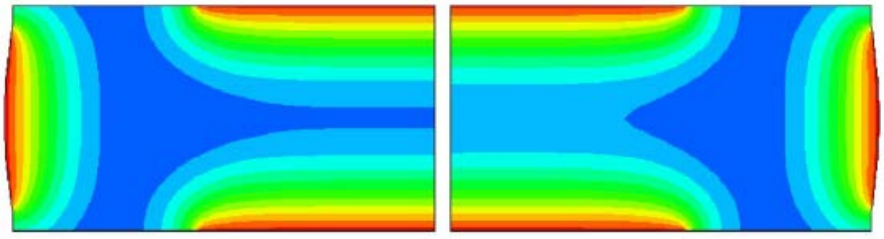

Fig. 1.9. Comparison of diffusive solute transport and combined diffusive/convective transport for small molecular weight solutes (400 Da). Following the subsequent 16 h of compressive loading and fluid expression, the net solute transport due to diffusion (left) and diffusion/convection (right) are of the same magnitude [33]

The results of an *in vivo* magnetic resonance imaging study shows that sustained compressive spinal loading of 50% of the subject's body weight for 4.5 hours in the supine position reduces small solute transport rates in intervertebral

discs, and authors summarise that sustained loading impairs diffusion to intervertebral discs and could accelerate disc degeneration [34]. An *ex vivo* study of bovine intervertebral discs [35] reveals that asymmetric static compressive loading increases cell death, structural disruption (Fig. 1.10) as well as production of catabolic and pro-inflammatory cytokine mRNA compared to uniformly loaded specimens.

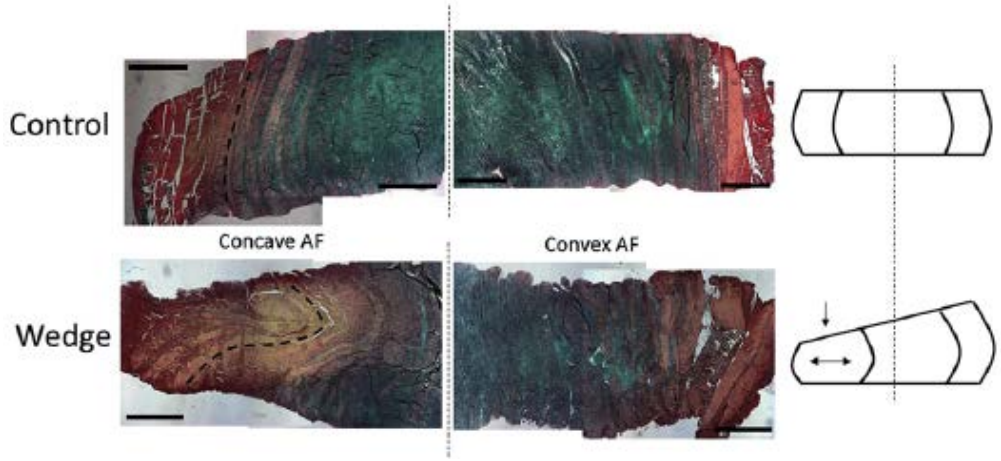

Fig. 1.10. Representative histology images of structural changes in the inner and outer annulus in control discs (top) and wedged discs (bottom). Dashed lines highlight the lamellar structure demonstrating intact lamellae in control discs and lamellar buckling in wedged discs. Tissue compaction and a shift of nucleus pulposus also occurred in wedged discs as seen in the scheme. The tissue has been stained with picrosirius red (collagen) and alcian blue (proteoglycans). Images were taken at 2.5x mag, scale bars represent 1.000 mm. [35]

Emanuel *et al*. [36] carried out a study of mechanical and osmotic influence on the intervertebral disc water content, height and nucleus pressure as caprice intervertebral discs were submerged in the physiological saline, and 4 loading steps were applied: 10 N compression (6 h) with the normal osmotic gradient, 150 N compression (24 h) with the normal osmotic gradient, 150 N compression (24 h) with a reduced osmotic gradient and 10 N compression (24 h) with a reduced osmotic gradient. Intradiscal pressure increased at the beginning of 150 N compression but quickly reached the lower counterbalanced value, and the reduction of the osmotic gradient resulted in no changes of intradiscal pressure. When the load was removed, intradiscal pressure decreased. The disc height was reduced under compression loading, and the rate of reduction was higher when the osmotic gradient was reduced. Also, the disc height did not reach the initial value when the load was removed, and the osmotic gradient was still reduced; thus the authors concluded that the osmotic gradient is essential in the restoration of the intervertebral disc (Fig. 1.11).

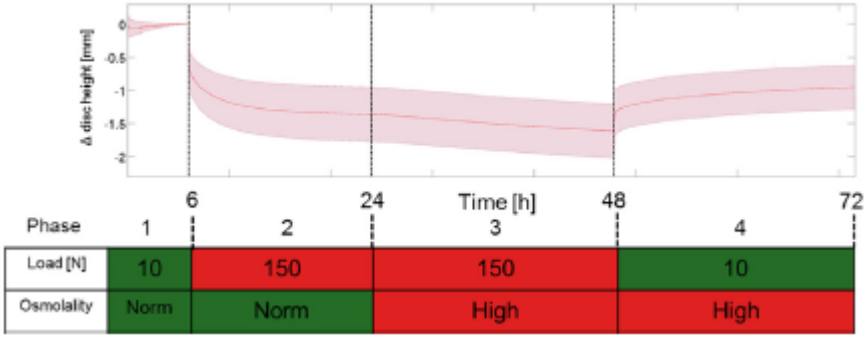

Fig. 1.11. Changes of intervertebral disc height (± SD) during different loading steps [36]

Flexion and extension

Flexion and extension movements are common during daily activities. The lumbar spine flexes between 8° to 14° when the move to touch the toes is performed from the erect standing position. Finite element analysis of the lumbar functional unit with the nucleus and the annulus modelled by using isotropic, incompressible, hyperelastic Mooney-Rivlin formulation [37] shows that the highest intradiscal pressure is generated by pure flexion, and the second highest value is generated by pure extension. Flexion and extension leads to shear strains in the posterior region. A finite element study of a non-linear lumbar spine (L3-sacrum) model [38] shows that progression of disc degeneration (changed material properties of the solid matrix of nucleus pulposus and annulus fibrosus) reduces the range of motion during flexion and extension. Another finite element study [39] modelled double level disc degeneration by modifying the bulk modulus of nucleus pulposus, annulus fibrosus and ligaments, and the disc height of L4-5 and L5-S1 discs showed that the range of motion depends of the spinal segments, on the degeneration grade, and on the position of the affected discs.

An *in vitro* study of ovine spinal segments by Veres *et al*. [40] shows that flexion reduces the disc's ability to survive high pressure and could result in herniation with the central posterior radial rupture. Even small moment but highly repetitive flexion/extension moves consistently result in herniation of *ex vivo* porcine discs [41]. As well as *in silico*, a trend of reduced ROM and significantly increased low flexibility zone stiffness are observed with increased disc degeneration in cadaveric lumbar spines [42].

A finite element study of flexion and extension reveals that higher stress values occur during flexion than extension [32], and that the trunk requires more stability to maintain the flexed than extended posture. Load sharing analysis [43] shows that, in the neutral standing position, the majority of the load is supported by the discs, while, in flexion, the importance of ligaments increases and that flexion enlarges the intervertebral disc pressure and strain in annulus fibers in all lumbar discs but mostly in L5-S1 (Fig. 1.12).

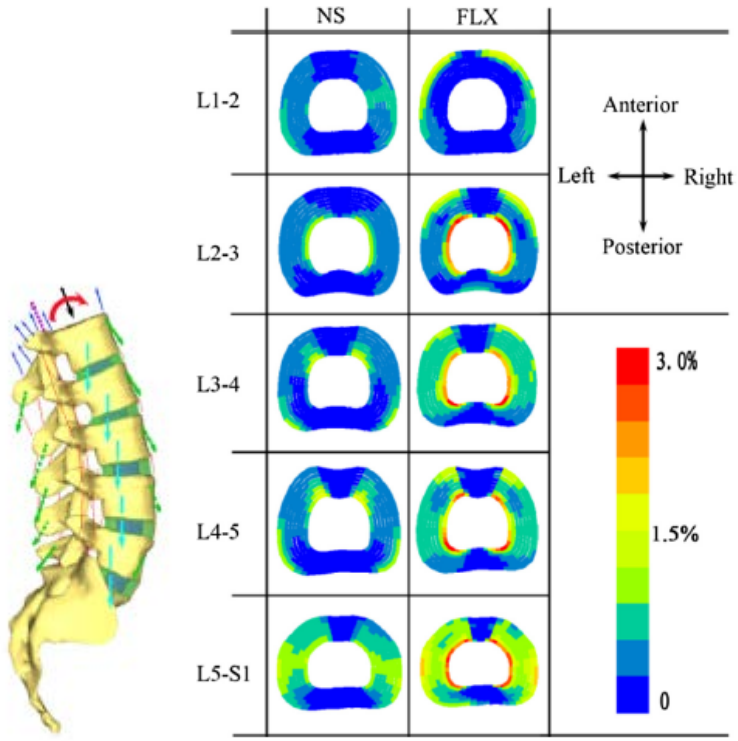

Fig. 1.12. Finite element model with loads taken from MSK model. Tensile strain distributions in annular fibres at L1-S1 levels (NS: neutral standing; FLX: forward flexion) [43]

Lateral bending

As lateral bending is performed less frequently than flexion and extension moves during the usual daily activities, it is also less researched, but it could still have a noteworthy impact on the spine as it is primarily accomplished by the movement of the spine while the hips movements contribute more to the flexion/extension and rotation moves of the trunk [44].

In vivo comparison of the coordination of the spine and the pelvis of young and older adults during lateral bending in the standing position [45] shows that the range of the motion of the lumbar spine of older adults decreases while the range of the motion of the thorax and the pelvis are similar in both groups, and the differences of the coupling angle between the straightening and bending phases exist only in older adults. The author concludes that age affects the coordination patterns during the bending phase and that older adults lack trunk control during lateral bending. A systematic review of *in vivo* studies [46] reveals that a limited range of the motion of the lumbar spine as well as limited lumbar lordosis and tight hamstring muscles may be predictive risk factors of the low back pain; therefore, the authors suggest that therapy methods targeted to reduce these factors may prevent the development of low back pain.

In silico and *in vitro* studies of lateral bending are mostly carried out when the main goal of the study is to compare the impact of all pure loading moments on the intradiscal pressure of nucleus pulposus or shear strain of annulus fibrosus. A finite element study [37] shows that pure lateral bending moments induce the lowest values of intervertebral disc pressure but the highest values of maximum shear strain compared with other cases of pure loading and even higher maximum shear strain values when lateral bending is combined with extension or flexion (Fig. 1.13). Also, a finite element study showed that intervertebral disc degeneration reduces the range of motion of lateral bending moves [38].

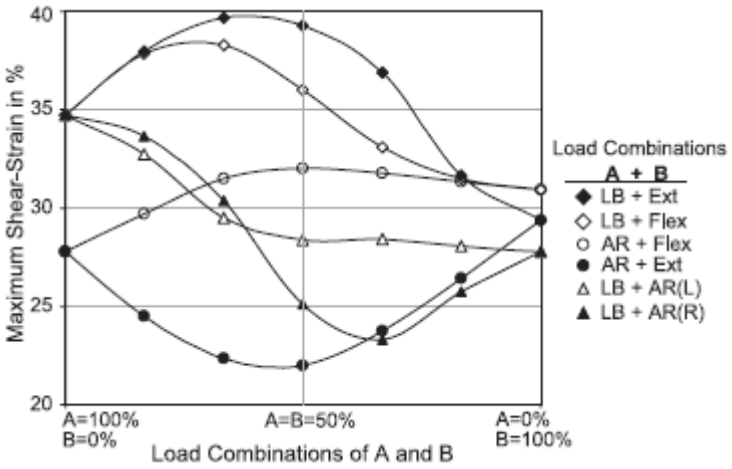

Fig. 1.13. Maximum shear strains in the annulus under combined loads: axial rotation plus flexion (AR(L) + Flex), axial rotation plus extension (AR(L) _ Ext), lateral bending plus flexion (LB _ Flex), lateral bending plus extension (LB _ Ext), lateral bending plus left axial rotation (LB _ AR(L)), and lateral bending plus right axial rotation (LB _ AR(R)) [37]

Axial Rotation

The results of an *in vivo* study show that the range of motion as well as the velocity and acceleration of axial rotation of the lumbar spine in neutral standing and standing with flexion is reduced in males with nonspecific chronic low back pain compared to the healthy group [47].

Changed torsional behaviour of the intervertebral disc also depends on the type of injury. An *in vitro* study of rat specimens reveals that torsional properties depend on the amount of intervertebral disc fiber disruption, while compressive properties change due to the loss of fluid which occurs due to the puncture and does not depend on the injury size [48].

The same *in silico* studies whose results related with flexion, extension and lateral bending were presented in the previous paragraphs also investigated axial rotation. Finite element analysis of the lumbar functional unit [37] reveals that pure axial rotation leads to medium values of intradiscal pressure and the lowest values of shear strains. The stiffness of axial rotation initially increases for moderate disc degeneration but decreases when the disc is severely degenerated [38], and the range

of motion also varies depending on the grade and location of the degenerated disc (Fig. 1.14) [39].

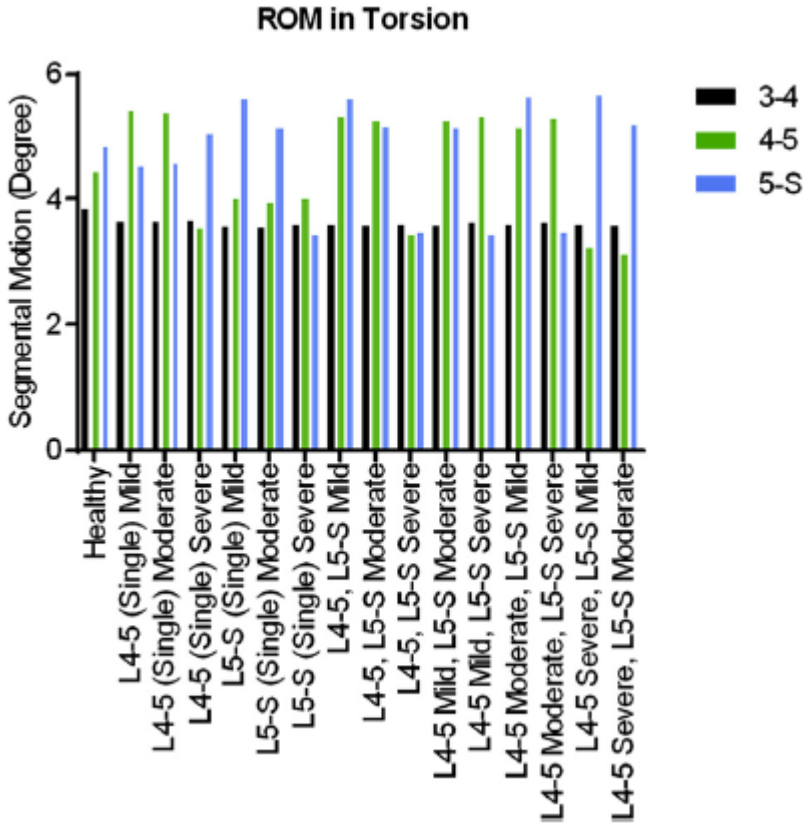

Fig. 1.14. Segmental range of motion in torsion depending on disc degeneration [39]

Vibrations

Knowledge related with the influence of vibrations on the lumbar spine is contradicting. It is widely accepted that whole body vibrations are a factor of low back pain. It was found that high frequency low amplitude whole body vibrations (45 Hz with the peak amplitude of 0.3g) applied to murine models and mimicking the conditions used clinically in humans induce processes related with disc degeneration [49]. Limited glucose or high frequency loading (10 Hz, 0.2 MPa) both led to a decrease of the cell viability of intervertebral discs compared to sufficient glucose and low frequency loading (0.2 Hz, 0.2 MPa), and combined limited glucose and high frequency loading results resulted in an even more decreased number of the viable cells [50].

However, a hypothesis that vibrations could increase the fluid flow within the intervertebral disc and improve the nutrition of cells also exists. Other scholars maintain that 90 Hz frequency low amplitude vibrations could help to avoid disc deterioration during hindlimb uploading in mice [51] or that 30 Hz frequency low

amplitude vibrations could reduce the negative effects of bed rest on the human spine [52]. Resonant frequency of the cadaveric intervertebral disc is found to be in the range of 8–10.4 Hz [53]. Vibrational loading (1000 N ± 10% with the frequency of 0.5, 1, 2, and 4 Hz) applied to the poroelastic model of the lumbar spinal unit L4-L5 leads to a larger loss of fluid volume of the intervertebral disc [54] than the vibrational static 1000 N compression force. An *in vivo* animal study also showed that convection induced by low frequency (0.5 Hz, 200 N) mechanical loading increases small molecule uptake [55]. Modelling performed by Huang and Hu [56] showed that the concentration of oxygen increases, and accumulation of lactic acid decreases when the intervertebral disc is dynamically (f = 0.1 Hz, amplitude of one tenth of the disc height) loaded. An *in silico* study revealed that dynamic loading could exert positive influence on the cell viability in degenerated IVDs as it facilitates nutrient diffusion [57]. An *in vitro* study shows that dynamic loading (f = 0.5 Hz, 0.6–1 MPa) significantly increases the diffusivity of low and large solutions through the CEP tissue compared to static loading [58].

Cyclic loading

A cyclic flexion and extension study with a compressive load of 1500 N and 1 Hz frequency of flexion/extension moves [59] shows that intradiscal pressure decreases with the increased number of cycles. 12 out of 14 porcine specimens of this study showed partial herniation, but no correlation between the damage type and the intradiscal pressure was found. Another *in vitro* study [41] of porcine specimens loaded by compressive force (260, 867, or 1472 N) and pure flexion/extension moments with angular and torque control revealed that herniation is more likely to occur due to high cyclic flexion/extension moments and not due to an excessive compression force. Thoreson *et al*. [60] noted that the majority of the porcine functional units cyclically flexed or extended 20,000 times at 1 Hz frequency with a load of 700 N had a decreased MRI (magnetic resonance imaging) signal in the growth zone of the superior vertebra, the inferior vertebrae and endplates, and an increased signal in the superior vertebral body that could be interpreted as a sign of fatigue. Furthermore, this loading leads to changes of the chondrocytes structure in the endplates and growth zones and the deformation of the extracellular matrix.

1.5. Treatment of low back pain and intervertebral disc degeneration

While the research of mechanisms of intervertebral disc degeneration has increased, most strategies of treatment still target reduction of the pain. The majority of the patients with low back pain associated with the degenerative disc disease are treated with rest, exercise and medications. If these approaches are not successful, surgical procedures, such as the removal of the degenerated tissue, spinal fusion and replacement of the whole disc or only nucleus pulposus, are considered.

A systematic review [61] reveals that the occurrence of the same level disc-herniation that requires reoperation is 6%, and 15% to 25% of patients start to feel low back pain two years after the operation. Phillips *et al*. [62] concludes that lumbar spine fusion is a viable treatment option for low back pain associated with

the disc degeneration disease, but, on the other hand, there is a risk of the acceleration of adjacent disc degeneration (it is a condition that may occur after spinal fusion or other spine surgery when the disc below or above the surgery site starts to degenerate due to the increased loading), especially in those patients who had laminectomy [63].

New treatment strategies of low back pain consider both mechanical and biological factors involved in intervertebral disc degeneration. Other possible approaches towards the degenerative disc disease are the regeneration of tissue, cell-based transplantation therapy, signalling molecules-based therapy which would help to restore the disc matrix, and injection of hydrogels [64], but currently they are mostly being studied *in vitro*, and the transfer of these methods to clinical use is still a major concern [65]. It is difficult to develop a regenerative therapy for the intervertebral disc because it has a unique structure of different regions, and both of these regions are mainly avascular, furthermore, biomolecules have a short half-life and, it is thought, that cell and biomolecule-based therapies will be successful only in the early stages of disc degeneration [64].

1.6. Exercise therapy

Physical activity is usually recommended as a treatment of low back pain, although, systemised reviews of randomised control trials suggest that the exercise therapy is more effective for chronic low back pain and is not more beneficial than other conservative therapy methods for acute low back pain [66, 67].

Without sufficient control, the vertebral column becomes vulnerable to excessive spinal mobility as well as postural misalignment, and this could lead to the degeneration of vertebral joints as well as other spinal issues which trigger low back pain [4]. Studies investigating the means and methods of the improvement of the condition of the lumbar spine usually focus on the strengthening of trunk muscles or study the influence of exercises on intervertebral discs. Below, some studies of each group are presented.

The efficiency of various exercise programmes for low back pain treatment, for example, proprioceptive neuromuscular facilitation, ball exercises, aerobic walking or pilates has been extensively researched [68, 69, 70, 71], but a dominating general conclusion is that the choice of the exercise regime should depend on the patient's and therapist's preferences [72], and it should challenge muscles because chronic low back pain is related with the lumbar spine's instability which is a consequence of the weakened trunk muscles but should not impose high loads on the joints [73].

The influence of specific standalone exercises or movements on the back muscles is less researched. One of the most widely studied movements is the intensive specific lumbar extension exercise which has been proven to be beneficial for strengthening the lumbar extensors when both full range of motion or limited range of motion exercises are performed once a week, and pain compared with control group is perceived to be reduced [74, 75, 76, 77]. The reason of the extensive number of these studies could also be the fact that there is a special machine which allows performing this exercise safely and efficiently (Fig. 1.15).

Flexion and extension movements are frequently used in therapy and widely researched, and, as it has already been mentioned, they are also most common during daily activities. It can be hypothesised that exercises consisting of other spine moves are necessary in order to ensure uniform spine loading and multidirectional mobility.

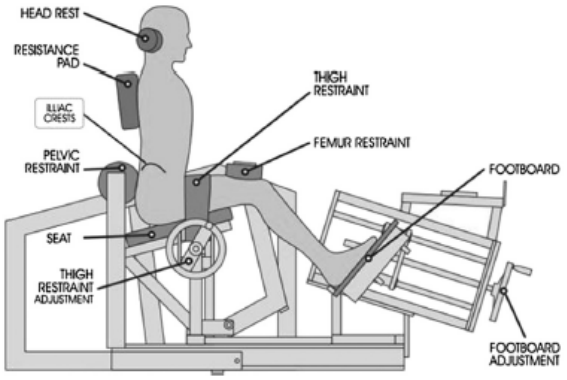

Fig. 1.15. *MedX* lumbar extension machine (*MedX*, Ocala, FL) [78]

Lateral bending is favourable for increasing the muscular activity of lateral latissimus dorsi and should be used in the evaluation of the latissimus dorsi function [79]. Due to the previously mentioned reason that lateral bending is primarily accomplished by the movement of the spine, lateral bending exercises show a potential to affect and improve the spine condition. Currently, lateral bending exercise is included in various pilates and core stabilization programmes, but it is not studied as a standalone exercise. In the currently available studies, lateral bending is performed in the standing, prone, supine and side positions. Subjects with low back pain or other spine disorders often are not able to perform pure lateral bending, and elements of rotation or asymmetry are observed in their standing position lateral bending movements. Moreover, asymmetrical lateral bending is one of the causes of spinal disorders [80]. Prone and supine lateral bending positions could allow reducing these negative effects.

Some studies show that the decreased activity of one muscle could be compensated by the increased activity of another muscle [81], and that a single muscle cannot be identified as the most important muscle for the lumbar spine stability as none of them produces spinal stability during all the different loadings, and extrinsic muscles are thus as important as the intrinsic ones [82, 83], while other researchers believe that intrinsic muscles play the crucial role and recommend to focus on activating the multifidus of the segmented level because multifidus muscle recovery does not occur spontaneously on remission of painful symptoms [84]. Multifidus strengthening is not the main target of common rehabilitation exercises, as only quadruped arm/lower extremity lift allows reaching MF muscle activity above 45% MVIC, which is necessary if we wish to increase the muscle strength in previously untrained subjects [85].

A study of Kingsley *et al*. [86] shows that moderate intensity running reduces the height and volume of intervertebral discs in thoracic and lumbar regions. The authors discuss that, although the reduced fluid content could lead to worsened load distribution and shock absorption, cyclic changes of the intradiscal pressure are necessary in order to ensure the health of intervertebral discs which depends on the diffusion and convention of nutrients and metabolites. An increased number of cells in annulus fibers and type II collagen, aggrecan and Sox-9 protein was found in rats which participated in a 3-week-long treadmill exercise programme [87], and authors hypothesise that regular exercise may improve the cell viability and matrix production. An *in vivo* study of young healthy adults [88] reveals that runners have better hydrated intervertebral discs with higher glycosaminoglycan levels, and the hydration is higher in the nucleus region than in the other regions. Belavy *et al*. in their review summarise [89] that the exercises which are performed regularly and are dynamic but not rapid and explosive may be beneficial for intervertebral discs.

1.7. Lumbar spine training and rehabilitation equipment

Most of the current training and rehabilitation equipment aimed at improving the shape of the back muscles relies on the flexion and extension moves of the spine. The majority of commercially available equipment represents various configurations of benches (Fig. 1.16), racks, roman chairs or other devices for sit-ups and back extension as already mentioned in Section 1.6.

Fig. 1.16. Lower back bench *Technogym Pure* [90]

Lateral bending, axial rotation and various combinations of these moves are less common. Some apparatus allowing to perform more unique movements have been found during the patent research. For example, the whole body exercise machine (Fig. 1.17) described in patent US2016106613 (A1) [91] allows circular orbital movement of the waist, longitudinal rotation and lateral-torsional rotation of the waist, and these movements, according to the authors, help to strengthen back muscles, although the specifically targeted muscles are not indicated.

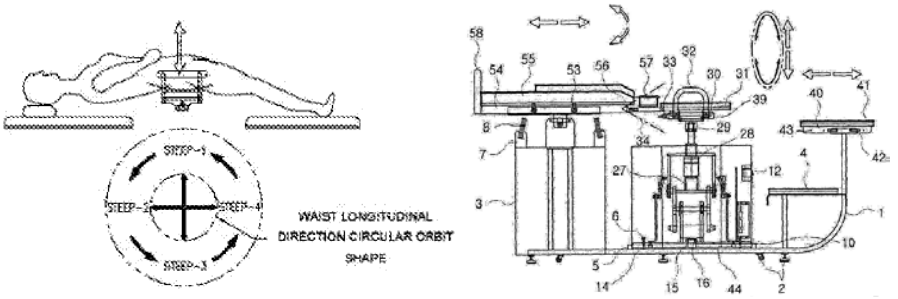

Fig. 1.17. Rehabilitation apparatus presented in patent US2016106613 (A1) [91]

The chiropractic treatment table (Fig. 1.18) presented in patent US6638299 (B2) [92] allows movements for pure longitudinal distraction or combined together with vertical flexion/rotation, lateral flexion and/or rotation. Although the structure of the table allows various movements, they can be performed only with the help of a therapist.

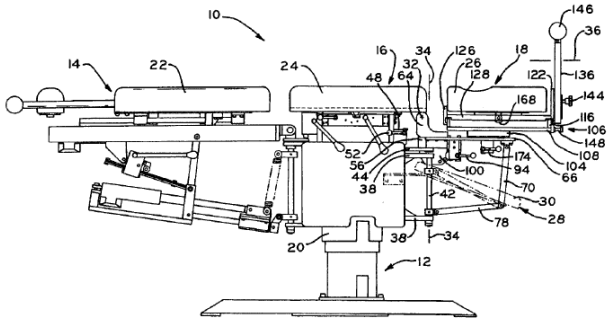

Fig. 1.18. Treatment table presented in patent US6638299 (B2) [92]

The apparatus for rehabilitation and training of the spine and other body parts (Fig. 1.19) presented in patent US005609599A [93] consists of the main body with a seat and an arched tube behind the seat that should be tied to the upper body of the patient and is actuated by pedals or an electric motor, moves rotationally and causes swinging movements of the patient. Besides, the apparatus has functions of controlled spine extension and low back massage. The author hypothesises that this exercise improves the strength of the back muscles and increases the oxygen concentration in the spine.

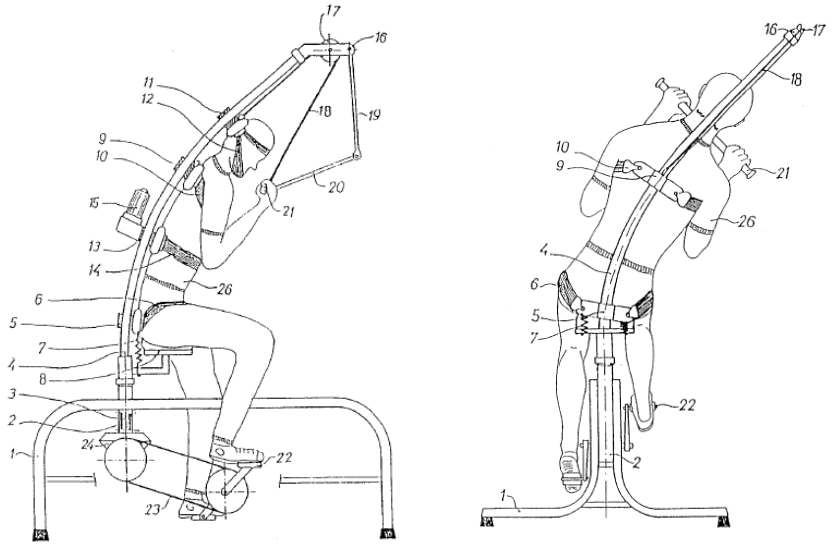

Fig. 1.19. Rehabilitation apparatus presented in patent US005609599A [93]

The spine training and rehabilitation device (Fig. 1.20) described in patent CN204207992U [94] allows to perform various crawling movements when the spine is forced to move laterally.

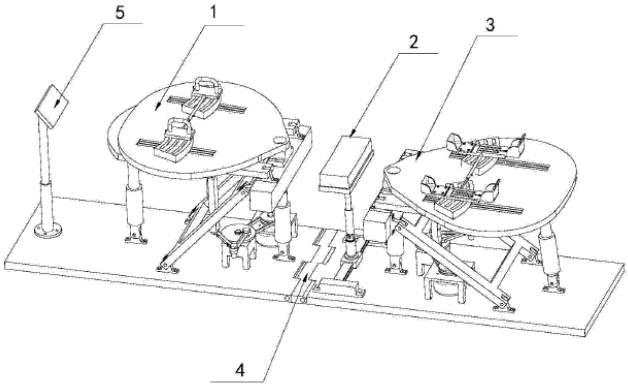

Fig. 1.20. Rehabilitation device presented in patent CN204207992U [94]

However, there is lack of scientific research on the influence of these or similar devices on the human spine, and the presented benefits are only presumed and not scientifically proven.

1.8. Formulation of thesis aim and objectives

Research of the human spine offers a lot of challenges. The spine is a complex structure to model, and some simplifications that reduce the accuracy of the results must be made. Different approaches are used to model the same behaviour, and it is important to choose the appropriate one for the specific question. For example, four

different methods to model intervertebral disc swelling are distinguished with fixed the boundary pressure and the fixed osmotic pressure models being more suitable for the calculations of the global quantities, and the biphasic swelling model being suitable for the evaluation of material properties [95]. Methods and protocols of *in vitro* and *in vivo* researches also differ within the studies, and this may be a reason of some contradicting results that have been reported. Furthermore, in the course of *in vitro* studies, it is difficult to repeat the environmental conditions that are *in vivo*, and common replacement of cadaveric material with animal models also requires careful consideration.

The majority of exercise equipment aimed to reduce low back pain is based on flexion and extension moves, and while there are some patented devices for the performance of other moves, their influence on the human spine has not been researched yet.

After thorough analysis of the literature, it is evident that there is still lack of novel research-based noninvasive methods and means of prevention and rehabilitation of various spinal disorders that would allow to reduce the risk of spinal disorders or to improve the condition of the spine, person's mobility or lifestyle in general.

The aim of this research is to numerically and experimentally investigate the biomechanical behaviour of the human lumbar spine and to propose methods and means for lumbar spine rehabilitation. In order to achieve this aim, the following objectives are formulated:

1. To conduct a comprehensive literature review on the human lumbar spine's biomechanical behaviour and rehabilitation methods.
2. To develop numerical models of the human spine intervertebral disc and the lumbar spine that would allow to investigate the human spine's biomechanical behaviour under various loadings.
3. To identify the equipment and methods for the experimental investigation of the lumbar spine's biomechanical behaviour by incorporating mechanical and medical measures.
4. To experimentally investigate the influence of cyclic and short-term dynamic loading on spine segments.
5. To develop innovative equipment for the improvement of lumbar spine rehabilitation and to conduct an experimental study that would evaluate its effectiveness.

2. MODELLING OF LUMBAR SPINE

Insufficient nutrition of intervertebral disc leads to the degenerative disc disease and other spinal disorders. Studies of nutrition mechanisms *in vivo* and *in vitro* is challenging as it is difficult to measure and evaluate the changes of the relevant parameters. Only a change of the height of intervertebral discs may be assessed *in vivo* without invasive procedures, and, during *in vitro* studies, it is difficult to ensure environmental conditions similar to those *in vivo*. Theoretical modelling of fluid flow and diffusion of nutrients can substitute invasive *in vivo* methods. The functional unit of the lumbar spine or the whole lumbar spine are widely modelled as mechanical systems, their stress and strain values are analysed, but there are fewer studies which evaluate and compare the influence of various biomechanical loading scenarios on the fluid flow and nutrient distribution within the intervertebral discs.

Comsol MultiPhysics (*COMSOL Inc*.) software was chosen for the modelling of the lumbar spine. Poroelasticity, Coefficient Form PDE, and Truss modules of *Comsol MultiPhysics* were used to create finite element models of the intervertebral disc and the lumbar spine.

2.1. Poroelastic model of lumbar intervertebral disc

As it was already explained in Chapter 1, the intervertebral disc consists of a solid matrix and a fluid; due to this reason, it may be considered as a poroelastic body. The fluid flow within the intervertebral disc depends on the deformation of its solid matrix determined by acting loads, for example, the height of the intervertebral disc reduces upon undergoing day loading, yet it regains its primary shape during the night rest.

As the condition of intervertebral discs significantly contributes to the health of the entire lumbar spine, theoretical investigation of the lumbar spine was started by creating a finite element model of the lumbar intervertebral disc. The model is based on the poroelasticity theory which defines fluid diffusion through the porous solid medium.

The relationship between the total stress, strain and fluid pore pressure is written as

$$\sigma = C\varepsilon - \alpha_B p_f I \tag{2.1}$$

where σ is the Cauchy stress tensor, C is the elasticity matrix under drained conditions, ε is the strain, α_B is the Biot-Willis coefficient, p_f is the fluid pore pressure and I is the tensor identity

Equation 2.1 may be split into a deviatoric part which does not depend on the pore-pressure coupling and the volumetric part:

$$p_m = -K_d \varepsilon_{vol} + \alpha_B p_f \tag{2.2}$$

where p_m is the total mean pressure, K_d is the bulk modulus of the drained porous matrix and ε_{vol} is the volumetric strain.

Effective stress that is defined as a product of $C\varepsilon$ may also be expressed as

$$C\varepsilon = \frac{1}{J}\frac{\partial W}{\partial F}F^T \tag{2.3}$$

where F is the deformation gradient tensor, J is the determinant of F, and W is the strain energy density of the drained matrix that is expressed as

$$W = \frac{G}{2}(I_1 - 3) + \frac{K}{2}(J-1)^2 \tag{2.4}$$

where I_1 is the first strain invariant, G is the shear modulus and K is the bulk modulus. For linear isotropic elastic materials, the shear and bulk modulus may be calculated by using Young's modulus E and Poisson's ratio v:

$$G = \frac{E}{2(1+\nu)} \tag{2.5}$$

$$K = \frac{E}{3(1-2\nu)} \tag{2.6}$$

The calculation of the fluid flow within the intervertebral disc is based on Darcy's generalised law:

$$q = -\frac{\kappa}{\mu}\nabla p \tag{2.7}$$

where q is the fluid flux, κ is the permeability of the porous medium, μ is the dynamic viscosity and ∇p is the pressure gradient vector.

Tissue permeability is considered to be isotropic and strain-dependent:

$$\kappa = \kappa_0 \left(\frac{e(1-e_0)}{e_0(1+e)}\right)^2 \exp\left(M\left(\frac{1+e}{1+e_0} - 1\right)\right) \tag{2.9}$$

where κ_0 is the initial permeability, e_0 represents the initial voids ratio, and M is the empirical constant. Voids ratio e is defined as

$$e = \frac{\phi}{1-\phi} \tag{2.10}$$

where ϕ is the tissue porosity which depends on volumetric strain ε_{vol}:

$$\phi = \left(1 - \frac{1-\phi_0}{\exp(\varepsilon_{vol})}\right)$$

Intervertebral disc swelling was simulated by applying the osmotic pressure gradient:

$$\Delta\pi = \varphi_i RT \sqrt{c_F^2 + 4\frac{\gamma_e^2}{\gamma_i^2} c_e^2 - 2\varphi_e RT c_e} \tag{2.11}$$

where φ_i and φ_e are internal and external osmotic coefficients, R is the universal gas constant, T is the absolute temperature, c_F is the fixed charge density, γ_i and γ_e are activity coefficients, and c_e is the external salt concentration.

The fixed charge density depends on volumetric deformations and is defined as:

$$c_F = c_{F0}\left(\frac{n_0}{n_0 - 1 + J}\right) \tag{2.12}$$

where c_{F0} is the initial fixed charge density, n_0 is the initial fluid volume fraction, and J is the determinant of the deformation gradient tensor.

A three-dimensional geometry of the finite element model of L4-L5 intervertebral disc has been created with SolidWorks (*Dassault Systèmes SolidWorks Corp*.). The width of the disc model is 35.9 mm, the length is 51.9 mm, and the total height is 11.4 mm. The model consists of nucleus pulposus which occupies 43% of the disc volume, annulus fibrosus, and 0.5 mm thick cartilaginous endplates. The composite behaviour of annulus fibrosus is represented by modelling the annulus fibrosus matrix and the seven layers of annulus fibers. Annulus fibers are modelled as tension-only elements with an inclination angle of ± 66° (Fig. 2.1.).

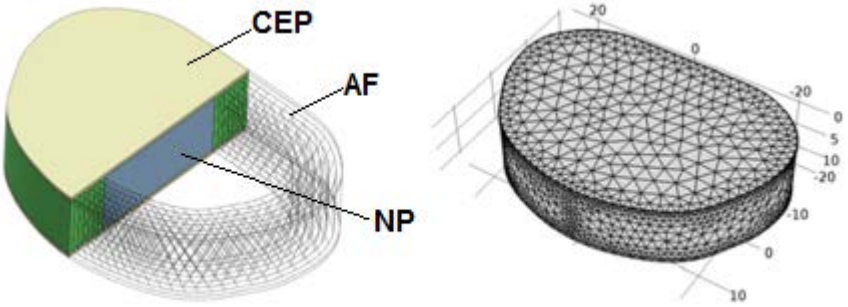

a) b)

Fig. 2.1. Intervertebral disc model: a) geometry of the disc (NP – nucleus pulposus, AF – annulus fibrosus, CEP – cartilaginous endplate), b) finite element model of the disc

The intervertebral disc matrix was meshed with tetrahedral finite elements that were refined around the edges of the disc. The total number of 62,135 tetrahedral elements was used to mesh the model.

Annulus fibers were defined with the elastic modulus of 100 MPa and Poisson's ratio of 0.33. The cross-sectional area of fiber elements equals to A = 0.07 mm^2. Other material properties representing healthy and degenerated (approximately the third degeneration class according to Thompson's scale) discs were taken from literature and are summarised in Table 2.1. The modelling of a degenerated disc requires to increase the elastic modulus and the initial permeability and to reduce

Poisson's ratio as well as the initial porosity of annulus fibrosus and nucleus pulposus, while the elastic modulus, Poisson's ratio and the initial permeability are decreased when modelling the endplates of a degenerated disc. The reduced initial permeability of endplates means that it is more difficult to supply oxygen and nutrients through to the central parts of the intervertebral disc.

The physical properties used in the model were as follows: fluid density ρ = 1000 kg/m^3, fluid viscosity μ = 1·10^{-3} Pa·s, internal and external osmotic coefficients φ_i = 0.83, φ_e = 0.92, universal gas constant R = 8.3145 J/mol·K, external salt concentration c_e = 150 mol/m^3, initial fixed charge density of nucleus pulposus and annulus fibrosus c_{f0_np} = 300 mol/m^3, c_{f0_af} = 180 mol/m^3, initial fluid volume fraction of nucleus pulposus and annulus fibrosus n_{0_np} = 0.8, n_{0_af} = 0.7. The drained density of nucleus pulposus and annulus fibrosus ρ_{d_np} = ρ_{d_af} = 1040 kg/m^3, the drained density of cartilaginous endplates ρ_{d_cep} = 2500 kg/m^3. Biot-Willis coefficient α_B = 1, compressibility 4·10^{-10} 1/Pa.

Table 2.1. Material properties of healthy and degenerated discs used in finite element analysis (Material properties are set according to Maladrino *et al*. [96]; Natarajan *et al*. [97]; Ferguson *et al*. [33]; or assumed)

Spinal component		Elastic modulus (MPa)	Poisson's ratio	Initial porosity	Initial permeability (mm^4/Ns)	M
Healthy disc	Annulus fibrosus	2.5	0.17	0.75	7.5·10^{-16}	8.5
	Nucleus Pulposus	1	0.17	0.83	7.5·10^{-16}	8.5
	Endplates	5	0.17	0.80	7.5·10^{-15}	8.5
Degene-rated disc	Annulus fibrosus	12	0.15	0.60	8.5·10^{-16}	8.5
	Nucleus Pulposus	1.6	0.15	0.78	8.5·10^{-16}	8.5
	Endplates	4	0.15	0.80	5·10^{-15}	8.5

2.2. Validation of poroelastic intervertebral disc model

The finite element model of the intervertebral disc was validated by calculating the decrease of the intervertebral disc height due to the static compression load and the reduction and recovery of the intervertebral disc height due to diurnal loading.

The total compression force of 500 N was uniformly applied to the upper surface of the top endplate and the inferior surface of the bottom endplate was constrained during the calculation of the decrease of the disc height (Fig. 2.2 a)). A loading value of 500 N was selected as it represents the average weight of the human upper body and is usually used in experimental studies. The calculated axial displacement meets the experimental values of 1–1.35 mm reported in literature [98].

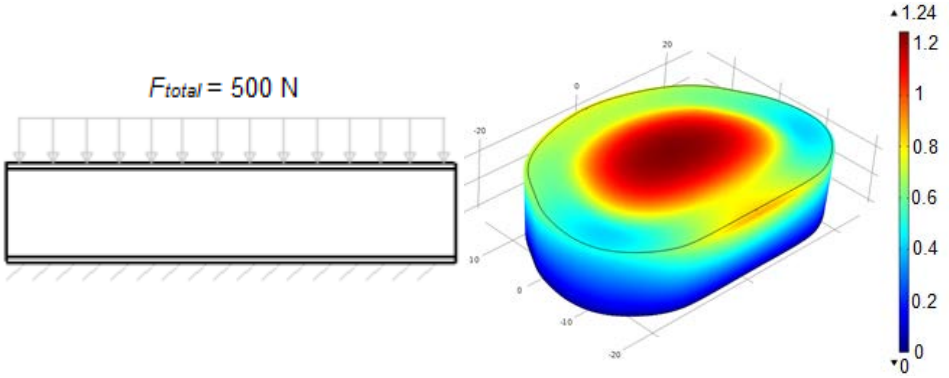

a) b)

Fig. 2.2. Validation of intervertebral disc model: a) loading scheme; b) intervertebral disc displacement

The validation of the disc swelling mechanism was performed by modelling the diurnal cycle loading. During the diurnal cycle loading, a compression force of 500 N was applied for 16 hours to the upper surface of the top endplate and then removed for another 8 hours. The inferior surface of the bottom endplate was constrained. It is known that 8 hours of rest should allow the intervertebral disc to return to its initial height. The modelled diurnal changes of the intervertebral disc height are shown in Fig. 2.3.

As both results are within the limits of experimental results reported in scientific literature, this model is valid and may be used to calculate other parameters of the intervertebral disc.

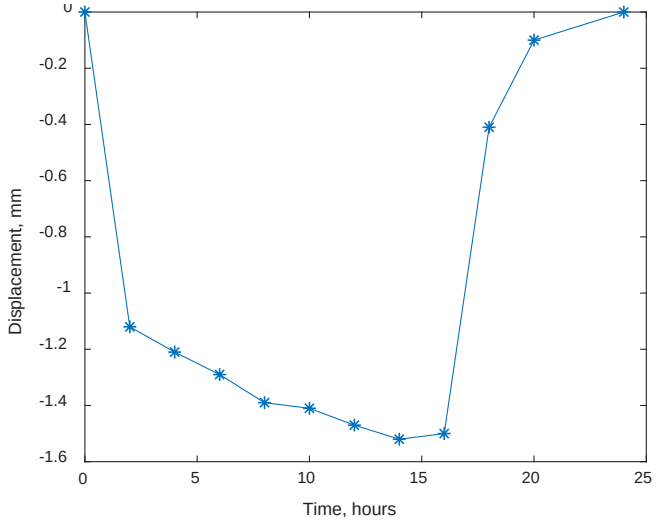

Fig. 2.3. Changes of intervertebral disc height during the day

2.3. Investigation of fluid flow velocity within the intervertebral disc

Some of the results presented in this chapter have been published in the article: Mikuckytė, S., Ostaševičius, V. Investigation of fluid flow velocity within the lumbar intervertebral disc. Mechanika. 2020, vol. 26, iss. 6.

A model of the healthy intervertebral disc was loaded with 7.5 Nm moments (*M*) of pure flexion, extension, lateral bending or axial rotation in order to calculate what fluid flow velocity may be caused by ordinary lumbar spine moves. The bottom surface of the lower cartilaginous endplate was constrained, and moments were uniformly applied to the top surface of the upper endplate (Fig. 2.4). Moments of 7.5 Nm were chosen as it is one of the values that are frequently used in various *in silico* studies, and it would allow to compare the obtained results. In order to evaluate the changes of the fluid flow velocity and to model the move of the human spine, loading moments were applied during one second and held at the maximum value for one second (Fig. 2.5).

It was calculated that the maximal fluid flow velocity due to flexion is 5.01 μm/s, 6.16 μm/s due to extension, 8.37 μm/s due to lateral bending and 0.53 μm/s due to axial rotation. Velocity fields through the surface of the intervertebral disc and the velocity magnitude at the middle plane horizontal section due to the particular moments at the loading time t = 1 s are given in Fig. 2.6 – Fig. 2.9. Horizontal section views show that the highest velocity magnitude values occur at the boundary between nucleus pulposus and annulus fibrosus and at the exterior region of annulus fibrosus.

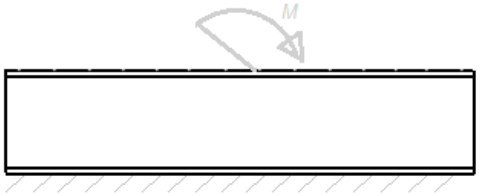

Fig. 2.4. Intervertebral disc loading scheme

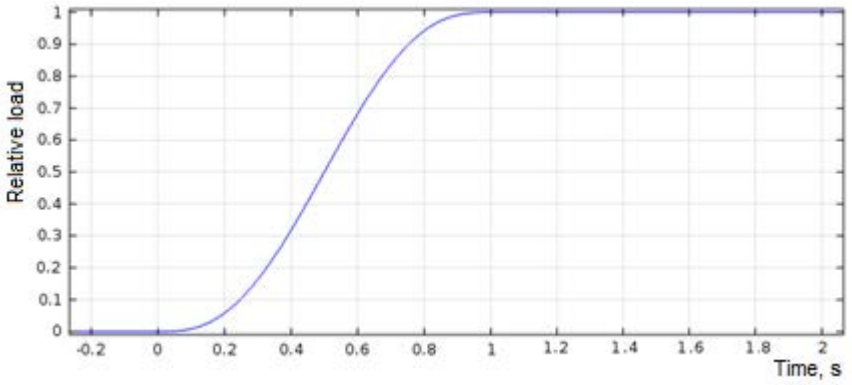

Fig. 2.5. Changes of intervertebral disc loading magnitude

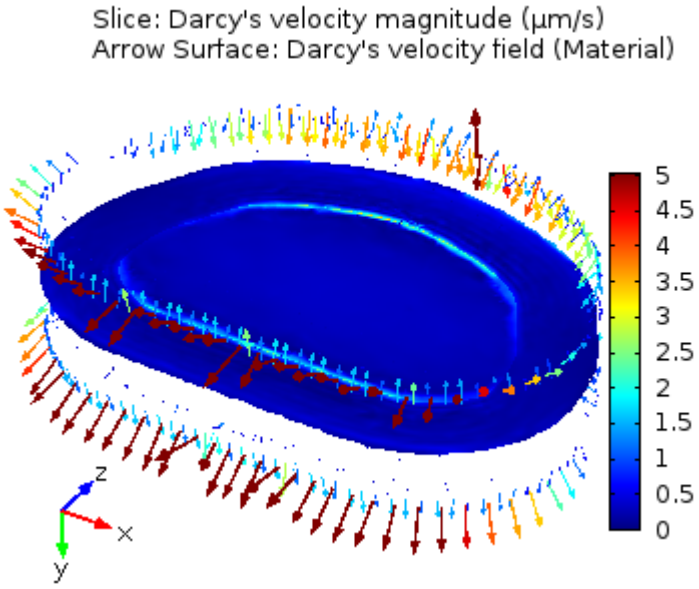

Fig. 2.6. Fluid flow velocity (µm/s) due to flexion

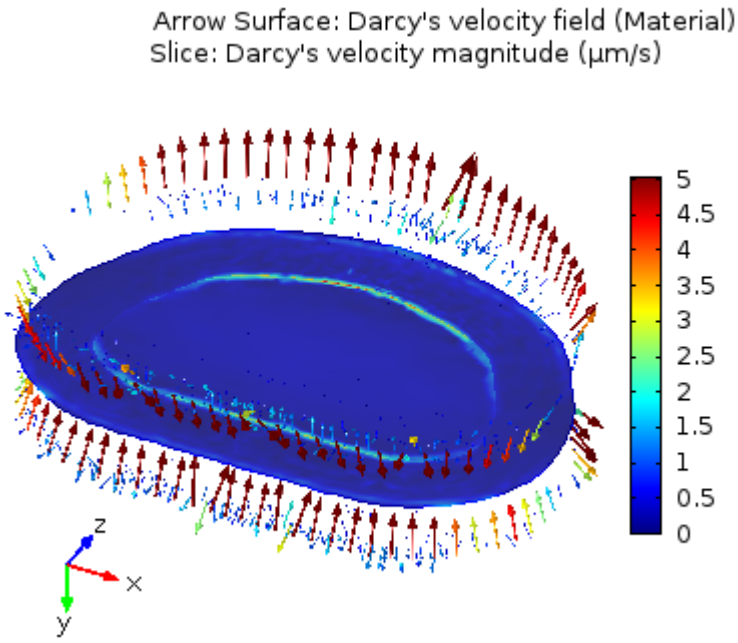

Fig. 2.7. Fluid flow velocity (µm/s) due to extension

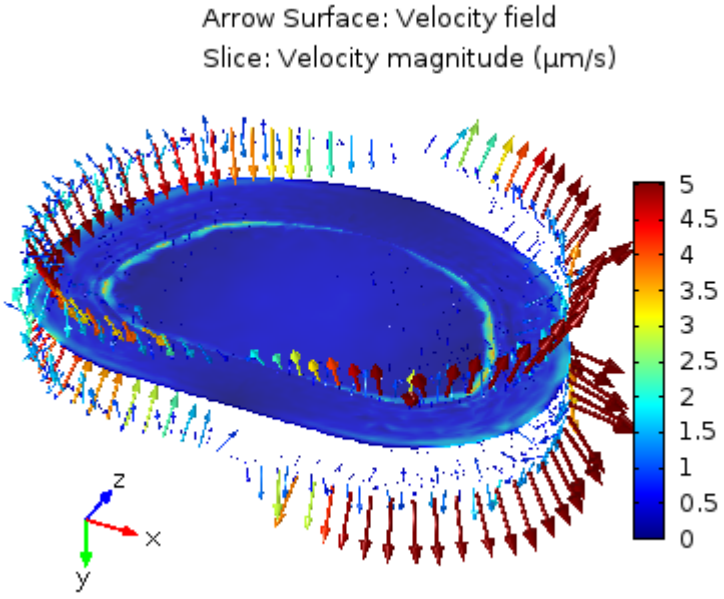

Fig. 2.8. Fluid flow velocity (µm/s) due to lateral bending

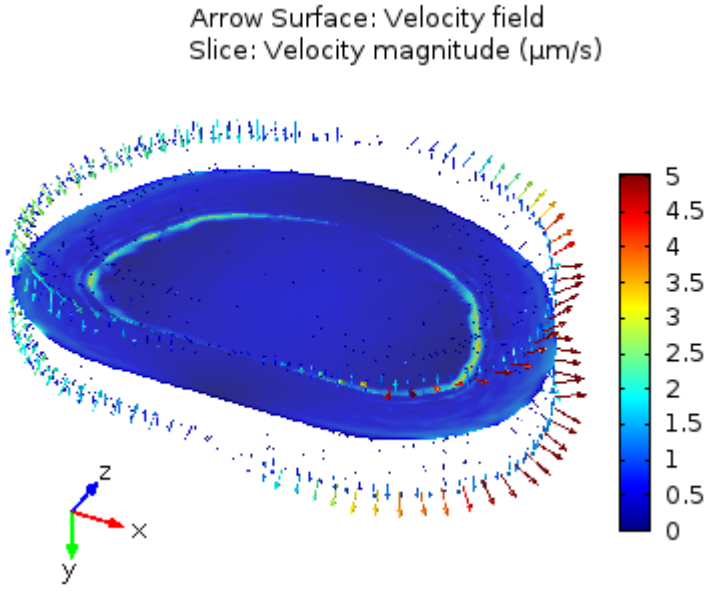

Fig. 2.9. Fluid flow velocity (µm/s) due to axial rotation

Fig. 2.10 – Fig. 2.13 show the average fluid flow velocity of the entire intervertebral disc, nucleus pulposus, annulus fibrosus and cartilaginous endplates, respectively, due to flexion, lateral bending, axial rotation and extension. The initial fluid flow velocity values are not equal to zero due to the applied osmotic pressure gradient for the simulation of the swelling of the disc. The highest average fluid flow velocity values are calculated due to flexion (0.0943 μm/s) and extension (0.0944 μm/s), and the lowest average velocity is calculated due to axial rotation (0.0313 μm/s). The average fluid flow velocity due to lateral bending is 0.0665 μm/s. It is necessary to emphasise that the average velocity values are analysed in this paragraph, and the average values are lower than the maximal velocity values given in the previous paragraph. The change of the average fluid flow velocity is the same for flexion and extension. This tendency is seen in particular parts of the intervertebral disc as well as the whole disc. In all loading scenarios, the highest average fluid flow velocity is calculated in cartilaginous endplates as most of the fluid that flows into the disc and out of it goes through the thin endplates as their initial permeability is 10 times higher than the permeability of the outer layer of annulus fibrosus. The lowest average fluid flow is calculated in nucleus pulposus as only a part of fluid reaches this central zone of the disc.

There is no significant difference between the times when velocity reaches its maximum average value, in all the cases and disc parts, this time is between 0.8 and 0.9 seconds after the loading starts, or, in other words, when the loading reaches its maximal value.

As the loading moment remains constant for the 2nd second of the loading, the fluid flow velocity decreases slower than it increased during the first second in all the cases of loading and parts of the intervertebral disc. The average fluid flow velocity of the whole disc during the 2nd loading second decreases the fastest when it was induced by lateral bending (a decrease of 30.31%), and the slowest when it was induced by axial rotation (a decrease of 21.37%). The slowest decrease of the average fluid flow velocity in all the loading cases is in nucleus pulposus and the fastest in annulus fibrosus and axial rotation leads to the most uniform decrease of the average fluid flow velocity in all the parts of the disc. All the values of the decrease of the average fluid flow velocity during the 2nd second of loading are given in Table 2.2.

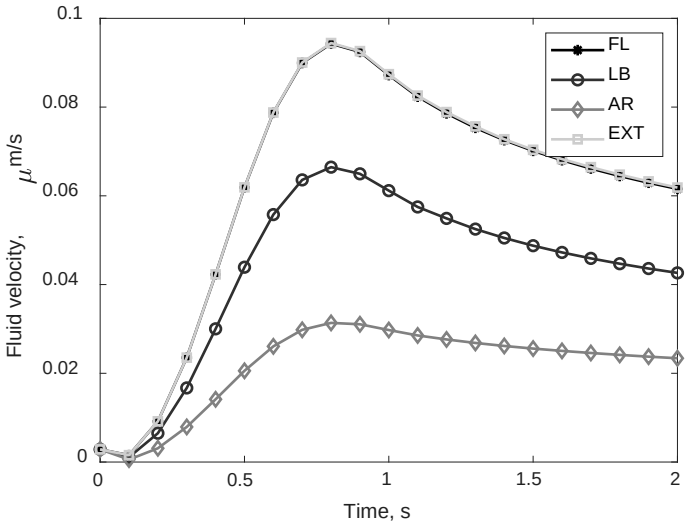

Fig. 2.10. Average intervertebral disc fluid flow velocity during pure loadings of 7.5 Nm (FL – flexion, LB – lateral bending, AR – axial rotation and EXT – extension)

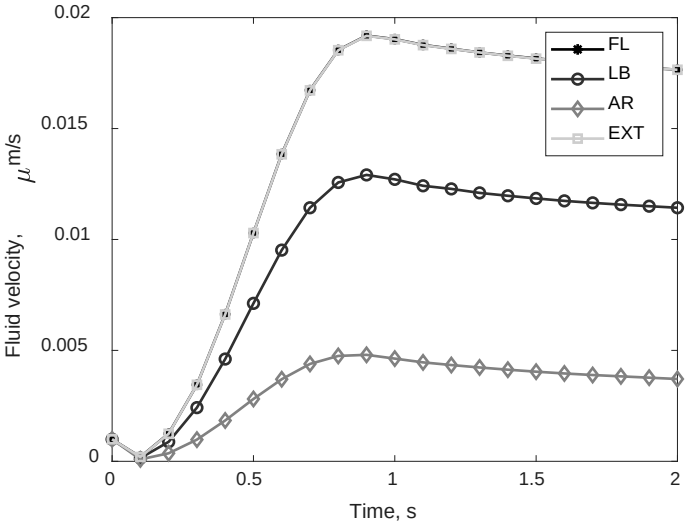

Fig. 2.11. Average fluid flow velocity in nucleus pulposus during pure loadings of 7.5 Nm (FL – flexion, LB – lateral bending, AR – axial rotation and EXT – extension)

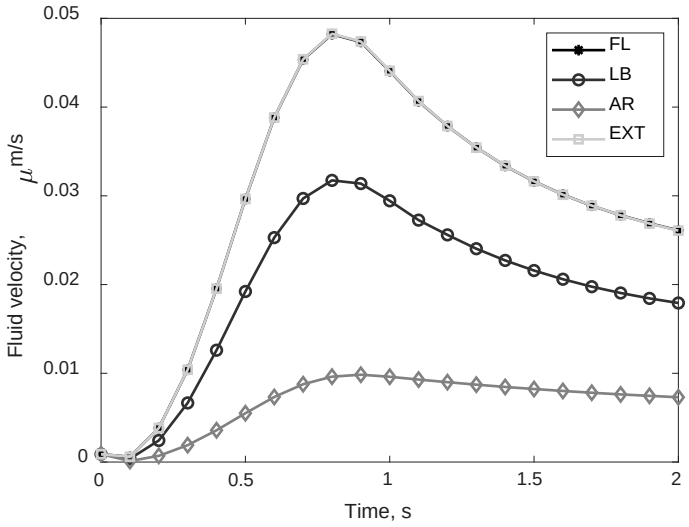

Fig. 2.12. Average fluid flow velocity in annulus fibrosus during pure loadings of 7.5 Nm (FL – flexion, LB – lateral bending, AR – axial rotation and EXT – extension)

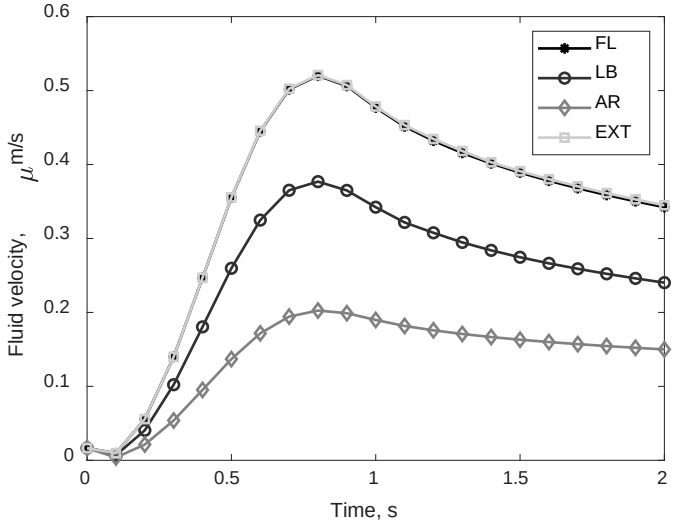

Fig. 2.13. Average fluid flow velocity in cartilaginous endplates during pure loadings of 7.5 Nm (FL – flexion, LB – lateral bending, AR – axial rotation and EXT – extension)

Table 2.2. Decrease of average fluid flow velocity during 2nd second of loading

	Flexion	Lateral bending	Axial rotation	Extension
Disc	29.41%	30.31%	21.38%	29.23%
NP	7.25%	10.07%	19.87%	7.20%
AF	40.73%	39.13%	24.04%	40.85%
CEP	28.23%	29.81%	20.99%	27.92%

Fig. 2.14 – Fig. 2.17 show the average fluid flow velocity component Y in the vertical direction of the intervertebral disc (the coordinate axes are seen in Fig. 2.6 – Fig. 2.9) of the whole intervertebral disc, nucleus pulposus, annulus fibrosus and cartilaginous endplates, respectively, due to flexion, lateral bending, axial rotation and extension. This direction is distinguished because most of the nutrients move from the endplates to nucleus pulposus, so this should be the main direction of the diffusion of nutrients. The calculated negative average velocity values represent the velocity in the opposite direction than the default *Y* direction. At it is seen, the average values of the fluid velocity component *Y* are significantly lower than the total average velocity values, especially in nucleus pulposus, and this direction of the fluid flow velocity is not dominant during all the cases of loading.

As well as in the case of the average magnitude values of fluid velocity, the highest average velocity component *Y* values are calculated in cartilaginous endplates, and the lowest is calculated in nucleus pulposus, but the patterns of the velocity changes are different.

The average fluid velocity component *Y* in the nucleus due to the direction of flexion changes at the beginning (the fluid flow direction due to flexion is different than due to the initial swelling) and reaches the maximum value at 0.6 s, it returns to the initial value and then starts to increase again, but as those values are very small, they may be considered only as small fluctuations around the initial value. The average fluid velocity component *Y* due to extension has a similarly changing pattern to that of component *Y* due to flexion, but the direction of the flow is opposite. Velocity component *Y* in the nucleus due to axial rotation moves towards zero as the load is applied. Axial rotation has the lowest influence on fluid flow velocity component *Y* in nucleus pulposus. Lateral bending exerts the most significant influence on velocity component *Y* in the nucleus as it reaches its maximum at 0.7 s and then starts moving towards the initial value.

Flexion and extension lead to the highest velocity component *Y* average values in annulus fibrosus. Velocity component *Y* induced by flexion decreases faster during the 2nd part of loading when the applied moment is constant than when component *Y* is induced by extension. Lateral bending has the lowest influence on fluid flow velocity component *Y* in annulus fibrosus.

Flexion and extension also lead to the highest velocity component *Y* average values in cartilaginous endplates. It is of interest that velocity component *Y* due to extension after some fluctuations reaches the average maximum value in the endplates only at 1.7 s.

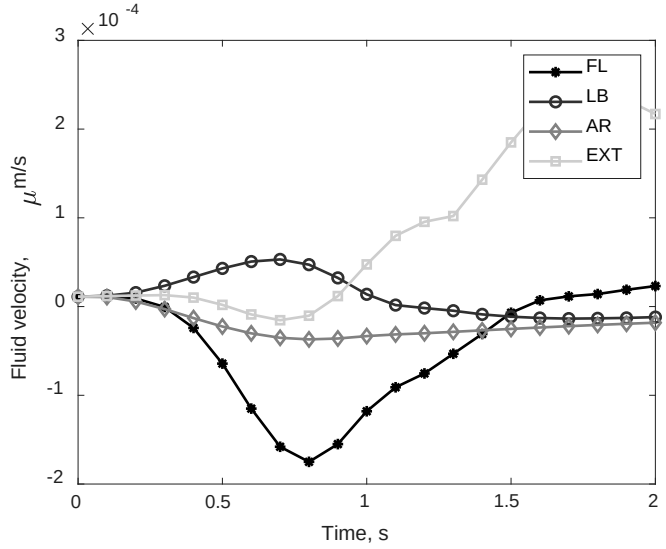

Fig. 2.14. Average intervertebral disc fluid flow velocity in the vertical direction during pure loadings of 7.5 Nm (FL – flexion, LB – lateral bending, AR – axial rotation and EXT – extension)

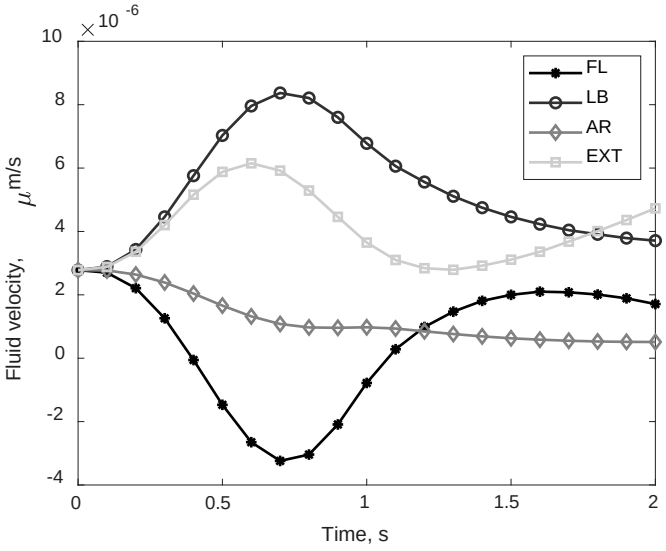

Fig. 2.15. Average fluid flow velocity in the vertical direction in nucleus pulposus during pure loadings of 7.5 Nm (FL – flexion, LB – lateral bending, AR – axial rotation and EXT – extension)

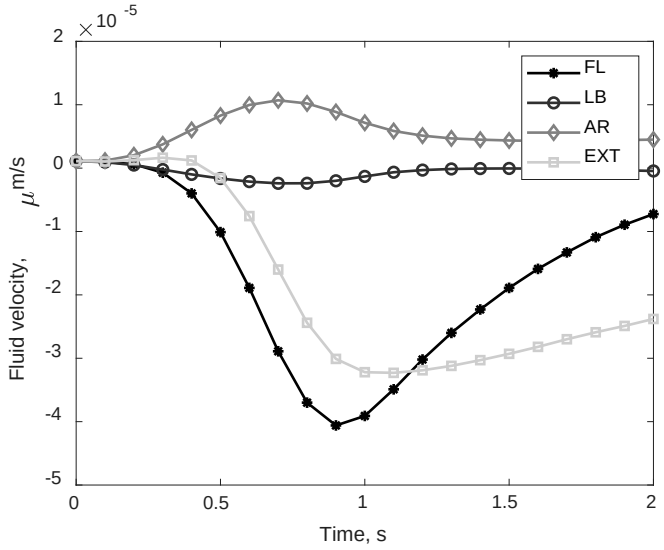

Fig. 2.16. Average fluid flow velocity in the vertical direction in annulus fibrosus during pure loadings of 7.5 Nm (FL – flexion, LB – lateral bending, AR – axial rotation and EXT – extension)

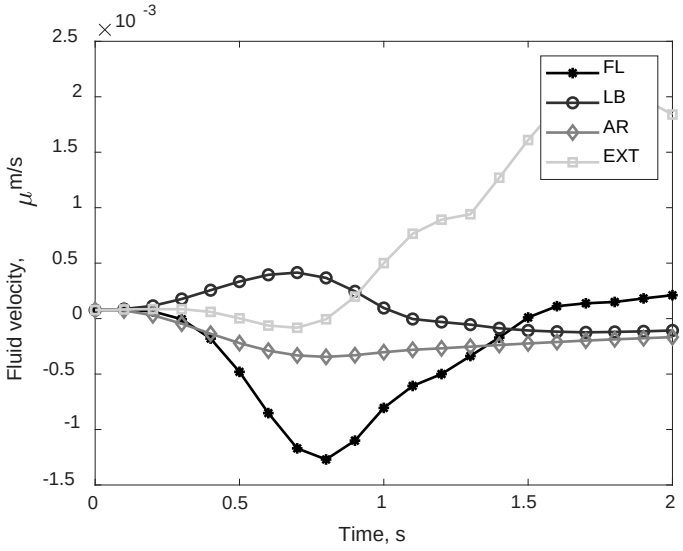

Fig. 2.17. Average fluid flow velocity in the vertical direction in cartilaginous endplates during pure loadings of 7.5 Nm (FL – flexion, LB – lateral bending, AR – axial rotation and EXT – extension)

2.4. Investigation of coupled lateral bending influence on the lumbar intervertebral disc

Results of previous investigations suggest that lateral banding moves may be used to improve the fluid flow into the intervertebral disc and also to increase the supply of nutrients. The purpose of this study is to investigate how pure lateral bending and coupled lateral bending (the loading of lateral bending and additional flexion, extension, or axial rotation) loads influences healthy and degenerated intervertebral discs. Some of the results presented in this chapter have been published in the article: Mikuckytė, Sandra; Ostaševičius, Vytautas. Numerical study of lateral bending influence on lumbar intervertebral disc. Vibroengineering procedia. 2017, 15, 71–76. DOI: 10.21595/vp.2017.19401.

The same intervertebral disc model described in Section 2 is used in this analysis. In order to investigate the influence of the pure lateral bending move on the intervertebral disc, a lateral bending angle of 10° was applied to the superior surface of the upper cartilaginous endplate as this value is near to the maximal failure-free lateral bending angle reported in literature. The same as in Section 2.3, the maximal loading value (in this case, the maximal bending angle) was reached in one second. In addition to lateral bending, flexion, extension, or axial rotation angles of 2° and 5° were applied to the disc. As it was already mentioned in Literature review, this type of additional moves is difficult to avoid when lateral bending exercises are performed in the standing position, especially, by older individuals. The inferior surface of the lower cartilaginous endplate was constrained in this study (Fig. 2.18).

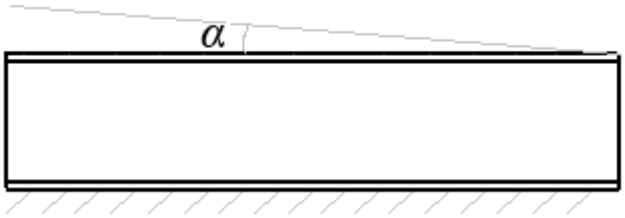

Fig. 2.18. Loading scheme

Fig. 2.19 shows the distribution of stress, pore pressure and fluid flow velocity values in the frontal section view of the healthy and degenerated intervertebral disc when a pure lateral bending displacement of 10° is applied. The stress values in healthy annulus fibrosus are higher than in nucleus pulposus. Due to disc degeneration, the stress values in annulus fibrosus significantly increase, but the values of nucleus pulposus remain similar to those of a healthy nucleus. The maximal stress value of a healthy annulus fibrosus is 3.15 MPa, and the maximal stress value of degenerated annulus fibrosus is 9.12 MPa.

The pore pressure of the disc also increases when the disc is degenerated and becomes unevenly distributed in the zones between nucleus pulposus and annulus fibrosus. In both cases, the highest pore pressure values occur in the compressed part of the disc.

Calculations show that the fluid flow velocity in the degenerated disc also increases, but the higher fluid velocity value in the degenerated disc does not mean that disc degeneration has any beneficial effects. Due to the reason that the exact lateral bending angle was prescribed in this study instead of lateral bending moments, it could be assumed that reactions and strain values of the degenerated disc are higher, as degeneration tends to increase the stiffness of the intervertebral disc, so that the same bending angle could induce critical stress values and increase the risk of failure.

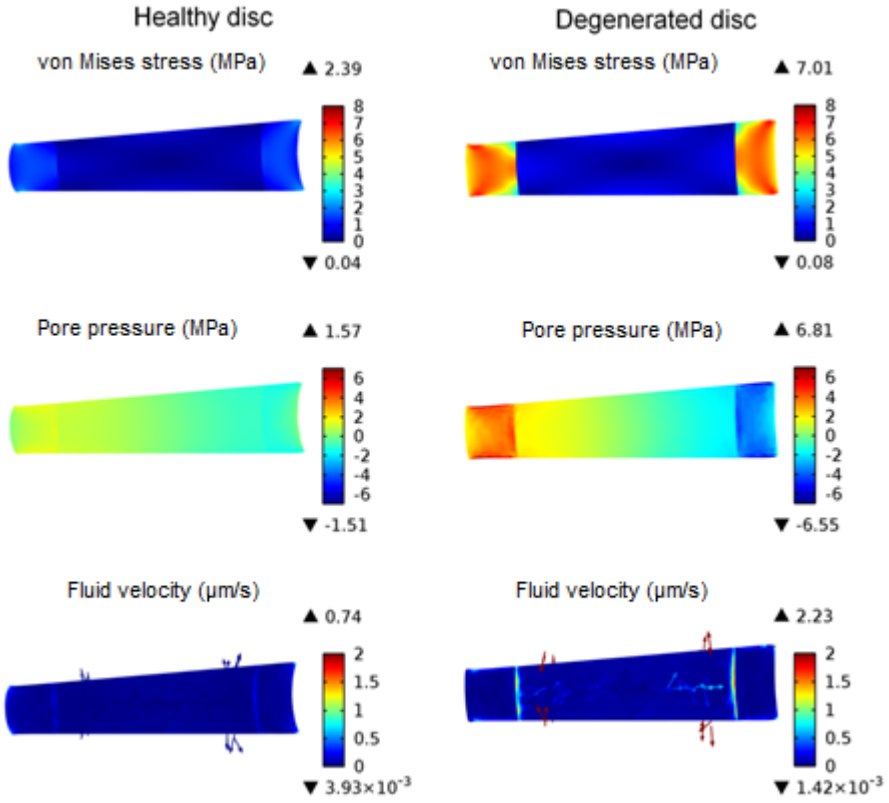

Fig. 2.19. Results of pure 10° lateral bending in healthy and degenerated intervertebral discs. Frontal plane cross-section view

The maximal stress values induced in the intervertebral disc due to pure and coupled lateral bending are shown in Fig. 2.20. Additional flexion or extension of 2° does not change the maximal stress value of 3.15 MPa, while axial rotations insignificantly reduce the maximal stress value of a healthy disc. Additional flexion or extension of 5° also does not have any apparent influence on the maximal stress value while the axial rotations of 5° decrease the maximal stress value more significantly.

The maximal stress values are significantly higher (about 3 times) when both pure lateral bending and coupled loads are applied to the degenerated intervertebral disc. Axial rotations of 2° and 5° reduce the maximal stress value while flexion and rotation, contrary to the case of a healthy disc, increase the maximal stress value. The highest maximal stress value of the intervertebral disc is calculated when an extension angle of 5° is applied together with lateral bending.

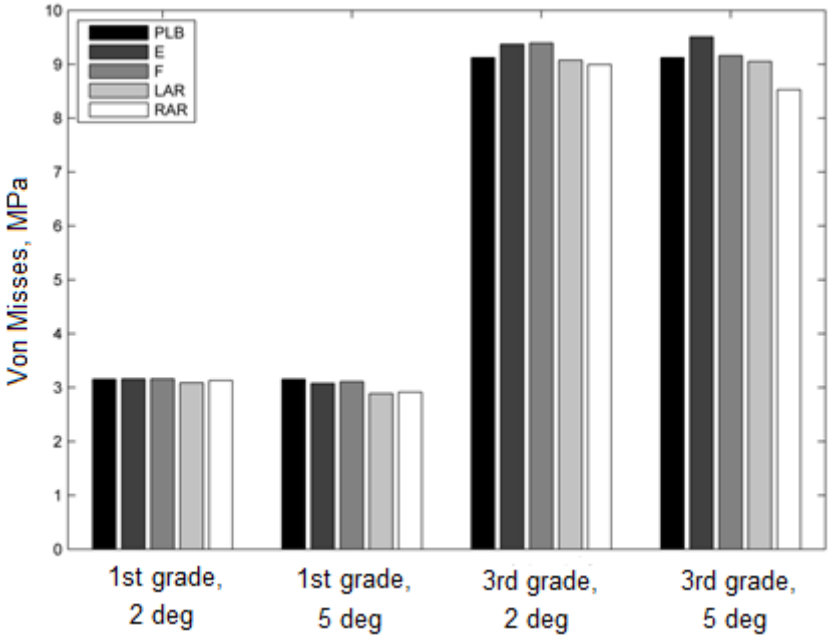

Fig. 2.20. Von Mises stress values induced by pure lateral bending and additional loads of 2° and 5° in healthy (1st grade) and degenerated (3rd grade) discs: PBL – pure 10° lateral bending, E – lateral bending + extension; F – lateral bending + flexion; LAR and RAR – lateral bending + axial rotation to the left or right

Coupled loading and disc degeneration also change the intervertebral disc pore pressure when compared to the case of pure lateral bending. The pore pressure values of nucleus pulposus and annulus fibrosus due to pure lateral bending and additional loads of 2° are shown in Fig. 2.21. The pore pressure value of a healthy nucleus is the highest when pure lateral bending is applied. The application of each of four additional loadings only insignificantly reduces the pore pressure. The maximal pore pressure values of a healthy annulus fibrosus are almost the same when pure bending or coupled loadings are applied with the exception of the case of additional axial rotation when the maximal pore pressure value is lower.

The maximal pore pressure of a degenerated nucleus pulposus is about 2.5 times higher than that of a healthy nucleus, and the maximal pore pressure of a degenerated annulus fibrosus is about 4.5 times higher than that of a healthy annulus. The changes of the maximal pore pressure values due to coupled loading

are insignificant, while additional extension leads to a higher pore pressure value than pure lateral bending.

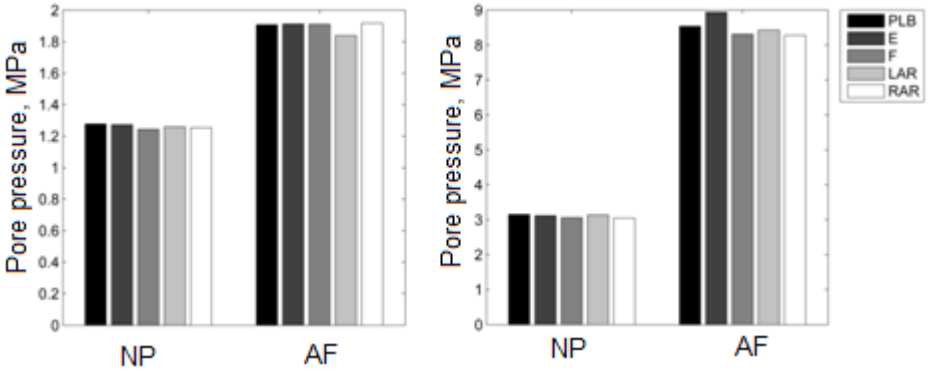

Fig. 2.21. Pore pressure comparison between cases of loading: healthy intervertebral disc (left) and degenerated intervertebral disc (right). PBL – pure 10° lateral bending, E – lateral bending + 2° extension; F – lateral bending + 2° flexion; LAR and RAR – lateral bending + 2° axial rotation to the left or right

The maximal fluid flow velocity values in a healthy nucleus pulposus are given in Fig. 2.22. All additional 2° and 5° angular displacements lead to lower fluid flow velocity values than the value induced only by lateral bending. 5° angular displacements lead to a higher decrease of the fluid flow velocity in all the cases of loading except when the angular displacement of extension is applied.

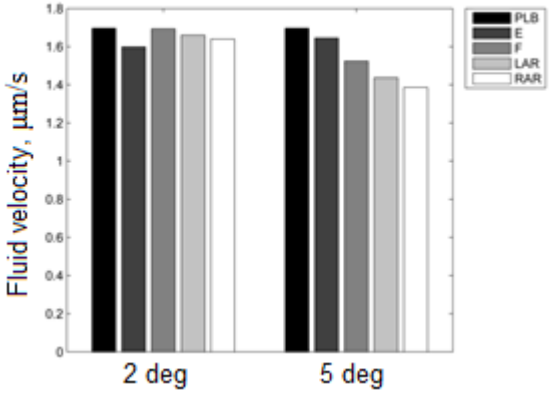

Fig. 2.22. Fluid velocity in healthy nucleus pulposus: PBL – pure 10° lateral bending, E – lateral bending + extension; F – lateral bending + flexion; LAR and RAR – lateral bending + axial rotation to the left or right

2.5. Investigation of loading distribution in the lumbar spine

The man goal of this study is to evaluate how flexion, extension, lateral bending and axial rotation loads are distributed in the lumbar spine. The geometry of lumbar spine segment T1-S1 has been created according to the mean dimensions of

the lumbar vertebrae and intervertebral discs presented in the literature. The main dimensions of the lumbar spine model geometry are given in Annex 1. Each intervertebral disc was modelled the same way as it is described in Section 2.1, and their material properties are given in Table 2.1, while the material properties of the vertebrae are given in Table 2.3. The ligaments that connect and stabilise the vertebral column were modelled as tension only elements, and their material properties are listed in Table 2.4. The lowest vertebra was constrained, and a moment was applied to the upper one (Fig. 2.23).

Table 2.3. Material properties of vertebrae

Elastic modulus, MPa	1000
Poisson's ratio	0.3
Initial porosity	0.048
Initial permeability, mm^4/Ns	$2 \cdot 10^5$

Table 2.4. Material properties of ligaments

	Tensile modulus, MPa	Poisson's ratio	Cross-sectional area, mm^2
Posterior longitudinal ligaments	20	0.35	25
Anterior longitudinal ligaments	8	0.35	20
Supraspinous Ligaments	30	0.35	35
Interspinous Ligaments	30	0.35	35
Ligamentum flava	30	0.35	40
Facet joints	10	0.4	40

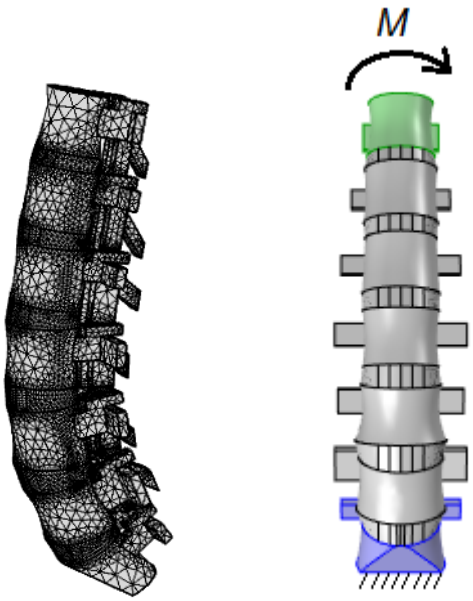

a) b)

Fig. 2.23. T12-S1 spine segment: a) finite element model, b) loading scheme

The material properties of separate ligaments were chosen during a widely used lumbar spine functional unit (two adjacent vertebrae and an intervertebral disc between them) validation procedure. The lumbar functional unit was loaded with pure 7.5 Nm moments of flexion, extension, right lateral bending and left axial rotation and compared with the values of an experimental study conducted by Heuer *et al*. [7]. A comparison of the modelled and given range of motion values is given in Table 2.5.

Table 2.5. Validation data of the lumbar spine model

Added elements	Anterior longitudinal lig.	Posterior longitudinal lig.	Vertebral arches	Facet capsules	Flaval lig.	Interspinous lig.	Supraspinous lig.	Intact
LB	6.43°	6.09°	6.14°	5.80°	5.64°	5.69°	5.66°	5.15°
LBM	6.26°	5.83°	5.91°	5.50°	5.45°	5.50°	5.34°	5.28°
Error, %	2.71	4.20	3.82	5.09	3.42	3.28	4.82	2.61
FL	10.11°	10.10°	9.73°	7.71°	7.13°	6.62°	6.55°	6.19°
FLM	9.74°	9.79°	9.21°	7.57°	6.98°	6.46°	6.42°	6.02°
Error, %	3.62	3.11	1.64	1.82	2.11	2.48	1.94	2.71
EX	10.28°	5.88°	5.82°	4.29°	4.46°	4.52°	4.45°	4.10°
EXM	10.63°	5.98°	5.75°	4.15°	4.27°	4.35°	4.35°	4.01°
Error, %	3.42	1.62	1.25	3.12	4.20	3.86	2.18	2.21
RO	2.70°	2.91°	2.94°	3.08°	3.29°	5.35°	5.47°	5.73°
ROM	2.63°	2.78°	3.03°	3.04°	3.37°	5.46°	5.65°	5.89°
Error, %	2.57	4.51	3.11	1.20	2.37	2.14	3.28	2.86

The strain values of annulus fibrosus induced due to lateral bending, flexion, extension and axial rotation of a healthy lumbar spine are shown in Fig. 2.24. The highest strain values occur due to lateral bending and axial rotation. In all the cases of loading, the highest strain values occur in the annulus fibrosus of intervertebral disc L5-S1, and it may be considered as the most vulnerable to traumas or degenerative changes.

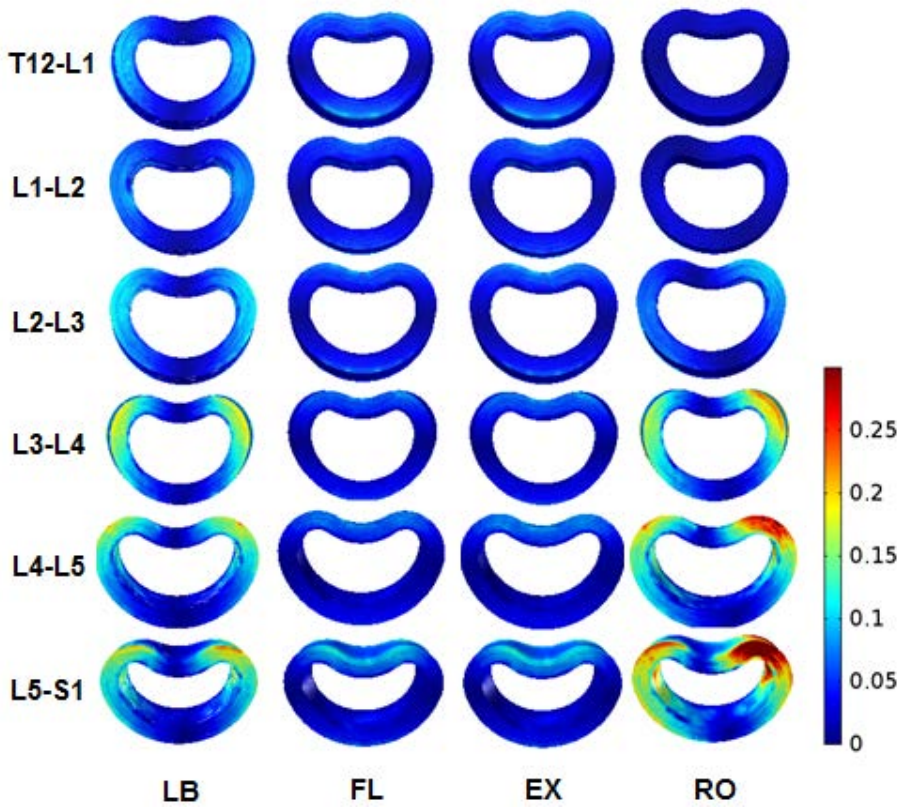

Fig. 2.24. Strain distribution in annulus fibrosus of lumbar intervertebral discs induced by lateral bending (LB), flexion (FL), extension (EX) and axial rotation (RO)

2.6. Section conclusions

The main purpose of this study was to develop finite element models that would allow to evaluate the fluid flow velocity within the intervertebral disc and to estimate the influence of various loading scenarios on the intervertebral disc and the lumbar spine.

The calculated maximal fluid flow velocity due to lateral bending is 8.37 μm/s, due to flexion – 5.01 μm/s, due to extension – 6.16 μm/s, and due to axial rotation – 0.53 μm/s. When comparing the average values of the flow velocity, the highest values are calculated due to flexion (0.0943 μm/s) and extension (0.0944 μm/s), but lateral bending leads to the highest value of the velocity component in the *Y* direction in nucleus pulposus ($8.370 \cdot 10^{-6}$ μm/s). As the average fluid flow velocity component *Y* values are significantly lower than the total average values, the assumption that lateral bending moves may be more useful for the health of the intervertebral disc than other moves cannot be sufficiently substantiated only by this data, these results of modelling show that the influence of lateral bending on the

intervertebral disc is similar to flexion and extension, and, as it is less performed in daily activities, should not be excluded from exercise programmes.

The results of the lateral bending of a poroelastic intervertebral disc show that the stress values in the intervertebral disc increase when a more degenerated intervertebral disc is bent. Disc degeneration also increases the pore pressure of the intervertebral disc, especially within annulus fibrosus, and this could lead to intervertebral disc disorders, such as disc herniation. Due to a significant influence of disc degeneration, the condition of the patient's spine should be evaluated before defining the intensity of the lateral bending exercise. While coupled loading simulations do not show any significant changes in the stress values of annulus fibrosus, the obtained results could imply that additional flexion and extension loads are more dangerous than axial rotations and could induce higher annulus fibrosus stresses than pure lateral bending. The fluid flow velocity reduced during combined loading could suggest that, in the frontal plane, the constrained lateral bending exercise is more beneficial than coupled moves in order to achieve a better nutrition of the intervertebral disc.

Lateral bending and axial rotation lead to the highest strains of annulus fibrosus. The highest strains due to all the moves of the lumbar spine occur in intervertebral disc L5-S1 which may be considered as the most vulnerable disc.

3. EXPERIMENTAL RESEARCH OF THE LUMBAR SPINE

The following section of the thesis describes experimental *in vitro* studies of the spine. *In vitro* studies are commonly used to investigate the biomechanical behaviour of human spine and are beneficial when it is necessary to measure parameters that would be difficult to measure *in vivo* or to apply loads that could cause damage to the spine. Due to very limited availability of fresh frozen cadaveric spines, animal specimens are widely used as an alternative. As animal specimens can be chosen by the desired age group, they have more uniform properties. Porcine, bovine, ovine or caprine models are the most common for *in vitro* investigation of the biomechanical behaviour of the spine. The porcine model was chosen for this research as it said to be the most resembling the human spine and was easier to obtain.

The main purpose of this study was to investigate how the spine reacts to various dynamic loading scenarios and to differentiate between positive and negative dynamic loading cases of the spine.

3.1. Measurement of porcine spine stiffness and response to impact load

The goal of this study was to measure the stiffness and response to an impact load of the spinal section in order to obtain basic knowledge about the porcine spine and to evaluate its condition.

A porcine spine with intact posterior elements, capsular structures and ligaments was obtained from a local abattoir. It was placed in the stiff specimen holder designed and manufactured for this study. The investigation was focused on the segment of 8 adjacent vertebrae that was placed between two supports of the specimen holder. An experimental setup (Fig. 3.1) consisting of a non-contact laser displacement sensor unit *LK-82G* (*Keyence Inc*.), an oscilloscope *Picoscope 3424* (*Picotech LTD*) and a personal computer was prepared in order to measure the stiffness and response to an impact load of the spinal section.

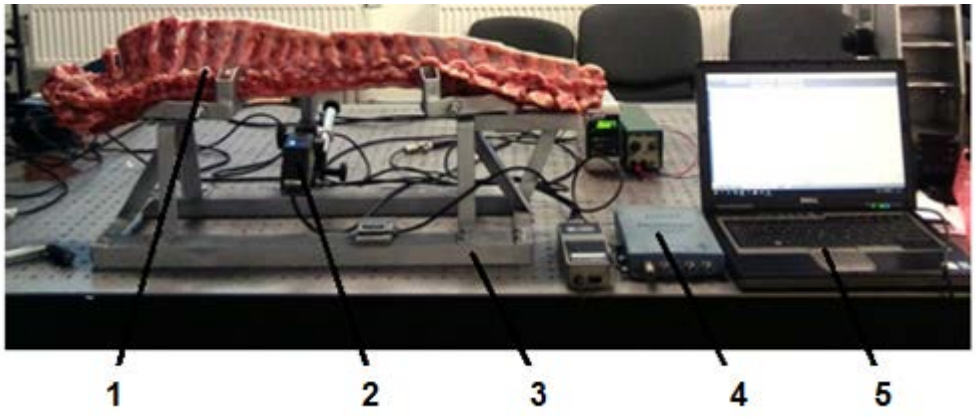

Fig. 3.1. Experimental setup: 1 – porcine spine specimen; 2 – displacement measurement unit laser *Keyence LK-G82*; 3 – specimen holder; 4 – oscilloscope *Picoscope 3424*; 5 – PC

Spine stiffness in the four main directions was assessed by applying load F = 1.5 N in the middle of the studied spine segment, measuring its displacement *x* and calculating stiffness value *k* from Equation:

$$k = \frac{F}{x} \tag{3.1}$$

The calculated values of spinal stiffness are given in Table 3.1. The studied part of the porcine spine is the stiffest in the sagittal extension direction presumably due to the presence of spinous processes. However, the calculated stiffness values are lower than the usually reported values of *in vivo* measurements of the human trunk stiffness [98], which shows that muscles are also an important factor for providing spinal stability.

Table 3.1. Results of porcine spine stiffness measurement

Plane and direction of applied load	Displacement, mm	Stiffness, N/mm	Average stiffness, N/mm
Sagittal, flexion	3.0	0.50	0.54
	2.6	0.58	
Sagittal, extension	1.9	0.79	0.77
	2.0	0.75	
Frontal, left	5.8	0.26	0.26
	5.8	0.26	
Frontal, right	4.4	0.34	0.40
	3.3	0.45	

The spine may be considered as a second order damped mechanical system whose movements may be defined by Equation

$$m\frac{d^2x}{dt^2} + c\frac{dx}{dt} + kx = F(t) \tag{3.2}$$

where *m* is the mass and inertia of the system, *c* is the energy dissipation and *k* is the stiffness of the system, *x* is the displacement, the first derivative of *x* is the velocity and the second derivative of *x* is the acceleration of the system.

The spine is a nonlinear system because *m*, *c* and *k* depend on the position and deformation of the spine, for example, the moment of inertia changes due to the bending of the spine and mass, whereas the damping and stiffness are related to the water content in the intervertebral discs.

The response of the segment of adjacent vertebrae to an impact load was measured in order to investigate its natural frequency and damping behaviour. The response of the segment to the impact load applied in the sagittal plane is shown in Fig. 3.2, and the response to the impact load applied in the frontal plane is shown in Fig. 3.3.

As it can be seen from these waveforms, the segment of adjacent vertebrae does not oscillate in any direction, so it may be considered as a critically damped or overdamped system.

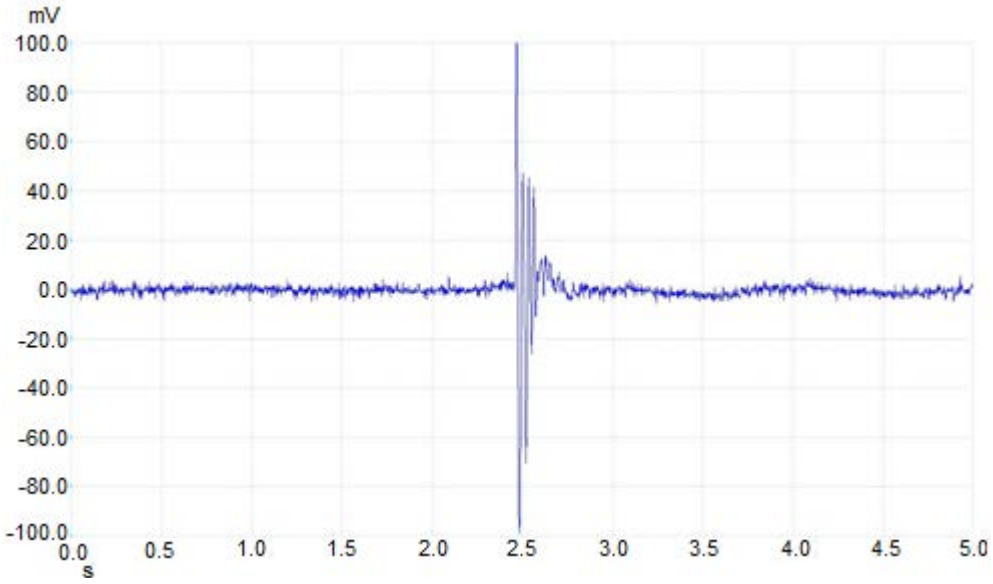

Fig. 3.2. Adjacent vertebrae segment response to impact load applied in the sagittal plane

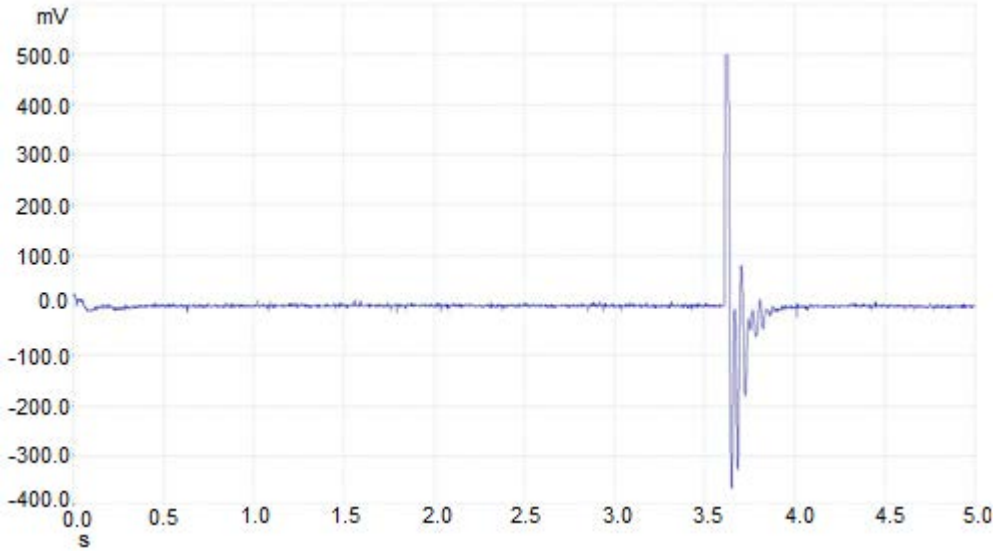

Fig. 3.3. Adjacent vertebrae segment response to impact load applied in the frontal plane

Although it was already mentioned above that the spine should be considered as a nonlinear system, for the sake of simplicity, the damping ratio of a linear system is given below:

$$\xi = \frac{c}{2\sqrt{mk}} \tag{3.3}$$

Depending on the value of the damping ration, mechanical systems are classified as underdamped ($\xi < 1$), critically damped ($\xi = 1$) and overdamped ($\xi > 1$).

A critically damped spinal system may be considered as healthy because then the spine smoothly moves from one position to another. Meanwhile, an underdamped system is related with non-sufficient stability of the spine when some oscillations of the spine may be observed, and additional efforts are necessary to move the spine to the required position.

As it can be seen from the damping ratio formula, the increased mass or inertia may lead to the lesser stability of the spine, and this means that tall or overweight people have a higher risk of spinal instability. Reduced energy dissipation, such as a reduced water content of intervertebral discs due to degeneration, also decreases the spinal stability.

Therefore, one of the factors to improve the spinal stability is related with the fluid content within intervertebral discs. On the other hand, healthy ligaments and back muscles also contribute to the damping of the spinal system and thereby to the spinal stability so the methods that would allow to improve their condition or pause their deterioration are also important and worth investigating.

3.2. Experimental investigation of coupled compressive loading

Some of the results presented in this chapter have been published in the article: Mikuckytė, S., Ostaševičius, V. Experimental Investigation of an Influence of Coupled Compressive Loading on Porcine Spine Specimens. Mechanika, 2021, vol. 27, iss, 1.

The goal of this study is to investigate the influence of cyclic compression and flexion on spinal sections as these are the most common moves during the day.

Two specimens consisting of four adjacent vertebrae and three intervertebral discs were separated from healthy porcine spines which were obtained from an abattoir, placed in plastic bags to decrease dehydration and environmental influence and fresh frozen at -20°C. Before testing, they were thawed in 0.9% (0.15 mol/l) saline overnight in a refrigerator (+4°C) to allow rehydration. This study consisted of three main stages: computed tomography (CT) scanning of the specimens, cycled loading and repeated CT scanning of the specimens to evaluate the influence of loading (Fig. 3.4). Between the scans and cyclic loading, the specimens were kept in moist cloths in order to prevent their dehydration.

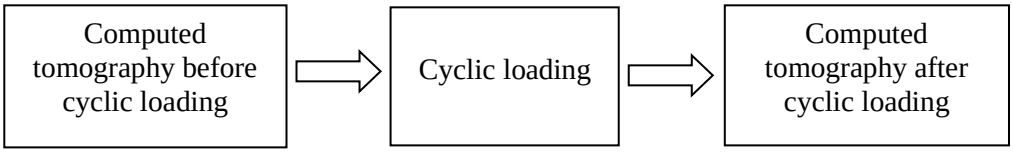

Fig. 3.4. Sequence of the experiment

Computed tomography imaging

Computed tomography is a medical diagnostic tool that allows visualising the inside structures of the human body. The computed tomography procedure is performed by generating cross-sectional images (slices) of the scanned body. A fan-shaped beam of X-ray produced by a rotating X-ray source is attenuated by the scanned object which it travels through, and this attenuation is captured by a rotating X-ray detector (Fig. 3.5) and converted into a digital signal for computed reconstruction. Measurements taken during one rotation result in a single 2D image. As the table where the scanned object is placed moves, a sequence of these images is produced, and this sequence can be used to create cross-sectional or three-dimensional views of the entire scanned object.

A *LightSpeed VCT* (*GE Healthcare*) computed tomography system whose main characteristics are given in Table 3.2 was used in this study. The CT dose index $CTDI_{vol}$ was 14.74 mGy, and the dose-length product DLP was 899.74 mGy/cm. A slice thickness of 0.625 mm was chosen for this study.

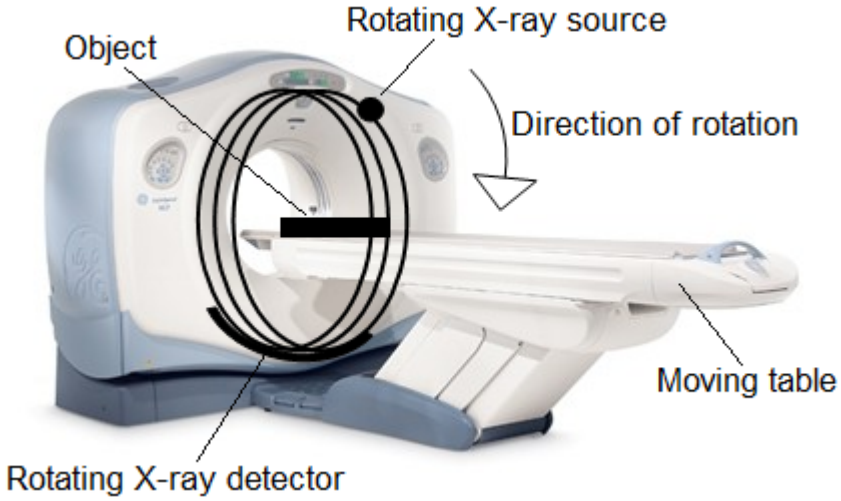

Fig. 3.5. Scheme of computed tomography imaging (a picture of *LightSpeed VCT* computed tomography system used to create this scheme was taken from **[99]**)

Table 3.2. Main technical features of computed tomography system *LightSpeed VCT*

Slices per rotation	64
Gantry diameter, cm	70
Minimum temporal resolution, ms	175
Maximum beam width, cm	4
X-ray generator kV range, kVp	80–140
Maximum scan range, cm	170

Cyclic loading

After the initial scanning, specimens were placed into holders designed to rigidly embed the lower and upper vertebrae of the specimens and to fit into chucks of a linear-torsion static and fatigue testing machine *Instron ElectroPuls E10000T* (Fig. 3.6). *Instron ElectroPuls E10000T* can be used for the static and dynamic testing of various materials and components. Its main characteristics are as follows: linear dynamic capacity ±10 kN; linear static capacity ±7 kN; torsional capacity ±100 Nm; stroke 60 mm; rotation ±135°, ±16 revolutions; load and torque weighing accuracy ±0.5 % of indicated load or torque, or ±0.005% of the load cell capacity; temperature chamber: -70 to +350°C.

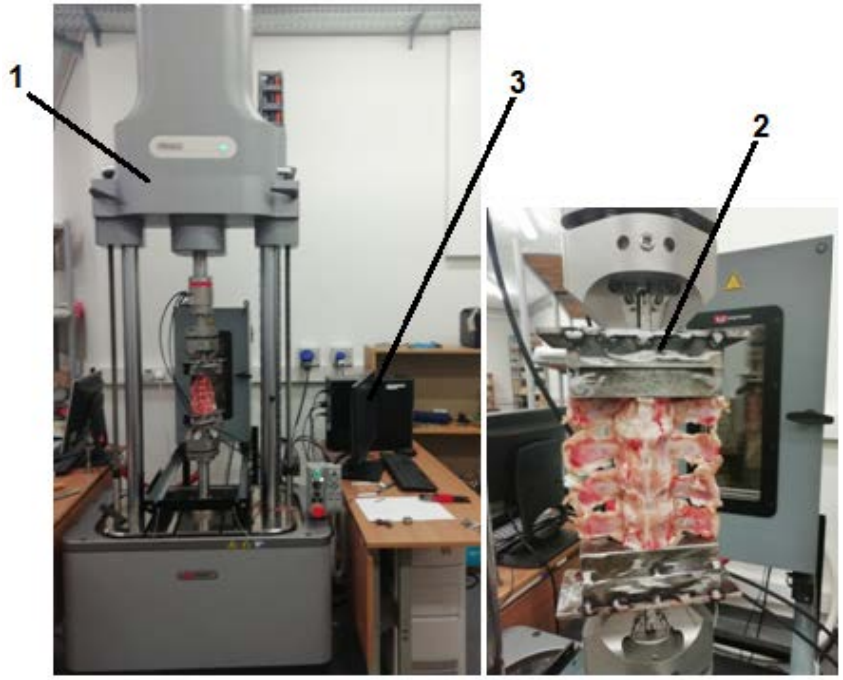

Fig. 3.6. Experimental setup: 1 – Linear-Torsion static and fatigue testing machine *Instron ElectroPuls E10000T*; 2 – specimen holder; 3 – PC

The specimens were loaded with 6,000 cycles of compressive load. Due to the comparatively long specimens and their curvature, the compressive load also forced them to flex, so specimens were loaded with coupled flexion and compression. The characteristics of the applied compressive loads are given in Table 3.3.

Table 3.3. Loading data

Specimen No.	1	2
Max cycle load, N	500	1000
Min cycle load, N	100	100
Loading frequency, Hz	2	5

Apparent deformations of intervertebral discs were seen during the loading cycle when, under maximum compression, the height of the discs decreased, and the discs themselves became more convex (Fig. 3.7). A significant decrease of the specimen height (Fig. 3.8) is observed during loading, mainly due to the loss of the fluid content within intervertebral discs.

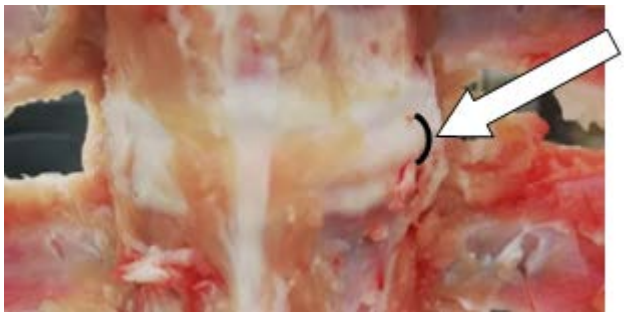

Fig. 3.7. Deformation of intervertebral disc during cyclic loading

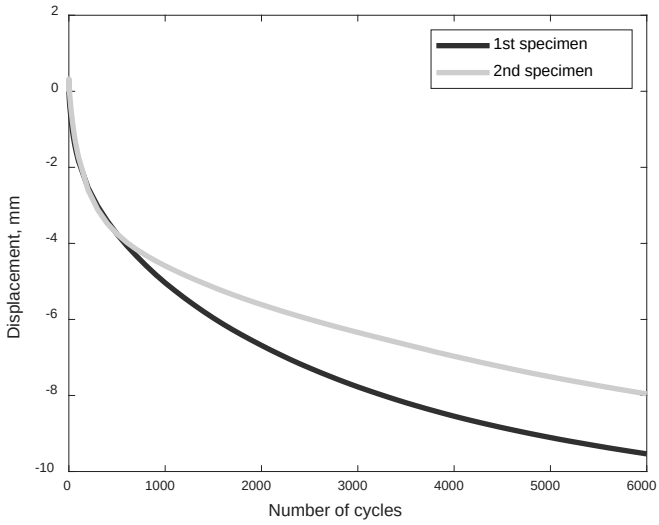

Fig. 3.8. Decrease of specimens' height

Repeated CT scanning and image processing

After cyclic loading, CT scanning was repeated in order to capture the current condition of the specimens. CT images were saved as *DICOM* (*Digital Imaging and Communications in Medicine*) files. As the sagittal plane of the spinal segments was not parallel to the vertical plane during the scanning, first of all, the *MATLAB* (*Mathworks Inc*.) code was used to rotate all the obtained CT images by 32°, while other information contained in these files was preserved. Then, the CT images were processed with *Sante DICOM Viewer 3D Pro* (*SanteSoft LTD*) software, and the sagittal sections of the specimens were created and analysed (Fig. 3.9).

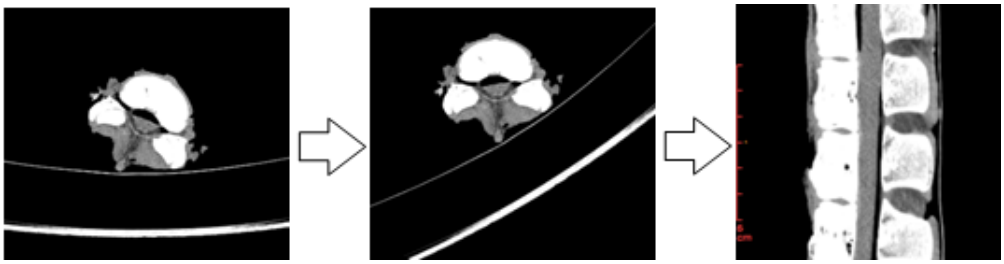

Fig. 3.9. Scheme of *DICOM* images processing: original image (left), rotated image (middle), midsagittal section of the specimen (right)

Midsagittal sections of CT scans of the first specimen are given in Fig. 3.10, and sections of the second specimen are given in Fig. 3.11. No obvious damage to the specimens was observed when comparing the images before and after loading. The anterior and posterior lines of vertebral columns remained smooth and intact. Also, no displacement of any vertebra over any other vertebra that is common due the degenerative disc disease is seen. The condition of the vertebra was observed by changing the software setting to the bone level window, and no fractures of the bones were observed.

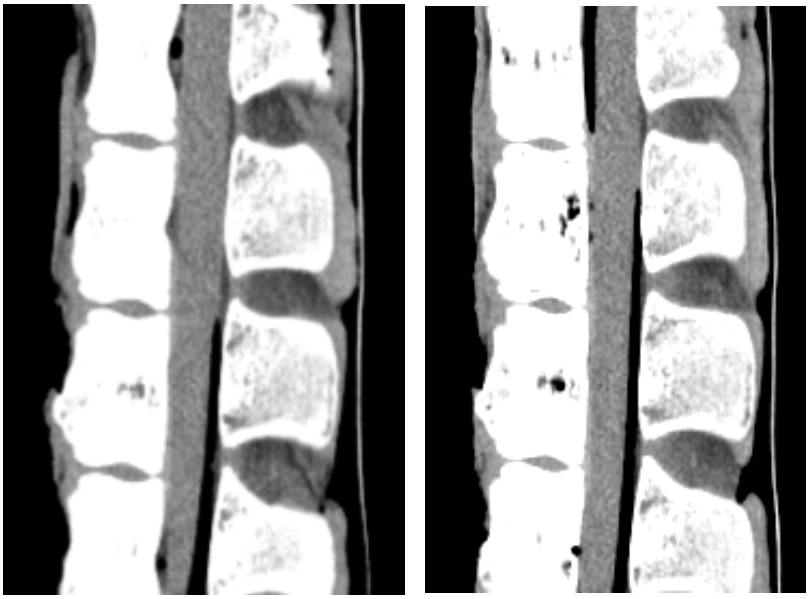

Fig. 3.10. Comparison of 1st specimen CT scans: before loading (left) and after loading (right)

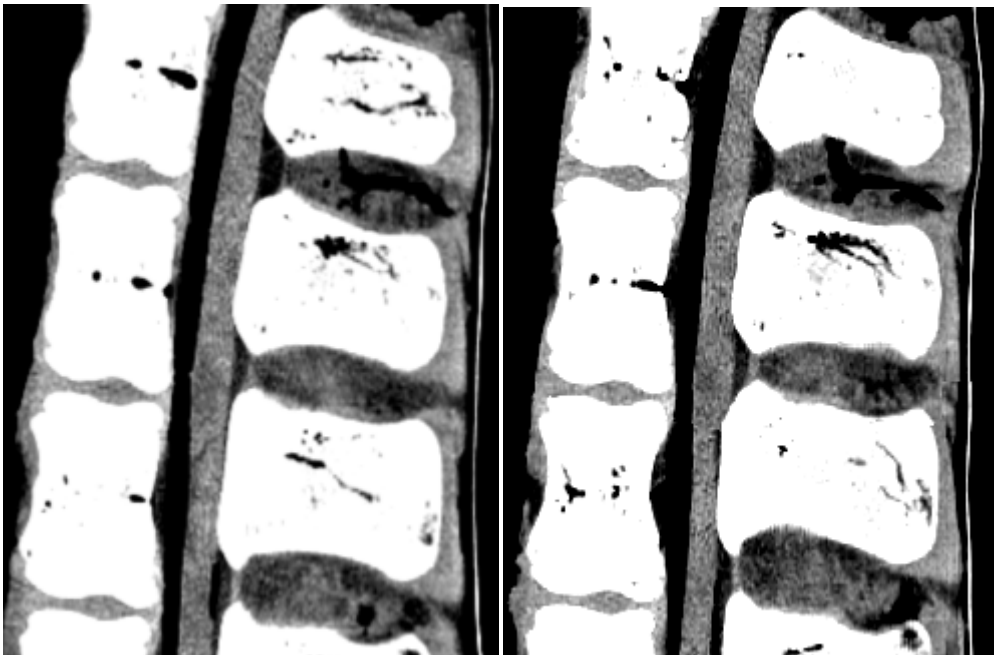

Fig. 3.11. Comparison of 2nd specimen CT scans: before loading (left) and after loading (right)

The height and the section area of the discs before and after loading were measured in the midsagittal section view. The height of the discs was measured at five locations of each intervertebral disc (Fig. 3.12). The results of the averaged values of these measurements are summarised in Table 3.4. One-way *ANOVA* (analysis of variance) was used for the statistical analysis of geometrical changes of the discs. There is a statistically significant difference between the differences of intervertebral disc heights before and after loading in both the first specimen ($p = 0.0224$) and the second specimen ($p = 0.0155$) with the lowest disc of both specimens decreasing the most and obviously losing the highest water content. The positive change of the middle disc of the fist specimen was found as, at three out of five measuring locations of this disc, increases of the height after loading were found. It may be explained by residual angular displacement of the vertebrae connected by this intervertebral disc.

Changes of the cross-sectional area also demonstrate the same tendency: the cross-sectional area of the lowest disc decreased the most. The increase of the cross-sectional area of the middle intervertebral disc of the first specimen may most likely be explained by the same reason as the increase of the height of this disc.

The results of the measurement of the changes of intervertebral discs after cyclic loading show that, even in short specimens of three sequenced intervertebral discs, the lowest discs are affected the most.

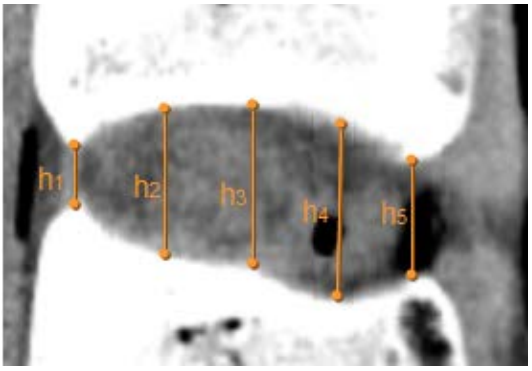

Fig. 3.12. Locations of measurement of intervertebral disc height

Table 3.4. Changes of disc height and section area ("–" represents the reduction of disc height Δh or cross-sectional area ΔA)

Disc	Δh, 1st spec., mm	Δh, 2nd spec., mm	ΔA, 1st spec., mm^2	ΔA, 2nd spec., mm^2
Upper	-0.508	-0.119	0	-0.100
Middle	0.242	-0.545	0.260	-0.050
Lower	-2.230	-2.005	-0.120	-0.400

3.3. Experimental investigation of short-term dynamic loading

The purpose of this study is to investigate the influence of short-term dynamic loading on functional units of the spine.

Six specimens of porcine spine functional units (2 adjacent vertebrae and the intervertebral disc between them) were separate from spinal columns at the zones of intervertebral discs above and below the functional units, placed in plastic bags to decrease dehydration and environmental influence and stored at -20°C. Before testing, they were thawed in 0.9% (0.15 mol/l) saline overnight in a refrigerator (+4°C) to allow rehydration. Before testing, each functional unit was placed in specimen holders which were inserted into the testing machine (Fig. 3.13).

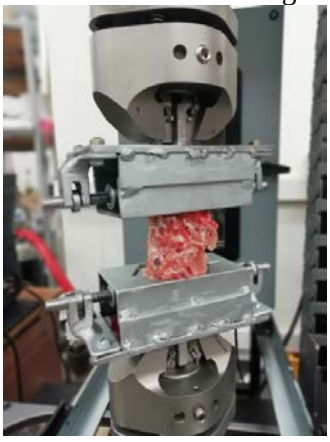

Fig. 3.13. Spinal functional unit placed in holders

The full experimental study of porcine functional units consisted of four stages (Fig. 3.14) in order to combine investigations of short term dynamic loading and cyclic compression into one study due to the limited number of specimens. As short-term dynamic loading of each specimen consisted only of 400 cycles and was significantly shorter than the cyclic compression (Stage 3) of 10,000 cycles, its influence on the results of cyclic compression may be neglected. At the beginning of the experiment, the specimens were preloaded with quasistatic compressive load for 10 minutes. After that, the specimens were impacted by 100 cycles of short-term loading with frequencies of 5, 10, 15 and 20 Hz. Then, the specimens were loaded with 10,000 cycles of compressive force, and, finally, short term cyclic loading with frequencies of 5, 10, 15 and 20 Hz was repeated. The complete loading data of each specimen is given in Table 3.5.

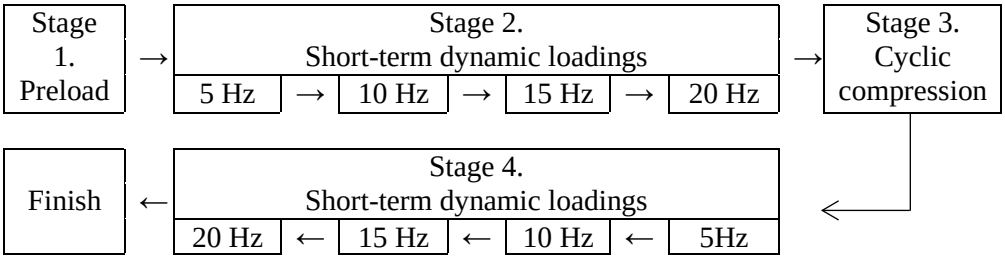

Fig. 3.14. Sequence of the experiment

Table 3.5. Loading data

Stage	I	II and IV				III		
Specimen No.	all	all				1	2	3
Number of cycles	60	100	100	100	100	10000		
Loading frequency, Hz	0.1	5	10	15	20	2	8	8
Mean cycle load, N	300	300	300	300	300	300	300	650
Max cycle load, N	320	500	500	500	500	500	500	1000
Min cycle load, N	280	100	100	100	100	100	100	300

In this section, the results of short-term dynamic loading are analysed. Detailed results of cyclic compression are given in Section 3.4.

The average decrease of the intervertebral disc height prior to cyclic compression during short term dynamic loading (loading stage II) is given in Fig. 3.15. The average loss of the intervertebral disc height after 5 Hz short term dynamic loading is 0.1963 ± 0,0962 mm, after 10 Hz loading is 0.2592 ± 0.1591 mm, after 15 Hz loading stands at 0.2314 ± 0.1294 mm, and after 20 Hz loading equals to 0.3138 ± 0.1409 mm.

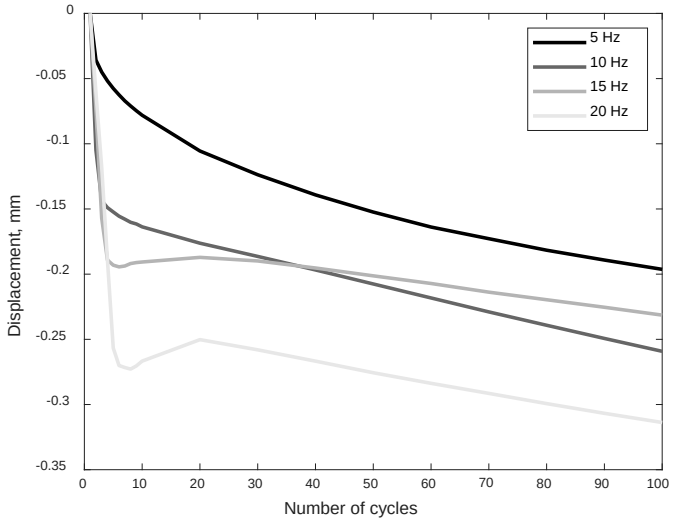

Fig. 3.15. Average decrease of intervertebral disc height (loading stage II)

The average decrease of the intervertebral disc height after cyclic compression during short term dynamic loading (loading stage IV) is given in Fig. 3.16. The average loss of the intervertebral disc height after 5 Hz short term dynamic loading is 0.1164 ± 0.0187 mm, after 10 Hz loading is 0.0978 ± 0.0366 mm, after 15 Hz loading stands at 0.1205 ± 0.04339 mm, and after 20 Hz loading equals to 0.1388 ± 0.0460 mm.

Loss of water during cyclic compression and no opportunity for rehydration may explain a decrease of the loss of the intervertebral disc height during short term loading after the discs were cyclically compressed.

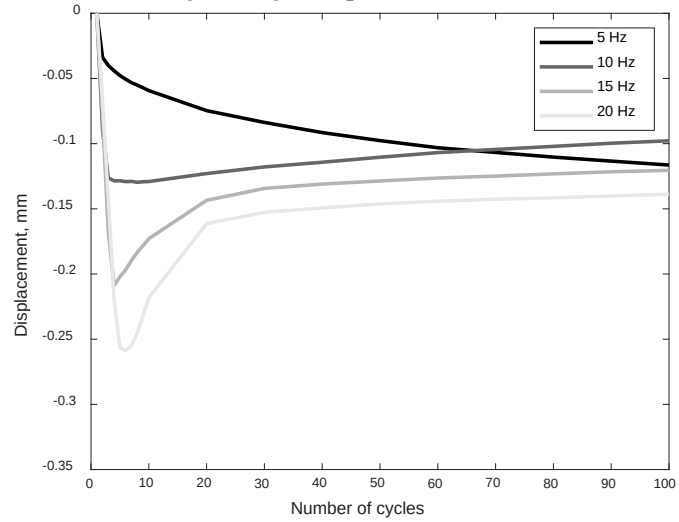

Fig. 3.16. Average decrease of intervertebral disc height (loading stage IV)

8 Hz 500 N cyclic compression leads to the smallest decrease of the intervertebral disc height during short term loading (Fig. 3.17) independently of the short-term loading frequency. The loss of the intervertebral disc height is almost equal when the specimens previously loaded with 2 Hz 500 N and 8 Hz 1000 N compression were short-term loaded with a frequency of 5 Hz. In other cases of short-term loading, the previous compression of 2 Hz and 500 N leads to the biggest loss of the intervertebral disc height.

A comparison of the influence of previous cyclic compression frequency on the changes of the intervertebral disc height during short term dynamic loading is shown in Fig. 3.18. Both specimens were loaded for 10,000 cycles with the maximum compression of 500 N. In all the cases of short-term dynamic loading, a bigger loss of intervertebral disc height is seen in the specimen previously loaded with 2 Hz frequency.

A comparison of the influence of the magnitude of previous cyclic compression on the changes of intervertebral disc height during short term dynamic loading is shown in Fig. 3.19. Both specimens were loaded for 10,000 cycles with a frequency of 8 Hz. In all the cases of short-term dynamic loading, previous loading of 1,000 N leads to a bigger loss of intervertebral disc height during short-term dynamic loading.

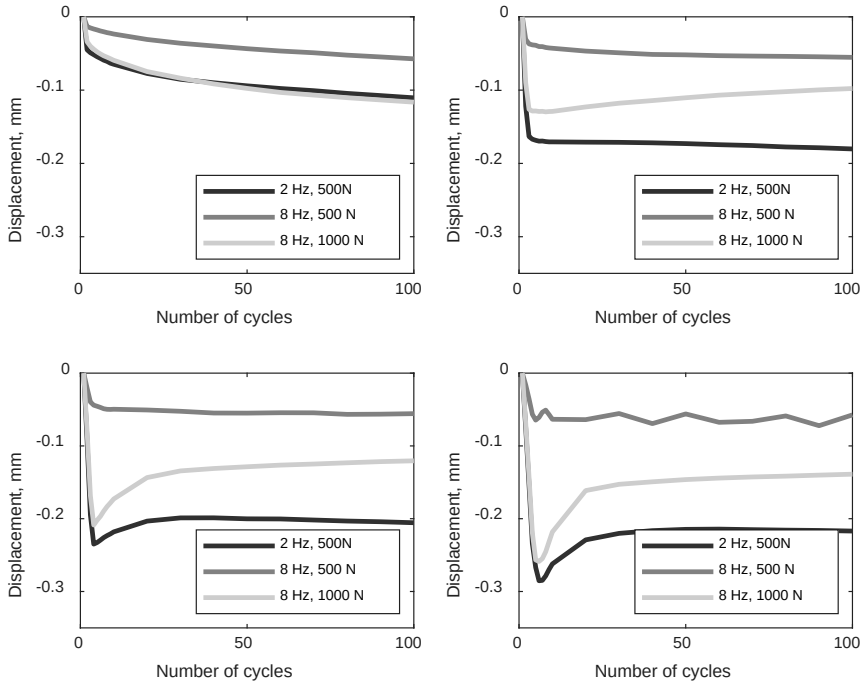

Fig. 3.17. Decrease of intervertebral disc height during short-term dynamic loading depending on previous compressive loading. Short-term loading frequency: 5Hz (top left); 10 Hz (top right); 15 Hz (bottom left); 20 Hz (bottom right)

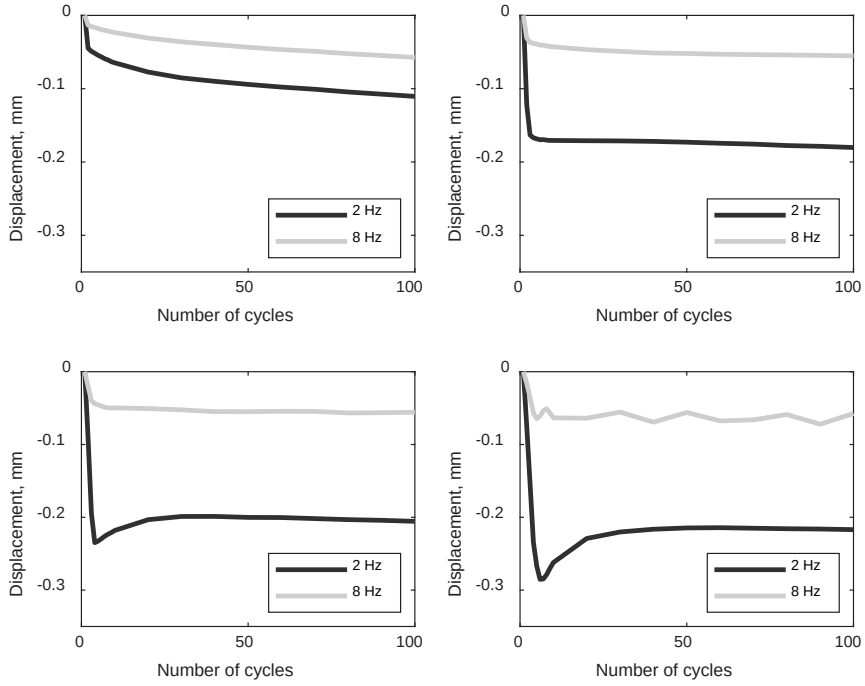

Fig. 3.18. Decrease of intervertebral disc height during short-term dynamic loading depending on the frequency of previous compressive loading Short-term loading frequency: 5Hz (top left); 10 Hz (top right); 15 Hz (bottom left); 20 Hz (bottom right)

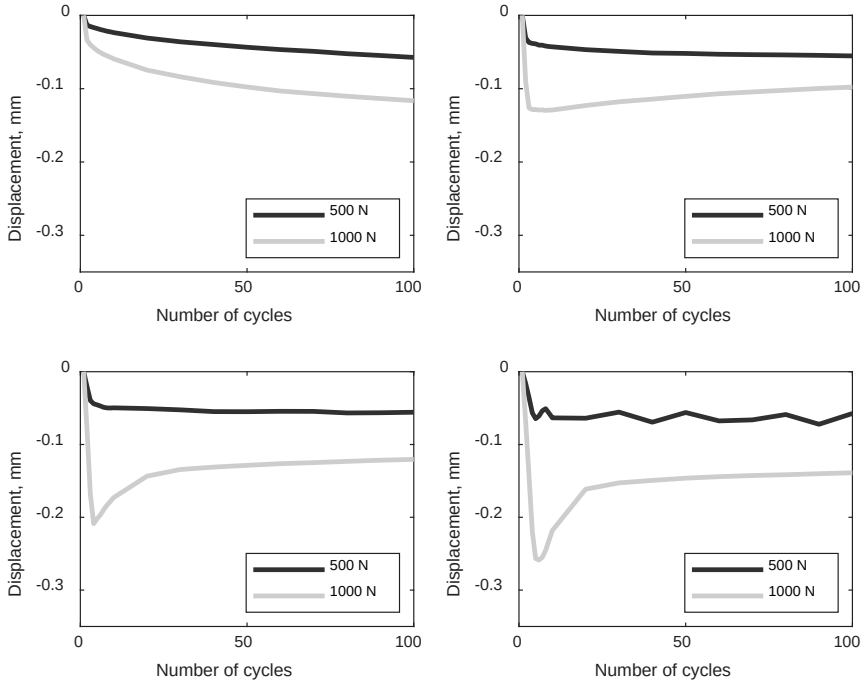

Fig. 3.19. Decrease of intervertebral disc height during short-term dynamic loading depending on the maximal magnitude of previous compressive loading. Short-term loading frequency: 5Hz (top left); 10 Hz (top right); 15 Hz (bottom left); 20 Hz (bottom right)

3.4. Experimental investigation of cyclic compression

In this section, the results of compressive cyclic loading (stage III) are discussed. The loss of intervertebral disc height after cyclic loading is represented in Fig. 3.20. A compressive load of 2 Hz frequency and 500 N amplitude leads to the highest loss of the intervertebral disc height which is equal to 6.6948 mm. The loss due to 8 Hz and 1000 N compression is equal to 3.0393 mm, and the loss due to 8 Hz and 500 N compression is 1.0498 mm.

After the loading, each specimen was cut through the intervertebral disc. Also, a not loaded specimen was cut as the control unit. The cross-sections of these specimens are given in Fig. 3.21. No obvious signs of intervertebral disc herniation are seen.

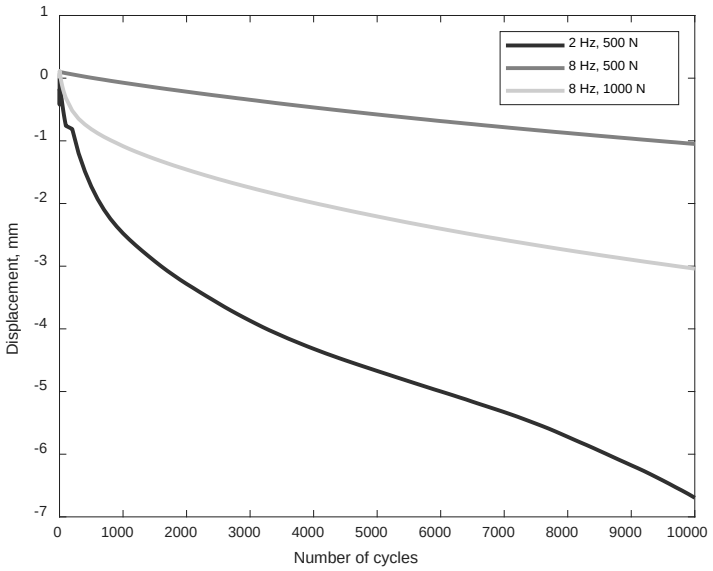

Fig. 3.20. Decrease of specimen height during cyclic compression

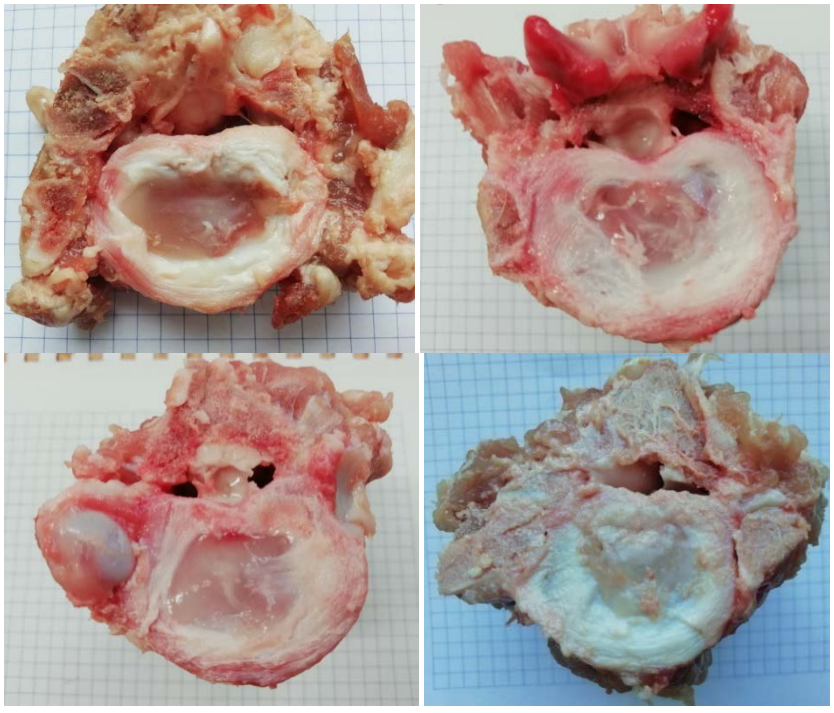

Fig. 3.21. Horizontal cross-sections of specimens: without loading (top left); 500 N 2 Hz cyclic loading (top right); 500 N 8 Hz cyclic loading (bottom left); 1000 N 8 Hz cyclic loading (bottom right)

3.5. Section conclusions

A healthy spine should be considered as an overdamped or a critically damped system as only such a system can secure the stability of the spine. Sufficiently hydrated intervertebral discs as well as intact ligaments and strong back muscles are the factors that determine the spine stability.

Coupled cyclic loading of 500 N or 1000 N compression and flexion did not induce intervertebral disc herniation or any other apparent damage to spine specimens. The maximal height loss was observed in the lowest intervertebral discs of the specimens. This once again confirms that the lower part of the spine, such as intervertebral discs L4-L5 and L5-S1, is the least prone to injuries and degeneration due to disturbed nutrition and the loss of the water content.

The results of the experimental investigation of short-term dynamic loading show that the higher magnitude of the previous compression load leads to a higher loss of the intervertebral disc height during short-term dynamic loading. However, in this study, the previous cyclic compression frequency of 2 Hz leads to a higher loss of the intervertebral disc height than the frequency of 8 Hz. In cases of short-term dynamic loading, the loading frequency of 20 Hz leads to a higher loss of the intervertebral disc height than frequencies of 5 Hz, 10 Hz and 15 Hz. These results suggest that different cyclic loading frequencies exert a different effect on the intervertebral disc, and that it is likely that higher frequencies do not necessarily result in a higher loss of the disc height or other residual changes; established the optimal frequencies as well as the optimal loading time should be established in the future in order to improve the disc condition.

A cyclic compression of 500 N and 1000 N did not cause intervertebral disc herniation or other significant damage during 10,000 cycles.

4. DEVELOPMENT OF NONINVASIVE LUMBAR SPINE REHABILITATION EQUIPMENT

4.1. Prototype of spinal actuator

As it was mentioned in the literature review, sufficient spine stability reduces the risk of low back pain and other spinal diseases. The deep layer back muscles are responsible for spinal stability, and these muscles are difficult to target during the usual training routine. Moreover, encouraging results of the fluid flow modelling within intervertebral discs during lateral bending allowed to formulate a hypothesis that lateral bending exercise could help to improve the nutrition of intervertebral discs as well as to strengthen the deep layer back muscles, especially multifidi. Therefore, a spinal actuator (Fig. 4.1) that helps to perform lateral bending moves has been developed and patented (A device for improving nutrition of intervertebral discs and strengthening deep layer back muscles: Lithuanian patent application number 2017 515, patent number 6585) at KTU Institute of Mechatronics. It consists of an oscillating plate (1) which allows oscillations with the maximum amplitude of 30 degrees, a sliding and rotating circle (2) is used to adjust the spinal actuator to suit the subject's height and to reduce friction during the exercise, sliding foot supports/pedals (3) which could be used to include the leg muscles into the exercise, a mechanism to regulate the resistance and amplitude (4), and an electromechanical gear (5) mounted on a stiff frame (6).

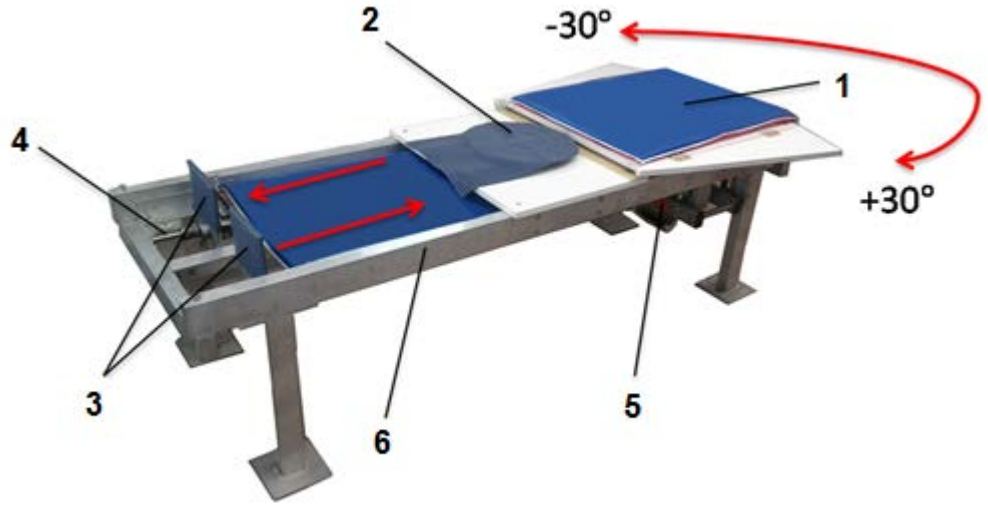

Fig. 4.1. Prototype of spinal actuator (Lithuanian patent number 6585): 1 – oscillating plate; 2 – sliding and rotating circle; 3 – pedals; 4 – electromechanical gear; 5 – frame; 6 – removable springs

A detailed drawing of the spinal actuator is given in Fig. 4.2. The oscillating plate consists of three parts: the central square part (its view is obstructed in Fig. 4.2), and two triangular side plates (1) which may be folded for easier transportation

of the spinal actuator. The movement of the oscillating plate is secured by thrust bearing (2). The bottom surface of the oscillating plate is covered by sheet metal and supported by 4 steel wheels (3) mounted on the frame (4). This configuration allows ensuring the stability and lower friction between the moving parts of the device. The rotating circle (5) consists of two circles of the same type. The bottom circle is fixed on a ball bearing telescopic slide (6) that is mounted on the supporting plate (7) and allows adjusting the rotating circle's position according to the subject's height. The upper circle can rotate with respect to the bottom one; it reduces friction during the movements. The pedals (8) are connected with the oscillating plate by rods (9) that slide in the guide rails (10), and their linear displacement depends on the angular displacement of the oscillating plate; that is why, regulators of the maximum allowable rotation (11) are mounted next to the pedals as they limit the maximum rotation of the oscillating plate by limiting the linear movement of the pedals. The electromechanical gear (12) for creating passive moves is mounted on the frame and can be activated by a handle (13) and a lifting mechanism (14); it is connected to the oscillating plate by a crankshaft mechanism (15).

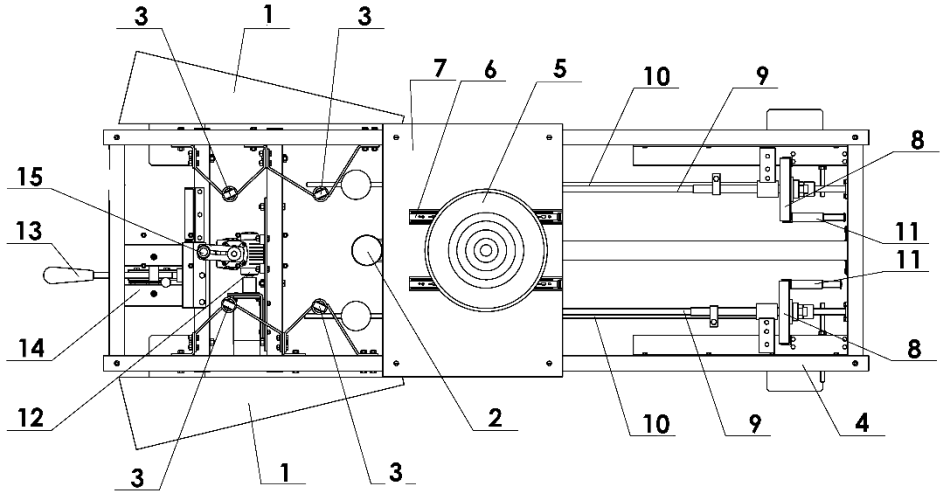

Fig. 4.2. Top view of the spinal actuator

Lateral bending moves to the right and left are produced by the trunk muscles while lying on the back with the thoracic spine placed on the oscillating plate and the pelvis placed on the sliding and rotating circle. This position ensures that lateral bending moves are performed in the frontal plane and that the spine is protected from combined loadings of lateral bending and flexion/extension which induce higher shear stress values in intervertebral discs. Also, a handle could be mounted on the oscillating plate in order to fixate the position of the arms during the exercise. This training device is versatile and can be adapted to fit various patients' needs. The subject's legs can be placed on the stationary frame when more loading on the trunk muscles is preferred, or used to pedal the foot supports in order to include leg muscles into the exercise and to decrease the loading on the trunk muscles.

Removable springs of various degrees of stiffness are mounted between the pedals and the frame and are used to provide a variable resistance load. When it is necessary for training, rehabilitation or research purposes, electromechanical gear can also be connected to the mechanism of the oscillating plate and used to generate passive lateral bending moves with a controlled amplitude and velocity. The spinal actuator allows not only to set the preferred value of the maximal lateral bending amplitude before starting the exercise, but also to measure the bending amplitude during each lateral bending cycle. This data is valuable for the evaluation of the subject's condition and monitoring of their progress.

4.2. Experimental study of spinal actuator's influence on trunk muscles

A study to investigate the presumable benefits of the lateral bending exercise performed on the spinal actuator was conducted by measuring the activity (electric signals created within the muscles) of four trunk muscles: internal oblique, transversus abdominis, multifidus and lumbar erector spinae. The internal oblique muscle forms the second layer of lateral abdominals, supports the abdominal wall, helps to raise pressure in the abdominal area, and, together with other muscles, rotates the trunk. Transverse abdominis is the deepest of the abdominal muscles and also supports the abdominal wall, helps to raise pressure in the abdominal area and to expel air during forced exhalation; moreover, one of its main functions is to stabilise the spine during movements. Multifidi muscles are a thick and most developed group of fibres in the lumbosacral region and provide extension torque, support and stability to the spine. Lumbar erector spinae is an extensive group of deep layer back muscles which controls gross flexion/extension, lateral bending and rotation movements of the spine.

Twelve young healthy males with an average age of 21.8 ± 0.6 years, average height of 185.0 ± 5.2 cm, average mass of 80.7 ± 12.0 kg and with no history of spine disorders were included into this study. Written informed consent of participation was obtained from all the participants.

The electromyographic activity (EMG) of left and right sides internal oblique, transverse abdominis, multifidus and lumbar erector spinae muscles was recorded with the telemetric EMG system *Telemyo 2400R G2* (*Noraxon USA, Inc*.) which has delivered in 16 analog output channels at a sampling frequency of 1500 Hz. The collected data was recorded and primarily processed with *Noraxon MR 3.8* software installed on a personal computer (Fig. 4.3).

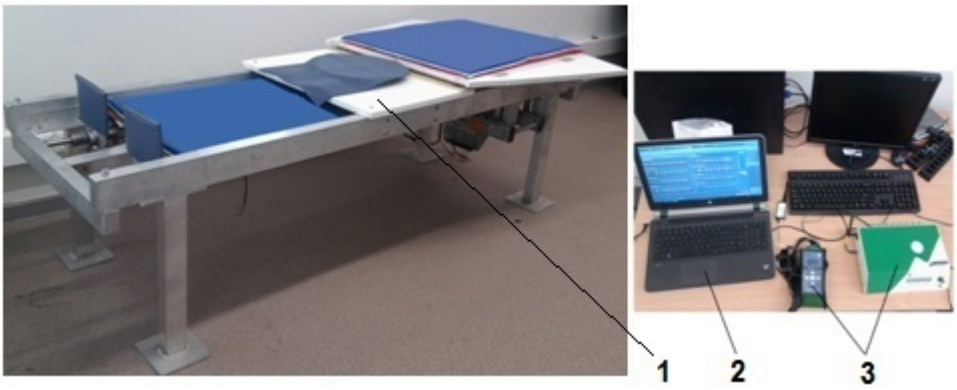

Fig. 4.3. Experimental setup: 1 – spinal actuator; 2 – PC; 3 – telemetry system *Telemyo 2400R G2*

During surface EMG, electric signals are measured by sensors placed on the skin above the muscles. Before disposable bipolar self-adhesive Ag/AgCl surface electrodes (*FIAB F3010*, 21 x 41 mm) were applied, the skin was shaved and cleaned with alcohol in order to reduce skin impedance. According to recommendations by *SENIAM* [100], the lumbar erector spinae electrodes were placed at a 2 finger width laterally from the spinous process of L1, and multifidus electrodes were placed at the level of L5 spinous process and aligned with the line extending from caudal tip posterior superior spina iliaca to the interspace between L1 and L2. According to a recommendation of McCook *et al*. [101], electrodes for the measurement of transverse abdominis were placed midway between the ribcage and the iliac crest and adjusted by palpation. Electrodes for the measurement of the internal oblique were placed at 3 cm medial and superior to the anterior superior iliac spine as recommended by Hodges and Richardson [102].

The lateral bending exercise was performed when commonly lying on a mat without any assisting equipment and on the spinal actuator in order to compare the influence of the spinal actuator on the activity of the trunk muscles. Foremost, the participants were asked to lie down on the mat in the supine position with arms raised above their head and bent at elbows. Then, the maximum voluntary isometric contraction (MVIC) was measured in order to normalise the EMG amplitudes during lateral bending exercises. While still lying on the mat, the participants performed seven cycles of lateral bending movements from the neutral position to the right, then to the left and back to the neutral position with the maximum comfortable amplitude (Fig. 4.4). After this, the participants were asked to lie down on the spinal actuator in the supine position and were instructed to place the thoracic spine on the oscillating plate, the pelvis on the sliding and rotating circle and the legs on the stationary frame, to raise their arms bent at elbows over the head and to perform the same seven cycles of lateral bending movements with the maximum comfortable amplitude (Fig. 4.5).

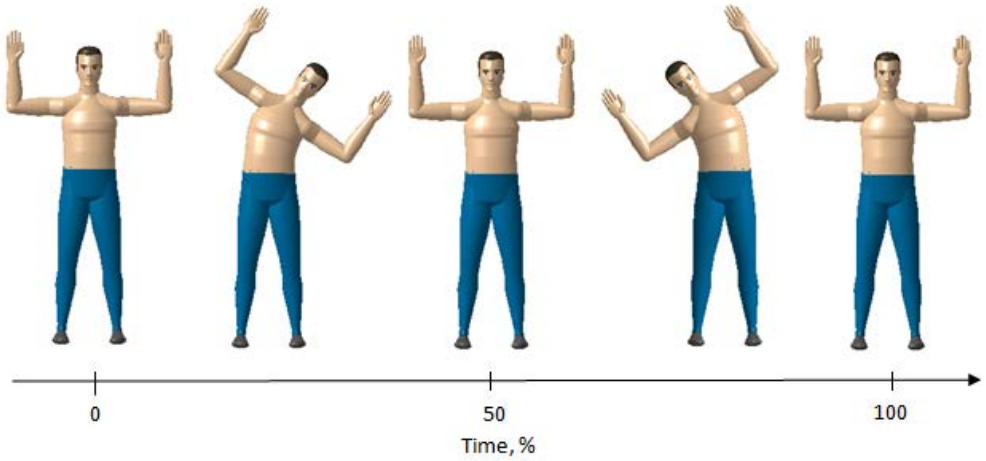

Fig. 4.4. A cycle of lateral bending exercise

Fig. 4.5. Subject performing lateral bending moves on spinal actuator with sensors placed on the skin above the muscles

The recorded raw EMG data was rectified, smoothed by root-mean-square (RMS) amplitude values, computed by using a 100 ms window, and bandpass filtered from 10 to 500 Hz. Then five least perturbed lateral bending cycles of each participant performed on the mat and five least perturbed lateral bending cycles of each participant performed on the spinal actuator were chosen for further statistical analysis which was performed by using *MATLAB* (*The MathWorks, Inc*.) software. The EMG data of trunk lateral bending cycles was time normalised and expressed as the percentage of MVIC values for each muscle.

As the Shapiro-Wilk normality test showed that the collected data is not normally distributed, the Friedman test with a significance level of 5% was chosen

to test for differences between the paired groups as it is a non-parametric alternative to the one-way ANOVA (analysis of variance) analysis.

A comparison of four trunk muscles EMG activity when lateral bending is performed on the mat and the spinal actuator is shown in Fig. 4.6, and mean muscle activity values (together with standard errors) are given in Table 4.1.

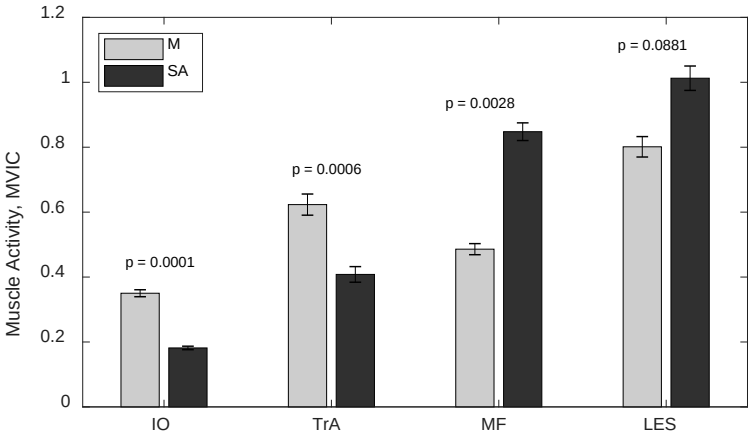

Fig. 4.6. Mean values of internal oblique (IO), transversus abdominis (TrA), multifidus (MF) and lumbar erector spinae (LES) muscle activity during lateral bending exercise on the mat (M) and on the spinal actuator (SA)

Table 4.1. Muscle activity (Mean ± SE, MVIC)

Muscle	IO	TrA	MF	LES
Left side, mat	0.3442 ± 0.0054	0.7164 ± 0.0209	0.4895 ± 0.0233	0.8272 ± 0.0205
Right side, mat	0.3496 ± 0.0055	0.5124 ± 0.0106	0.4757 ± 0.0191	0.7440 ± 0.0309
Total, mat	0.3469 ± 0.0055	0.6144 ± 0.0166	0.4826 ± 0.0087	0.7856 ± 0.0160
Left side, actuator	0.1605 ± 0.0019	0.5143 ± 0.0164	0.7542 ± 0.0134	1.1664 ± 0.0239
Right side, actuator	0.2147 ± 0.0034	0.3055 ± 0.0054	0.8835 ± 0.0143	0.8106 ± 0.0125
Total, actuator	0.1876 ± 0.0027	0.4099 ± 0.0123	0.8189 ± 0.0139	0.9885 ± 0.0192

The analysis of EMG data reveals that there is a statistically significant difference ($p = 0.025$) between the mean values of the internal oblique, transverse abdominis, multifidus and lumbar erector spinae muscle activities during lateral bending on the mat, but there is no significant difference between mean values of these four muscles activities when left ($p = 0.138$) and right ($p = 0.093$) sides are analysed separately. Also, there is a statistically significant difference ($p < 0.001$) between the mean values of internal oblique, transverse abdominis, multifidus and lumbar erector spinae muscle activities during lateral bending on the spinal actuator as well as when the left ($p = 0.007$) and right ($p < 0.001$) sides are analysed separately. This means that when the lateral bending exercise is performed on the mat, all the four investigated muscles are activated more uniformly and that the lateral bending exercise on the spinal actuator actually targets multifidus and lumbar erector spinae muscles.

Detailed descriptions of the activities of each muscle are given in the following paragraphs.

Muscle activity of internal oblique

The average internal oblique muscle activity during the lateral bending exercise on the mat is 35% of MVIC. There is no statistically significant difference ($p = 1$) between the left and right side values of the activity of the internal oblique muscle when the lateral bending exercise is performed on the mat. The mean muscle activity of internal oblique decreases by 1.85 times to the value of 19% when the exercise is performed on the spinal actuator. Statistically significant differences exist between the left side values ($p = 0.0067$), the right side values ($p = 0.0067$) and the total values ($p = 0.0001$) of the internal oblique muscle activity when comparing the two types of exercises, but the tendency that there is no statistically significant difference ($p = 0.0833$) between the left and right side values of the internal oblique muscle activity remains when the lateral bending exercise is performed on the spinal actuator. The activity of the internal oblique muscle has distinct left and right side activity peaks when the exercise is performed on the mat while the exercise on the spinal actuator flattens the curves, and the changes of the muscle activity during one exercise cycle are almost inconspicuous (Fig. 4.7).

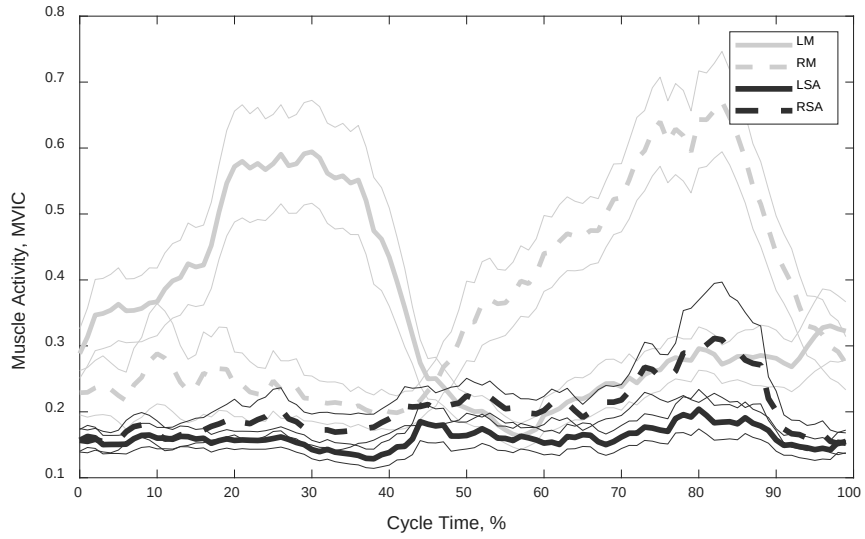

Fig. 4.7. Activity of internal oblique muscles. LM – left side, exercise on the mat; RM – right side, exercise on the mat; LSA – left side, exercise on the spinal actuator; RSA – right side, exercise on the spinal actuator. Thicker lines show the mean values; thinner lines represent standard errors

Muscle activity of transverse abdominis

The average activity of the transverse abdominis muscle during the lateral bending exercise on the mat is 61% of MVIC. There is no statistically significant difference ($p = 0.5637$) between the left and right side values of the transverse

abdominis muscle activity when the lateral bending exercise is performed on the mat. The mean muscle activity of transverse abdominis also decreases by 1.50 times to the value of 41% MVIC when the exercise is performed on the spinal actuator. Statistically significant differences exist between the left side values ($p = 0.0348$), the right side values ($p = 0.0067$) and the total values ($p = 0.0006$) of the transverse abdominis muscle activity when comparing the two types of exercises, but the tendency that there is no statistically significant difference ($p = 0.2482$) between the left and right side values of the transverse abdominis muscle activity remains when the exercise is performed on the spinal actuator. The activity of the transverse abdominis muscle exhibits distinct left and right side activity peaks when the exercise is performed on the mat, and, while the peak values decrease when the exercise is performed on the spinal actuator, they remain distinct (Fig. 4.8).

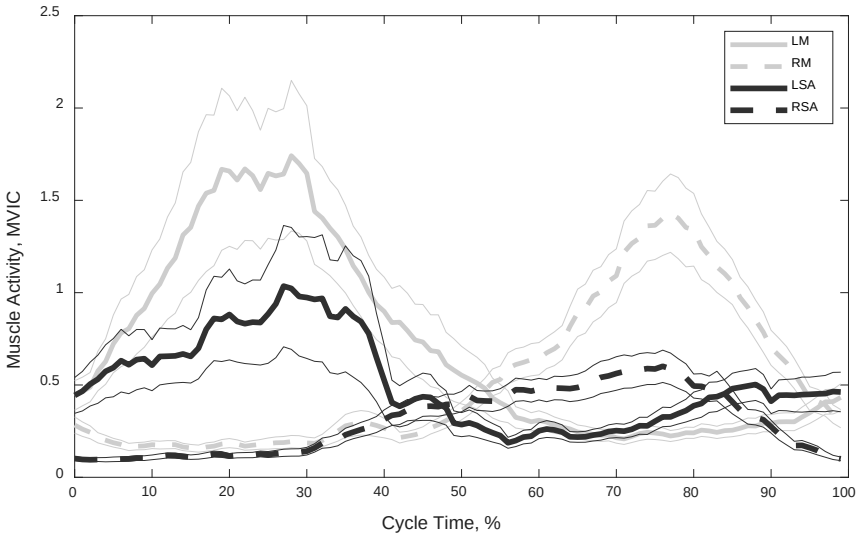

Fig. 4.8. Activity of transversus abdominis muscles. LM – left side, exercise on the mat; RM – right side, exercise on the mat; LSA – left side, exercise on the spinal actuator; RSA – right side, exercise on the spinal actuator. Thicker lines show the mean values; thinner lines represent standard errors

Muscle activity of multifidus

The average activity of the multifidus muscle during the lateral bending exercise on the mat is 48% of MVIC. There is no statistically significant difference ($p = 0.0833$) between the left and right side values of the multifidus muscle activity when the lateral bending exercise is performed on the mat. However, to the contrary of the muscle activities of internal oblique and transverse abdominis, the mean muscle activity of multifidus increases by 1.70 times to the value of 82% MVIC when the lateral bending exercise is performed on the spinal actuator. Statistically significant differences exist between the left side values ($p = 0.0348$), the right side values ($p = 0.0348$) and the total values ($p = 0.0028$) of the multifidus muscle activity when comparing the two types of exercises, but the tendency that there is no

statistically significant difference (p = 0.0833) between the left and right side values of the multifidus muscle activity remains when the lateral bending exercise is performed on the spinal actuator. The activity of the multifidus muscle has distinct left and right side activity peaks when the exercise is performed on the mat. Although the peak values remain at the same level when the exercise is performed on the spinal actuator, the muscle activities remain at those peak values for longer time periods, the muscles of the respective side are activated to the maximum values almost immediatelly after the move to that side starts (before the spine reaches the straight position), and this leads to higher mean values of the multifidus activity during the cycle of the lateral bending exercise (Fig. 4.9).

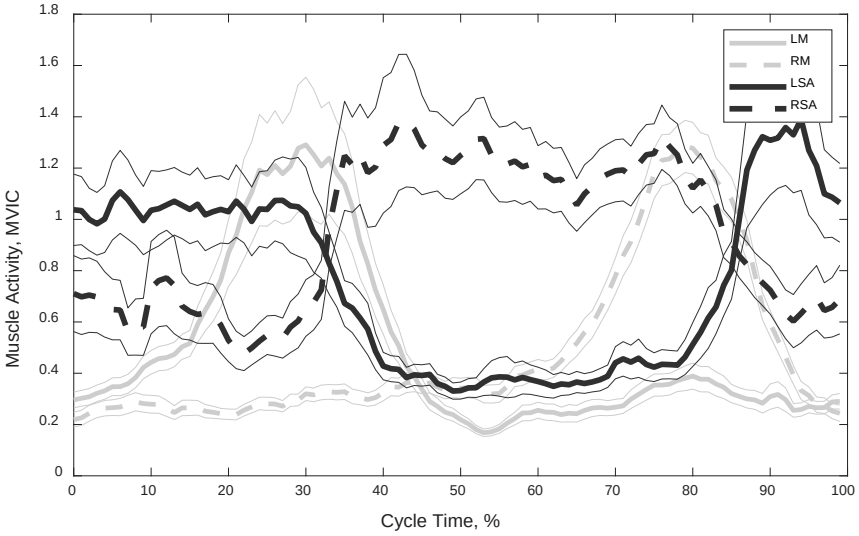

Fig. 4.9. Activity of multifidi muscles. LM – left side, exercise on the mat; RM – right side, exercise on the mat; LSA – left side, exercise on the spinal actuator; RSA – right side, exercise on the spinal actuator. Thicker lines show the mean values; thinner lines represent standard errors

Muscle activity of lumbar erector spinae

The average activity of the lumbar erector spinae muscle during the lateral bending exercise on the mat is 79% of MVIC. There is no statistically significant difference (p = 0.5637) between the left and right side values of the lumbar erector spinae muscle activity when the lateral bending exercise is performed on the mat. The muscle activity of lumbar erector spinae increases to the value of 99% MVIC when the exercise is performed on the spinal actuator, but the differences between the left side values (p = 0.3657), the right side values (p = 0.1317) and the total values (p = 0.0881) of the lumbar erector spinae muscle activity are not statistically significant when comparing the two types of exercises. The same tendency observed in all muscle activities remains, and there is no statistically significant difference (p = 0.2482) between the left and right side values of the lumbar erector spinae muscle activities when the lateral bending exercise is performed on the spinal actuator.

Lumbar erector spinae has distict left and right side activity peaks when the exercise is performed on the mat. When it is performed on the spinal actuator, the maximal values of the muscle activity are smaller, but the activation periods are longer, and, due to this reason, there is no significant diference between the mean values of the lumbar erector spinae muscle activity (Fig. 4.10).

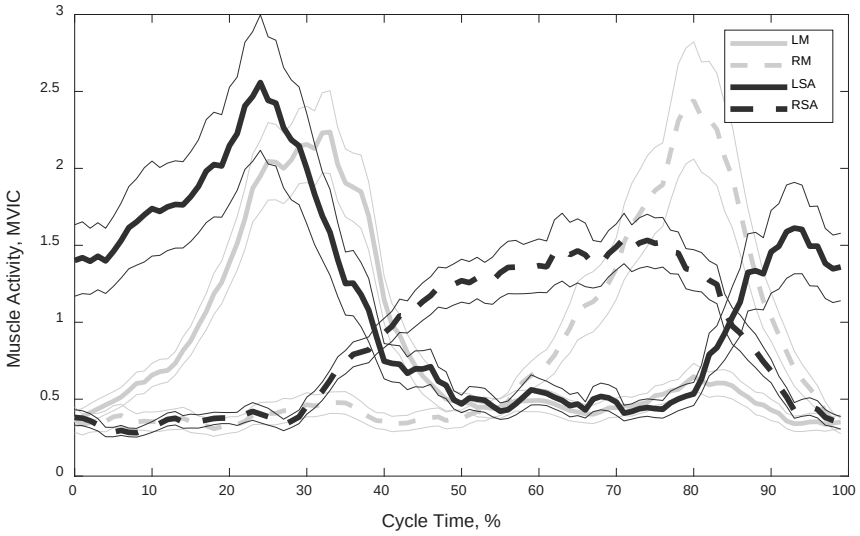

Fig. 4.10. Activity of lumbar erector spinae muscles. LM – left side, exercise on the mat; RM – right side, exercise on the mat; LSA – left side, exercise on the spinal actuator; RSA – right side, exercise on the spinal actuator. Thicker lines show the mean values; thinner lines represent standard errors

4.3. Experimental study comparing influence of lateral bending exercise with and without abdominal hollowing on trunk muscles

During the experimental study of the influence of the spinal actuator on the trunk muscles, the participants were asked to perform the lateral bending exercise with abdominal hollowing after they performed the standard lateral bending exercise on the spinal actuator in order to check the hypothesis that the exercise performed with abdominal hollowing may increase the activity of the trunk muscles.

The results of this study show that there is a statistically significant difference ($p = 0.007$) between the mean values of the internal oblique, transverse abdominis, multifidus and lumbar erector spinae muscle activities during lateral bending on the spinal actuator with abdominal hollowing, but there is no significant difference between the mean values of the internal oblique, transverse abdominis, multifidus and lumbar erector spinae activities when the left ($p = 0.2407$) and right ($p = 0.7291$) sides are analysed separately.

A comparison of the EMG activities of the four trunk muscles when lateral bending is performed on the spinal actuator without and with abdominal hollowing is shown in Fig. 4.11, and the mean muscle activity values are given in Table 4.2.

More detailed descriptions of the activities of each muscle are given in the following paragraphs.

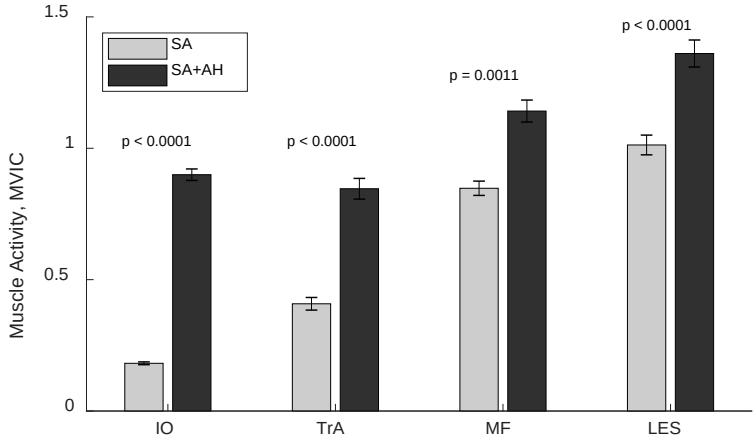

Fig. 4.11. Mean values of internal oblique (IO), transversus abdominis (TrA), multifidus (MF) and lumbar erector spinae (LES) muscle activity during lateral bending exercise on the spinal actuator (SA) and the spinal actuator with abdominal hollowing (SA+AH)

Table 4.2. Muscle activity (Mean ± SE, MVIC)

Muscle	IO	TrA	MF	LES
Left side, SA + AH	0.8460 ± 0.0092	1.0303 ± 0.0270	1.0479 ± 0.0233	1.2540 ± 0.0205
Right side, SA + AH	0.9742 ± 0.0128	0.6327 ± 0.0083	1.1561 ± 0.0191	1.3825 ± 0.0309
Total, SA + AH	0.9101 ± 0.0111	0.8315 ± 0.0201	1.1020 ± 0.0214	1.3183 ± 0.0263

Muscle activity of internal oblique

The average activity of the internal oblique muscle during the lateral bending exercise on the spinal actuator with abdominal hollowing is 91% of MVIC. There is no statistically significant difference ($p = 0.5637$) between the left and right side values of the internal oblique muscle activity when the lateral bending exercise is performed on the spinal actuator with abdominal hollowing. The average muscle activity of internal oblique increases by 4.85 times when the exercise with abdominal hollowing is performed on the spinal actuator compared to the exercise without abdominal hollowing. Statistically significant differences exist between the left side values ($p = 0.0005$), the right side values ($p = 0.0005$) and the total values ($p < 0.0001$) of the internal oblique muscle activity when the exercise is performed on the spinal actuator without and with abdominal hollowing. The activity of the internal oblique muscle maintains a similar activity pattern when the exercise is performed on the spinal actuator without and with abdominal hollowing, but the activity values with abdominal hollowing, as it was mentioned above, are significantly higher and are more widely spread (Fig. 4.12).

It also should be mentioned that the muscle activity of internal oblique during the lateral bending exercise on the spinal actuator is 2.62 times higher than during the lateral bending exercise on the mat, thus, although, the lateral bending exercise on the spinal actuator reduces the activity of internal oblique by 1.85 times (as presented in Section 4.2), the exercise on the spinal actuator with abdominal hollowing may increase the activity of internal oblique even when comparing with the activity values during the exercise without the assisting equipment.

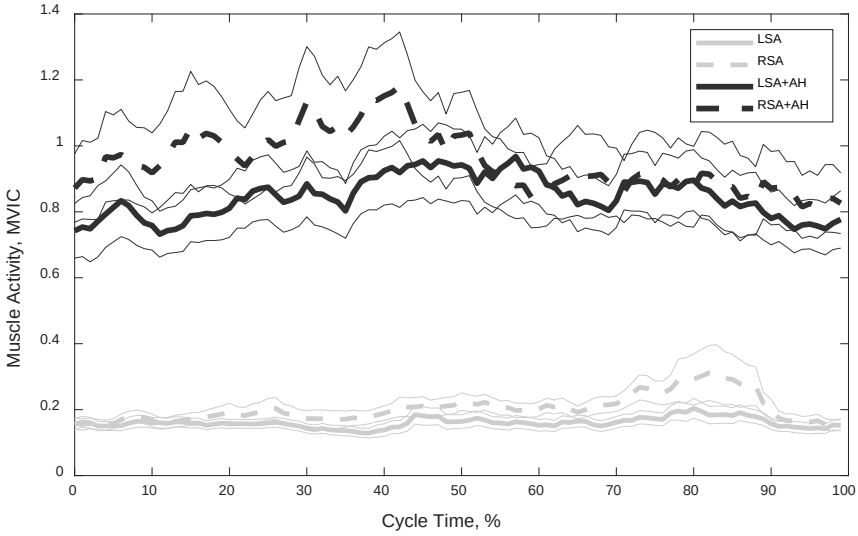

Fig. 4.12. Activity of internal oblique muscles. LSA – left side, exercise on the spinal actuator; RSA– right side, exercise on the spinal actuator; LSA+AH – left side, exercise on the spinal actuator with abdominal hollowing; RSA + AH– right side, exercise on the spinal actuator with abdominal hollowing. Thicker lines show the mean values; thinner lines represent standard errors

Muscle activity of transverse abdominis

The average activity of the transverse abdominis muscle during lateral bending exercise on the spinal actuator with abdominal hollowing is 83% of MVIC. There is no statistically significant difference ($p = 0.0833$) between the left and right side values of the transverse abdominis muscle activity when the lateral bending exercise is performed on the spinal actuator with abdominal hollowing. The average muscle activity of transverse abdominis increases by 2.03 times when the exercise with abdominal hollowing is performed on the spinal actuator. Statistically significant differences exist between the left side values ($p = 0.0039$), right side values ($p = 0.0005$) and the total values ($p < 0.0001$) of the transverse abdominis muscle activity when the exercise on the spinal actuator is performed with and without abdominal hollowing. The activity of the transverse abdominis muscle maintains a similar activity pattern when the exercise is performed on the spinal actuator without and with abdominal hollowing, but the activity values with abdominal hollowing, as it

was mentioned, are significantly higher, and a tendency that the left side peak values are higher than the right side values remains (Fig. 4.13).

A well as in the case of internal oblique, the muscle activity of transversus abdominis during the lateral bending exercise on the spinal actuator is higher than during the lateral bending exercise on the mat, in this case by 1.35 times, and, although the lateral bending exercise on the spinal actuator reduces the activity of internal oblique by 1.50 times compared to the exercise on the mat (as presented in Section 4.2), the exercise on the spinal actuator with abdominal hollowing may increase the activity of transversus abdominis even when comparing with the activity values during the exercise without the assiting equipment.

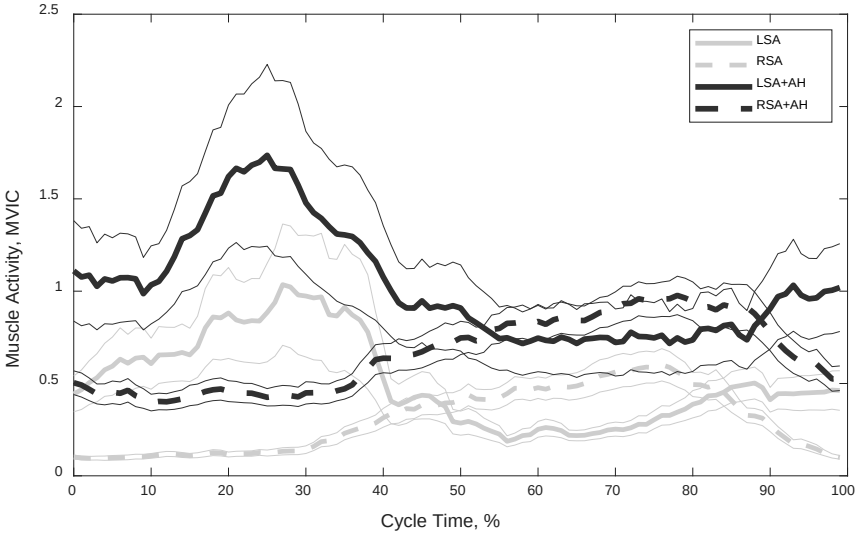

Fig. 4.13. Activity of transversus abdominis muscles. LSA – left side, exercise on the spinal actuator; RSA– right side, exercise on the spinal actuator; LSA+AH – left side, exercise on the spinal actuator with abdominal hollowing; RSA + AH– right side, exercise on the spinal actuator with abdominal hollowing. Thicker lines show the mean values; thinner lines represent standard errors

Muscle activity of multifidus

The average activity of the multifidus muscle during the lateral bending exercise on the spinal actuator with abdominal hollowing is 110% of MVIC. There is no statistically significant difference ($p = 1$) between the left and right side values of the multifidus muscle activity when the lateral bending exercise is performed on the spinal actuator with abdominal hollowing. The average muscle activity of multifidus increases by 1.35 times when the exercise with abdominal hollowing is performed on the spinal actuator. Statistically significant differences exist between the left side values ($p = 0.0209$), the right side values ($p = 0.0209$) and the total values ($p = 0.0011$) of the multifidus muscle activity when the exercise on the spinal actuator is performed without and with abdominal hollowing. The activity of the multifidus muscle maintains a similar activity pattern when the exercise is

performed on the spinal actuator without and with abdominal hollowing, but the activity values with abdominal hollowing, as it was mentioned above, are significantly higher (Fig. 4.14).

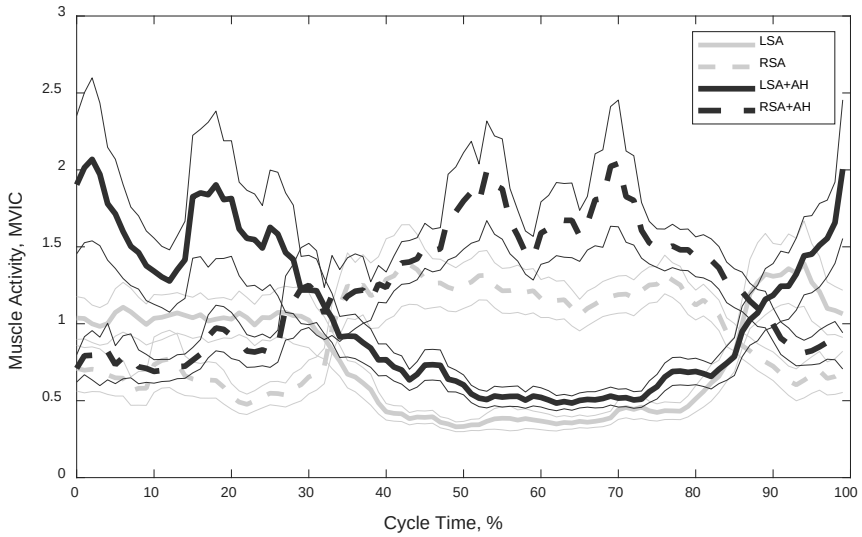

Fig. 4.14. Activity of multifidi muscles. LSA – left side, exercise on the spinal actuator; RSA– right side, exercise on the spinal actuator; LSA+AH – left side, exercise on the spinal actuator with abdominal hollowing; RSA + AH– right side, exercise on the spinal actuator with abdominal hollowing. Thicker lines show the mean values; thinner lines represent standard errors

Muscle activity of lumbar erector spinae

The average activity of the lumbar erector spinae muscle during the lateral bending exercise on the spinal actuator with abdominal hollowing is 132% of MVIC. There is no statistically significant difference ($p = 0.2482$) between the left and right side values of the lumbar erector spinae muscle activity when the lateral bending exercise is performed on the spinal actuator with abdominal hollowing. The average muscle activity of lumbar erector spinae increases by 1.33 times when the exercise with abdominal hollowing is performed on the spinal actuator. Statistically significant differences exist between the left side values ($p = 0.0039$), the right side values ($p = 0.0039$) and the total values ($p < 0.0001$) of the lumbar erector spinae muscle activity when the exercise on the spinal actuator is performed without and with abdominal hollowing. The activity of lumbar erector spinae maintains a similar activity pattern when the exercise is performed on the spinal actuator without and with abdominal hollowing, but the activity values with abdominal hollowing, as it was mentioned above, are significantly higher. Hovewer, while there is no difference between the mean activity values of the left and right sides when the exercise is performed with abdominal hollowing, it can still be seen that the activity patterns and peak values actually differ (Fig. 4.15).

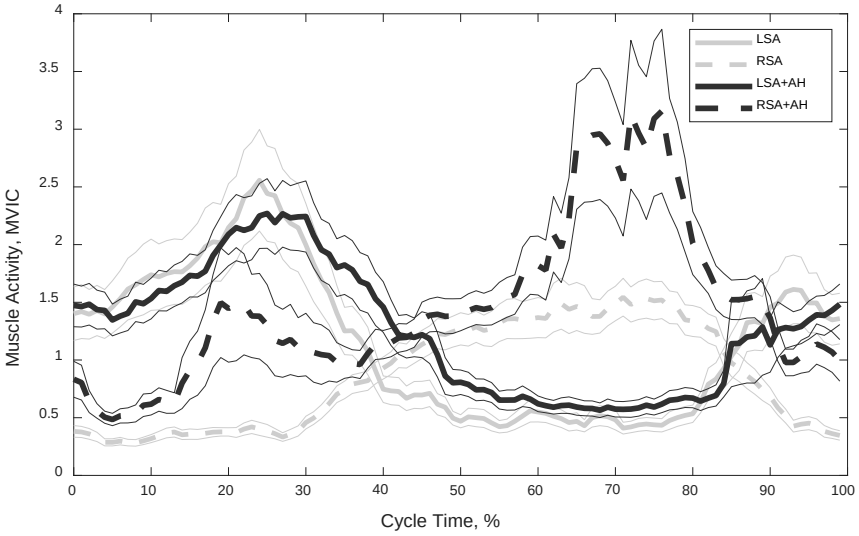

Fig. 4.15. Activity of lumbar erector spinae muscles. LSA – left side, exercise on the spinal actuator; RSA– right side, exercise on the spinal actuator; LSA+AH – left side, exercise on the spinal actuator with abdominal hollowing; RSA + AH– right side, exercise on the spinal actuator with abdominal hollowing. Thicker lines show the mean values; thinner lines represent standard errors

4.4. Section conclusions

In this section, the prototype of a spinal actuator and experimental studies investigating the benefits of this prototype were presented. The prototype of a spinal actuator that allows to perform the lateral bending exercise has been developed due to the reasons that most of lumbar spine training and rehabilitation equipment offered on the market relies on the performance of flexion and extension moves, while literature review and modelling results are uniform in suggesting that lateral bending may be beneficial to the spine and deep layer back muscles. The main purpose of the presented experimental study was to investigate the influence of the spinal actuator on the trunk muscles.

The results of the experimental study show that the lateral bending exercise activates multifidus and lumbar erector spinae above the value of 45% MVIC, which is necessary to increase the muscle strength in previously untrained subjects in both cases: without the assisting equipment and on the spinal actuator. Due to this reason, the lateral bending exercise is suitable for strengthening the back muscles which are important for securing the stability of the lumbar spine and for preventing intervertebral disc degeneration and low back pain.

During the experimental study, it was observed that the ability to perform the lateral bending exercise in the frontal plane depends on the physical condition of the participants. For less physically active ones, it was difficult to maintain the upper body which had to be slightly lifted in order to perform the lateral bending moves on the mat at the same height. Also, a tendency to engage in additional rotational

movements and various leg movements was observed, which could lead to various traumas. The lateral bending exercise on the spinal actuator is easier to perform as the thoracic spine is pressed against the plate and is allowed to move only in one plane, thus it may be presumed that the lateral bending exercise on the spinal actuator is less trauma-prone than the exercise on the mat.

The lateral bending exercise on the spinal actuator compared to the exercise on the mat leads to statistically significant decreases of the activities of internal oblique (by 1.85 times) and transverse abdominis (by 1.50 times) muscles and to a statistically significant increase of the muscle activity of multifidus (by 1.70 times) by changing the pattern of muscle activation as the peak values of muscle activity remain at the same level, but the maximal activation periods are significantly longer. The muscle activity of lumbar erector spinae also increases, but the difference is not statistically significant.

The lateral bending exercise on the spinal actuator with abdominal hollowing leads to statistically significant increases of the activity of the internal oblique (by 4.85 times), transverse abdominis (by 2.03 times), multifidus (by 1.35 times) and lumbar erector spinae muscles (by 1.33 times), thus it may be presumed that abdominal hollowing is beneficial for enhancing the effectiveness of the lateral bending exercise.

CONCLUSIONS

1. A comprehensive literature review on spine reactions to biomechanical loading, intervertebral disc degeneration and rehabilitation methods was conducted. It was determined that lateral bending moves of the human spine may have a positive impact on the nutrition of the intervertebral discs and the strength of the back muscles, but it is still scarcely researched, and lateral bending exercises are not widely included in spine rehabilitation programmes since there is lack of available equipment.
2. Poroelastic finite element models of the intervertebral disc and the lumbar spine were developed thus allowing to evaluate the influence of various biomechanical loadings. It has been found that lateral bending induces a higher maximum fluid flow velocity within the nucleus pulposus of the intervertebral disc than other spinal moves: 1.36 times higher than extension, 1.67 times higher than flexion, and 15.79 times higher than axial rotation. When comparing the average flow velocity, the highest values are induced due to flexion and extension, but lateral bending induces the highest value of the velocity component in the axial direction of the spinal column in nucleus pulposus. Pure lateral bending is safer and more beneficial to perform as it leads to lower stress values of annulus fibrosus and a higher fluid flow velocity than coupled lateral bending.
3. An experimental setup consisting of a fatigue testing machine and a computed tomography system was developed in order to investigate the structural and geometrical changes of intervertebral discs due to cyclic loading. The results of this study showed that intervertebral discs positioned lower in the spinal segment lose more height than the upper discs, and that 2 Hz loading frequency leads to a more significant height loss than 5 Hz loading frequency.
4. An experimental *in vitro* study of porcine specimens showed that a pure compressive load of 1000 N or the same compressive load combined with flexion moves does not cause any noticeable damage to intervertebral discs. A study of short-term dynamic loading revealed that previous 8 Hz compressive loading leads to a smaller loss of the intervertebral disc height than a previous compressive load of 2 Hz frequency, and that the optimal loading frequency and time should be chosen in order to induce a positive effect of loading on the disc.
5. A spinal actuator – a piece of training equipment which allows performing lateral bending moves – has been developed and patented. The experimental study has shown that the lateral bending exercise is beneficial for strengthening the multifidus and lumbar erector spinae muscles as it activates these muscles above the value of 45% maximum voluntary isometric contraction, which is necessary to increase the muscle strength in previously untrained subjects. Moreover, the lateral bending exercise performed on the spinal actuator significantly increases the activity of the multifidi muscles by 1.70 times compared with the lateral bending exercise without any assisting equipment and is an even more effective way to strengthen the deep layer back muscles. Abdominal hollowing during the lateral bending exercise on the spinal actuator significantly increases the muscle activity of all the four measured muscles.

REFERENCES

1. GBD 2015 DISEASE AND INJURY INCIDENCE AND PREVALENCE COLLABORATORS. Global, regional, and national incidence, prevalence, and years lived with disability for 310 diseases and injuries, 1990-2015: a systematic analysis for the Global Burden of Disease Study 2015. *Lancet*, 2016, 388(10053), 1545-1602. doi:10.1016/S0140-6736(16)31678-6.
2. HARTVIGSEN, J., *et al*. What low back pain is and why we need to pay attention. *Lancet.* 2018, 391(10137), 2356-2367. doi:10.1016/S0140-6736(18)30480-X.
3. HOY, D., *et al*. A Systematic Review of the Global Prevalence of Low Back Pain. *Arthritis & Rheumatology*. 2012, 64(6), 2028-2037. doi:10.1002/art.34347.
4. NEUMANN, D. A. *Kinesiology of the Musculoskeletal System: Foundation for Rehabilitation.* St. Louis : Mosby Elsevier, 2010. ISBN 9780323287531
5. EBRAHEIM, N. A., *et al*. Functional anatomy of the lumbar spine. *Seminars in Pain Medicine.* 2004, 2(3), 131-137. doi:10.1016/j.spmd.2004.08.004.
6. BOGDUK, N. *Clinical Anatomy of the Lumbar Spine and Sacrum.* 3rd ed. Elsevier Health Sciences: 1997. ISBN 0443060142
7. HEUER, F., *et al*. Stepwise reduction of functional spinal structures increase range of motion and change lordosis angle. *Journal of Biomechanics.* 2007, 40(2), 271-280. doi:10.1016/j.jbiomech.2006.01.007.
8. MOORE, R. J. The vertebral endplate: disc degeneration, disc regeneration. *European Spine Journal.* 2006, 15(Suppl 3), 333–337. doi: 10.1007/s00586-006-0170-4.
9. SETTON, L. A., BONASSAR, L. and MASUDA, K. *Regeneration and Replacement of the Intervertebral Disc*. In: Lanza, R., Langer, R., and Vacanti, J. *Principles of Tissue Engineering*. 4th ed. Academic Press, 2014, 877-896 doi:10.1016/B978-012370615-7/50062-7.
10. HUANG, Y. C., URBAN, J. P. G. and LUK, K. D. K. Intervertebral disc regeneration: do nutrients lead the way? *Nature Reviews Rheumatology.* 2014, 10(9), 561-566. doi:10.1038/nrrheum.2014.91.
11. JUNGER, S., *et al*. Effect of Limited Nutrition on In Situ Intervertebral Disc Cells Under Simulated-Physiological Loading. *Spine.* 2009, 34(12), 1264-71. doi:10.1097/BRS.0b013e3181a0193d.
12. WONG, J., *et al*. Nutrient supply and nucleus pulposus cell function: effects of the transport properties of the cartilage endplate and potential implications for intradiscal biologic therapy. *Osteoarthritis and Cartilage.* 2019, 27(6), 956-964. doi:10.1016/j.joca.2019.01.013.
13. SHIRAZI-ADL, A., TAHERI, M. and URBAN, J. P. Analysis of cell viability in intervertebral disc: Effect of endplate permeability on cell population. *Journal of Biomechanics.* 2010, 43(7), 1330-1336. doi:10.1016/j.jbiomech.2010.01.023.
14. MALANDRINO, A., NOAILLY, J. and LACROIX, D. Numerica lexploration of the combined effect of nutrient supply,tissue condition and deformation in the intervertebral disc. *Journal of Biomechanics.* 2014, 47(6), 1520-1525. doi:10.1016/j.jbiomech.2014.02.004.

15. WU, Y., *et al*. Region and strain-dependent diffusivities of glucose and lactate in healthy human cartilage endplate. *Journal of Biomechanics.* 2016, 49(13), 2756-2762. doi:10.1016/j.jbiomech.2016.06.008.
16. QASEEM, A., *et al*. Noninvasive Treatments for Acute, Subacute, and Chronic Low Back Pain: A Clinical Practice Guideline From the American College of Physicians. *Annals of Internal Medicine.* 2017, 166(7), 514-530. doi:10.7326/M16-2367.
17. NIJS, J., *et al*. Low Back Pain: Guidelines for the Clinical Classification of Predominant Neuropathic,Nociceptive, or Central Sensitization Pain. *Pain Physician Journal.* 2015, 18(3), E333-346.
18. AIRAKSINEN, O., *et al*. European guidelines for the management of chronic nonspecific low back pain. *European Spine Journal.* 2006, 15, S192–S300. doi:10.1007/s00586-006-1072-1.
19. HAYASHI, Y. Classification, Diagnosis, and Treatment of Low Back Pain. *Japan Medical Association Journal.* 2004, 47(5), 227-233.
20. CALIFORNIA BRAIN & SPINE. *Ankylosing Spondylitis* [online] [viewed 04 March 2019]. Available from: http://www.californiabrainandspine.com/ankylosing-spondylitis.
21. LIVSHITS, G., *et al*. Lumbar disc degeneration and genetic factors are the main risk factors for low back pain in women: the UK Twin Spine Study. *Annals of the Rheumatic Diseases.* 2011, 70(10), 1740-1745. doi:10.1136/ard.2010.137836.
22. ZHENG, C. J. and CHEN, J. Disc degeneration implies low back pain. *Theoretical Biology and Medical Modelling.* 2015, 12(24), 1-10. doi:10.1186/s12976-015-0020-3.
23. URBAN, J. P. and ROBERTS, S. Degeneration of the intervertebral disc. *Arthritis Research & Therapy.* 2003, 5(3), 120-130. doi:10.1186/ar629.
24. THOMPSON, J. P., *et al*. Preliminary evaluation of a scheme for grading the gross morphology of the human intervertebral disc. *Spine.* 1990, 15(5), 411-415. doi:10.1097/00007632-199005000-00012.
25. PFIRRMANN, C. W., *et al*. Magnetic resonance classification of lumbar intervertebral disc degeneration. *Spine.* 2000, 26(7), 1873-1878. doi:10.1097/00007632-200109010-00011.
26. BOOS, N., *et al*. Classification of age-related changes in lumbar intervertebral discs: 2002 Volvo award in basic science. *Spine.* 2002, 27(23), 2631-2644. doi:10.1097/00007632-200212010-00002.
27. ADAMS, M.A. and ROUGHLEY, P.J. What is Intervertebral Disc Degeneration, and What Causes It? *Spine.* 2006, 31(18), 2151–2161. doi:10.1097/01.brs.0000231761.73859.2c.
28. FENG, Y., EGAN, B. and WANG, J. Genetic factors in intervertebral disc degeneration. *Genes & Diseases.* 2016, 3, 178-185. doi:10.1016/j.gendis.2016.04.005.
29. WANG, D., *et al*. Spine degeneration in a murine model of chronic human tobacco smokers. *Osteoarthritis and Cartilage.* 2012, 20(8), 896-905. doi:10.1016/j.joca.2012.04.010.
30. BOUBRIAK, O. A. Factors regulating viable cell density in the intervertebral disc: blood supply in relation to disc height. *Journal of Anatomy.* 2013, 222(3), 341–348. doi:10.1111/joa.12022.

31. URRUTIA, J., *et al*. The Pfirrmann classification of lumbar intervertebral disc degeneration: an independent inter- and intra-observer agreement assessment. *European Spine Journal.* 2016, 25(9), 2728-2733. doi:10.1007/s00586-016-4438-z.
32. ZANJANI-POUR, S., *et al*. Estimation of *in vivo* inter-vertebral loading during motion using fluoroscopic and magnetic resonance image informed finite element models. *Journal of Biomechanics.* 2018, 70, 134-139. doi:10.1016/j.jbiomech.2017.09.025.
33. FERGUSON, S. J., ITO, K. and NOLTE, L. P. Fluid flow and convective transport of solutes within the intervertebral disc. *Journal of Biomechanics.* 2003, 37(2), 213-221. doi:10.1016/s0021-9290(03)00250-1.
34. ARUN, R., *et al*. 2009 ISSLS Prize Winner: What influence does sustained mechanical load have on diffusion in the human intervertebral disc?: an *in vivo* study using serial postcontrast magnetic resonance imaging. *Spine.* 2009, 34(21), 2324-2337. doi:10.1097/BRS.0b013e3181b4df92.
35. WALTER, B. A., *et al*. Complex loading affects intervertebral disc mechanics and biology. *Osteoarthritis and Cartilage.* 2011, 19(8), 1011-1018. doi:10.1016/j.joca.2011.04.005.
36. EMANUEL, K. S., *et al*. Osmosis and viscoelasticity both contribute to time-dependent behaviour of the intervertebral disc under compressive load: A caprine *in vitro* study. *Journal of Biomechanics.* 2017, 70, 10-15. doi:10.1016/j.jbiomech.2017.10.010.
37. SCHMIDT, H., *et al*. Intradiscal Pressure, Shear Strain, and Fiber Strain in the Intervertebral Disc Under Combined Loading. *Spine.* 2007, 32(7), 748-755. doi:10.1097/01.brs.0000259059.90430.c2.
38. ELLINGSON, A. M., *et al*. Comparative Role of Disc Degeneration and Ligament Failure on Functional Mechanics of the Lumbar Spine. 2015, 19(9), 1009-1018. doi:10.1080/10255842.2015.1088524.
39. WU, Y., *et al*. Study of Double-level Degeneration of Lower Lumbar Spines by Finite Element Model. *World Neurosurgery.* 2016, 86, 294-299. doi:10.1016/j.wneu.2015.09.038.
40. VERES, S.P., ROBERTSON, P. A. and BROOM, N. D. The morphology of acute disc herniation: a clinically relevant model defining the role of flexion. *Spine.* 2009, 34(21), 2288-2296. doi:10.1097/BRS.0b013e3181a49d7e.
41. CALLAGHAN, J. P. and MCGILL, S. M. Intervertebral disc herniation: studies on a porcine model exposed to highly repetitive flexion/extension motion with compressive force. *Clinical biomechanics (Bristol, Avon).* 2001, 16(1), 28-37. doi:10.1016/s0268-0033(00)00063-2.
42. MARIUKI, M. G., *et al*. Effects of Motion Segment Level, Pfirrmann Intervertebral Disc Degeneration Grade and Gender on Lumbar Spine Kinematics. *Journal of Orthopaedic Research.* 2016, 34(8), 1389-1398. doi:10.1002/jor.23232.
43. LIU, T., *et al*. Load-sharing in the lumbosacral spine in neutral standing & flexed postures – A combined finite element and inverse static study. *Journal of Biomechanics.* 2018, 70, 43-50. doi:10.1016/j.jbiomech.2017.10.033.
44. LEE, R. Y. and WONG, T. K. Relationship between the movements of the lumbar spine and hip. *Human Movement Science.* 2002, 21(4), 481-494. doi:10.1016/s0167-9457(02)00117-3.
45. SUNG, P. S. Different coordination and flexibility of the spine and pelvis during lateral bending between young and older adults. *Human Movement Science.* 2016(46), 229-238. doi:10.1016/j.humov.2016.01.001.

46. SADLER, S. G., *et al*. Restriction in lateral bending range of motion, lumbar lordosis, and hamstring flexibility predicts the development of low back pain: a systematic review of prospective cohort studies. *BMC Musculoskeletal Disorders.* 2017, 18(179), 1-15. doi:10.1186/s12891-017-1534-0.
47. HAJ, A., WEISMAN, A. and MASHARAWI, Y. Lumbar axial rotation kinematics in men with non-specific chronic low back pain. *Clinical Biomechanics.* 2019, 61, 192-198. doi:10.1016/j.clinbiomech.2018.12.022.
48. MICHALEK, A. J., FUNABASHI, K. L. and IATRIDIS, J. C. Needle puncture injury of the rat intervertebral disc affects torsional and compressive biomechanics differently. *European Spine Journal.* 2009, 19(12), 2110–2116. doi:10.1007/s00586-010-1473-z.
49. MCCANN, M. R., *et al*. Repeated Exposure to High-Frequency Low-Amplitude Vibration Induces Degeneration of Murine Intervertebral Discs and Knee Joints. *Arthritis & Rheumatology.* 2015, 67(8), 2164-2175. doi:10.1002/art.39154.
50. ILLIEN-JÜNGER, S., *et al*. The Combined Effects of Limited Nutrition and High-Frequency Loading on Intervertebral Discs With Endplates. *Spine.* 2010, 35(19), 1744-1752. doi:10.1097/BRS.0b013e3181c48019.
51. HOLGUIN, N., *et al*. Brief daily exposure to low-intensity vibration mitigates the degradation of the intervertebral disc in a frequency-specific manner. *Journal of Applied Physiology.* 2011, 111(6), 1846-1853. doi:10.1152/japplphysiol.00846.2011.
52. HOLGUIN, N., *et al*. Short applications of very low-magnitude vibrations attenuate expansion of the intervertebral disc during extended bed rest. *The Spine Journal.* 2009, 9(6), 470-477. doi:10.1016/j.spinee.2009.02.009.
53. IZAMBERT, O., *et al*. Dynamic stiffness and damping of human intervertebral disc using axial oscillatory displacement under a free mass system. *European Spine Journal.* 2003, 12(6), 562-566. doi:10.1007/s00586-003-0569-0.
54. CHEUNG, J. T., ZHANG, M. and CHOW, D. H. Biomechanical responses of the intervertebral joints to static and vibrational loading: a finite element study. *Clinical biomechanics (Bristol, Avon).* 2003, 18(9), 790-799. doi:10.1016/s0268-0033(03)00142-6.
55. GULLBRAND, S. E., *et al*. Low rate loading-induced convection enhances net transport into the intervertebral disc *in vivo*. *The Spine Journal.* 2015, 15(5), 1028-1033. doi:10.1016/j.spinee.2014.12.003.
56. HUANG, C. Y. and GU, W. Y. Effects of mechanical compression on metabolism and distribution of oxygen and lactate in intervertebral disc. *Journal of Biomechanics.* 2008, 41(6), 1184-1196. doi:10.1016/j.jbiomech.2008.02.002.
57. ZHU, Q., JACKSON, A. R. and GU, W. Y. Cell viability in intervertebral disc under various nutritional and dynamic loading conditions:3d Finite element analysis. *Journal of Biomechanics.* 2012, 45(16), 2769-2777. doi:10.1016/j.jbiomech.2012.08.044.
58. SAMPSON, S. L., SYLVIA, M. and FIELDS, A. J. Effects of dynamic loading on solute transport through the human cartilage endplate. *Journal of Biomechanics.* 2019, 83(23), 273-279. doi:10.1016/j.jbiomech.2018.12.004.
59. NOGUCHI, M., *et al*. Is intervertebral disc pressure linked to herniation?: An in-vitro study using a porcine model. *Journal of Biomechanics.* 2016, 49(9), 1824-1830. doi:10.1016/j.jbiomech.2016.04.018.
60. THORESON, O., *et al*. The effect of repetitive flexion and extension fatigue loading on the young porcine lumbar spine, a feasibility study of MRI and

histological analyses. *Journal of Experimental Orthopaedics.* 2017, 4(16). doi:10.1186/s40634-017-0091-7.

61. PARKER, S. L., *et al*. Incidence of Low Back Pain After Lumbar Discectomy for Herniated Disc and Its Effect on Patient-reported Outcomes. *Clinical Orthopaedics and Related Research.* 2015, 473(6), 1988-1999. doi:10.1007/s11999-015-4193-1.
62. PHILLIPS, F. M., *et al*. Lumbar Spine Fusion for Chronic Low Back Pain Due to Degenerative Disc Disease. *Spine.* 2013, 38(7), E409-422. doi:10.1097/BRS.0b013e3182877f11.
63. EKMAN, P., *et al*. A prospective randomised study on the long-term effect of lumbar fusion on adjacent disc degeneration. *European Spine Journal.* 2009, 18(8), 1175-1186. doi:10.1007/s00586-009-0947-3.
64. WHATLEY, B. R. and WEN, X. Intervertebral disc (IVD): Structure, degeneration, repair and regeneration. *Materials Science and Engineering.* 2012, 32(2), 61-77. doi:10.1016/j.msec.2011.10.011.
65. HENRY, N., *et al*. Innovative strategies for intervertebral disc regenerative medicine: From cell therapies to multiscale delivery systems. *Biotechnology Advances.* 2018, 36(1), 281-294. doi:10.1016/j.biotechadv.2017.11.009.
66. VAN TULDER, M. W., *et al*. Exercise Therapy for Low Back Pain. *Cochrane Database of Systematic Reviews.* 2000, 2.
67. HAYDEN, J.A., *et al*. Exercise therapy for treatment of non-specific low back pain. *Cochrane Database of Systematic Reviews.* 2005, 20(3). doi:10.1002/14651858.CD000335.pub2.
68. DONZELLI, S., *et al*. Two different techniques in the rehabilitation treatment of low back pain: a randomized controlled trial. *Europa Medicophysica.* 2006, 42(3), 205-210.
69. SHNAYDERMAN, I. and KATZ-LEURER, M. An aerobic walking programme versus muscle strengthening programme for chronic low back pain: a randomized controlled trial. *Clinical Rehabilitation.* 2013, 27(3), 207-214. doi:10.1177/0269215512453353.
70. WAJSWELNER, H., METCALF, B. and BENNELL, K. Clinical pilates versus general exercise for chronic low back pain: randomized trial. *Medicine & Science in Sports & Exercise.* 2012, 44(7), 1197-1205. doi:10.1249/MSS.0b013e318248f665.
71. LEE, C., HWANGBO, K. LEE, I. The Effects of Combination Patterns of Proprioceptive Neuromuscular Facilitation and Ball Exercise on Pain and Muscle Activity of Chronic Low Back Pain Patients. *The Journal of Physical Therapy Science*. 2014, 26(1), 93-96. doi:10.1589/jpts.26.93
72. SARAGIOTTO, B. T., *et al*. Motor control exercise for chronic non-specific low-back pain. *Cochrane Database of Systematic Reviews.* 2016(8), 1. doi:10.1002/14651858.CD012004
73. MCGILL, S. M. Low Back Exercises: Evidence for Improving Exercise Regimens. *Physical Therapy.* 1998, 78(7), 754-765. doi:10.1093/ptj/78.7.754.
74. RISCH, S. V., *et al*. Lumbar strengthening in chronic low back pain patients. Physiologic and psychological benefits. *Spine.* 1993, 18(2), 232-238.
75. NELSON, B. W., *et al*. The clinical effects of intensive, specific exercise on chronic low back pain: a controlled study of 895 consecutive patients with 1-year follow up. *Orthopedics.* 1995, 18(10), 971-981.

76. BRUCE-LOW, S., *et al*. One lumbar extension training session per week is sufficient for strength gains and reductions in pain in patients with chronic low back pain ergonomics. *Ergonomics.* 2012, 55(4), 500-507. doi:10.1080/00140139.2011.644329.
77. STEELE, J., *et al*. A Randomized Controlled Trial of Limited Range of Motion Lumbar Extension Exercise in Chronic Low Back Pain. *Spine.* 2013, 38(15), 1245-1252. doi:10.1097/BRS.0b013e318291b526.
78. FISHER, J., BRUCE-LOW, S. and SMITH, D. A randomized trial to consider the effect of Romanian deadlift exercise on the development of lumbar extension strength. *Physical Therapy in Sport.* 2013, 14(3), 139-145. doi:10.1016/j.ptsp.2012.04.001.
79. PARK, S. Y., *et al*. Comparison of isometric exercises for activating latissimus dorsi against the upper body weight. *Journal of Electromyography and Kinesiology.* 2015, 25(1), 47-52. doi:10.1016/j.jelekin.2014.09.001.
80. GOMBATTO, S. P., *et al*. Patterns of lumbar region movement during trunk lateral bending in 2 subgroups of people with low back pain. *Physical Therapy.* 2007, 87(4), 441-454. doi:10.2522/ptj.20050370.
81. NG, J. K., *et al*. EMG activity of trunk muscles and torque output during isometric axial rotation exertion: a comparison between back pain patients and matched controls. *Journal of Orthopaedic Research.* 2002, 20(1), 112-121. doi:10.1016/S0736-0266(01)00067-5.
82. CHOLEWICKI, J. and VAN VLIET, J.J. Relative contribution of trunk muscles to the stability of the lumbar spine during isometric exertions. *Clinical Biomechanics.* 2002, 17(2), 99-105. doi:10.1016/s0268-0033(01)00118-8.
83. KAVCIC, N., GRENIER, S. and MCGILL, S. M. Quantifying tissue loads and spine stability while performing commonly prescribed low back stabilization exercises. *Spine.* 2004, 29(20), 2319-2329. doi:10.1097/01.brs.0000142222.62203.67.
84. HIDES, J. A., RICHARDSON, C. A. and JULL, G. A. Multifidus Muscle Recovery Is Not Automatic after Resolution of Acute, First-Episode Low Back Pain. *Spine.* 1996, 21(23), 2763-2769. doi:10.1097/00007632-199612010-00011.
85. EKSTROM, R. A., DONATELLI, R. A. and CARP, K. C. Electromyographic analysis of core trunk, hip and thigh muscles during 9 rehabilitation exercises. *Journal of Orthopaedic and Sports Physical Therapy.* 2007, 37(12), 754-762. doi:10.2519/jospt.2007.2471.
86. KINGSLEY, M. I., *et al*. Moderate-intensity running causes intervertebral disc compression in young adults. *Medicine & Science in Sports & Exercise.* 2012, 44(11), 2199-2204. doi:10.1249/MSS.0b013e318260dbc1.
87. BRISBY, H., *et al*. The effect of running exercise on intervertebral disc extracellular matrix production in a rat model. *Spine.* 2010, 35(15), 1429-1436. doi:10.1097/BRS.0b013e3181e0f5bc.
88. BELAVY, D. L., *et al*. Running exercise strengthens the intervertebral disc. *Scientific Reports.* 2017, 7. doi:10.1038/srep45975.
89. BELAVY, D. L., *et al*. Can Exercise Positively Influence the Intervertebral Disc? *Sports Medicine.* 2015, 46(4), 473-485. doi:10.1007/s40279-015-0444-2.
90. TECHNOGYM. *Pure - Lower Back Bench* [online]. 2018 [viewed 11 May 2018]. Available from: https://www.technogym.com/us/lower-back-bench-pure.html.

91. OVERTECH CO. Ltd. *Whole body exercise machine capable of circular orbital movement of waist*. Inventor: SEUNG, H. O. 21 April 2016. Appl: 21 March 2014. US20160106613A1.
92. JCC&P LLC. *Chiropractic treatment table and method for spinal distraction.* Inventor: COX, J. M. 20 March 2003. Appl: 14 September 2001. US20030055456A1
93. PUPOVIC, M. *Apparatus for treatment, physical therapy, rehabilitation, recreation and training of spine and other human body parts.* 03 November 1997. Appl: 26 October 1993. US5609566A
94. YI, Z. *Multifunctional spine lateral bending rehabilitation training device.* 18 March 2015. Appl: 07 November 2014. CN204207992U.
95. GALBUSERA, F., *et al*. Comparison of four methods to simulate swelling in poroelastic finite element models of intervertebral discs. *Journal of the Mechanical Behavior of Biomedical Materials.* 2011, 4(7), 1234-1241. doi:10.1016/j.jmbbm.2011.04.008.
96. MALADRINO, A., PLANELL, J. A. and LACROIX, D. Statistical factorial analysis on the poroelastic material properties sensitivity of the lumbar intervertebral disc under compression, flexion and axial rotation. *Journal of Biomechanics.* 2009, 42, 2780-2788. doi:10.1016/j.jbiomech.2009.07.039.
97. NATARAJAN, R. N., WILLIAMS, J. R. and ANDERSSON, G. B. J. Modeling changes in intervertebral disc mechanics with degeneration. *The Journal of Bone & Joint Surgery.* 2006, 88(2), 36-40. doi:10.2106/JBJS.F.00002.
98. HEUER, F., *et al*. Creep associated changes in intervertebral disc bulging obtained with a laser scanning device. *Clinical Biomechanics.* 2007, 22, 737–744. doi: 10.1016/j.clinbiomech.2007.04.010.
99. VETTE, A. H., *et al*. Multidirectional quantification of trunk stiffness and damping duringunloaded natural sitting. *Medical Engineering and Physics.* 2014, 36, 102-109. doi:10.1016/j.medengphy.2013.10.005.
100. BCTECHNICAL. *VTC-64* [online]. [viewed: 21 November 2018]. Available from: https://bctechnical.com/systems/vct-64/.
101. SENIAM. *Recommendations for sensor locations on individual muscles* [online]. [viewed: 13 May 2017]. Available from: http://seniam.org/sensor_location.htm.
102. MCCOOK D. T., VICENZINO, B. and HODGES P.W. Activity of deep abdominal muscles increases during submaximal flexion and extension efforts but antagonist co-contraction remains unchanged. *Journal of Electromyography and Kinesiology*. 2009, 19(5), 754-762. doi: 10.1016/j.jelekin.2007.11.002.
103. HODGES, P. W. and RICHARDSON, C. A. Contraction of the Abdominal Muscles Associated With Movement of the Lower Limb. *Physical Theraphy*. 1997, 77(2), 134-142. doi: 10.1093/ptj/77.2.132.

LIST OF AUTHOR'S PUBLICATIONS

Indexed in the Web of Science with Impact Factor

Ostaševičius, Vytautas; Jurėnas, Vytautas; Gaidys, Rimvydas; Golinka, Ievgeniia; Kižauskienė, Laura; Mikuckytė, Sandra. Development of a Piezoelectric Actuator for Separation and Purification of Biological Microparticles. Actuators. 2020 (in edition).

Mikuckytė, Sandra; Ostaševičius, Vytautas. Experimental Investigation of Short-Term Cyclic Loading Influence on the Intervertebral Disc Height. European Spine Journal. 2020 (in edition).

Mikuckytė, Sandra; Ostaševičius, Vytautas; Jurėnas, Vytautas. The Influence of on the Frontal Plane Constrained and Free Lateral Bending on Trunk Muscles. Journal of Electromyography and Kinesiology (in edition).

[S1 LT] Mikuckytė, Sandra; Ostaševičius, Vytautas. Investigation of fluid flow velocity within the lumbar intervertebral disc. Mechanika // Mechanika / Kaunas University of Technology, Vilnius Gediminas Technical University, Lithuanian Academy of Sciences. Kaunas: KTU. 2020, vol. 26, iss. 6.

[S1 LT] Mikuckytė, Sandra; Ostaševičius, Vytautas. Experimental Investigation of an Influence of Coupled Compressive Loading on Porcine Spine Specimens. Mechanika // Mechanika / Kaunas University of Technology, Vilnius Gediminas Technical University, Lithuanian Academy of Sciences. Kaunas: KTU. 2021, vol. 27, iss, 1.

[S1; SI] Ostaševičius, Vytautas; Gaidys, Rimvydas; Daukševičius, Rolanas; Mikuckytė, Sandra. Study of vibration milling for improving surface finish of difficult-to-cut materials // Strojniški Vestnik = Journal of mechanical engineering. Ljubljana: Association of Mechanical Engineers and Technicians of Slovenia. ISSN 0039-2480. 2013, vol. 59, no. 6, p. 351-357. DOI: 10.5545/sv-jme.2012.856.

[S1; LT] Daukševičius, Rolanas; Milašauskaitė, Ieva; Ostaševičius, Vytautas; Jūrėnas, Vytautas; Mikuckytė, Sandra. Experimental study of coupled dynamic and electric characteristics of piezoelectric energy harvester under variable resistive load // Journal of Vibroengineering / Vibromechanika, Lithuanian Academy of Sciences, Kaunas University of Technology, Vilnius Gediminas Technical University. Vilnius: Vibromechanika. ISSN 1392-8716. 2012, Vol. 14, iss. 3, p. 1435-1443.

Articles in conference proceedings

[P1c; LT] Ostasevicius, V.; Markevicius, V.; Venslauskas, M.; Mikuckyte, S.; Domeika, A.; Grigaliunas, V.; Aleknaite-Dambrauskiene, I. Conceptual solutions for driver-vehicle interfaces and interaction // Transport means 2019: Sustainability: research and solutions: proceedings of the 23rd international scientific conference, October 02–04, 2019, Palanga, Lithuania / conference organized by Kaunas University of Technology in cooperation with Klaipeda University, IFToMM National Committee of Lithuania, Lithuanian Society of Automotive Engineers, The Division of Technical Sciences of Lithuanian Academy of Sciences, Vilnius Gediminas Technical University. Kaunas: Kaunas University of Technology. ISSN

1822-296X. eISSN 2351-7034. 2019, Pt. 3, p. 1485-1490. [Scopus] [M.kr.: T 003] [Input: 0.142]

[P1c; LT] Mikuckytė, Sandra; Ostaševičius, Vytautas. Numerical study of lateral bending influence on lumbar intervertebral disc // Vibroengineering procedia: 29th International conference on vibroengineering, Vilnius, Lithuania, December 1st 2017. Kaunas: JVE International. ISSN 2345-0533. 2017, vol. 15, p. 71-76. DOI: 10.21595/vp.2017.19401. [Scopus; Academic Search Complete] [M.kr.: T009] [Input: 0.500]

[P1e; LT] Mikuckytė, Sandra; Ostaševičius, Vytautas. Investigation of intervertebral discs degeneration influence on lumbar spine load distribution // Mechanika 2017: proceedings of the 22nd international scientific conference, 19 May 2017, Kaunas University of Technology, Lithuania / Kaunas University of Technology, Lithuanian Academy of Science, IFTOMM National Committee of Lithuania, Baltic Association of Mechanical Engineering. Kaunas: Kaunas University of Technology. ISSN 1822-2951. 2017, p. 267-271. [M.kr.: T009] [Input: 0.500]

Patents registered by the State Patent Bureau of the Republic of Lithuania

[N5; LT] Ostaševičius, Vytautas (inventor); Venslauskas, Mantas (inventor); Jurėnas, Vytautas (inventor); Mikuckytė, Sandra (inventor). Įrenginys tarpslankstelinių diskų mitybai gerinti bei giliesiems nugaros raumenims stiprinti / inventors: Vytautas Ostaševičius, Mantas Venslauskas, Vytautas Jurėnas, Sandra Mikuckytė; ownership: Kaunas University of Technology s. LT 6585 B. 2019-01-25. 11 p. [Espacenet] [FOR: T009] [Input: 0.250]

Bubulis, Algimantas (inventor); Jurėnas, Vytautas (inventor); Mikuckytė, Sandra (inventor); Ostaševičius, Vytautas (inventor); Minchenya, Vladimir (inventor). Akustinių bangų poveikio žmogaus kūno organams įrenginys. Application No. LT2018 551.

ANNEXES

Annex 1

Table A1. Main dimensions of lumbar spine model

Vertebrae	T12	L1	L2	L3	L4	L5	S1
Width of upper surface, mm	26.7	29.0	28.9	30.4	28.9	27.6	29
Width of bottom surface, mm	27.7	29.7	29.0	29.7	29.6	27.4	–
Length of upper surface, mm	34.5	38.7	38.1	40.6	42.4	43.9	41.6
Length of bottom surface, mm	36.4	39.7	41.1	40.2	47.9	46.6	–
Angle of vertebra, °	14.18	13.37	10.92	4.58	-5.12	-20.96	-35.19
Intervertebral discs	T12-L1	L1-L2	L2-L3	L3-L4	L4-L5	L5-S1	
Disc height, mm	7.3	8.4	9.3	10.1	10.5	9.4	
Angle of disc, °	14.24	13.2	8.3	0.32	-11.65	-30.3	

SL344. 2020-07-14, 12,25 leidyb. apsk. l. Tiražas 12 egz.
Išleido Kauno technologijos universitetas, K. Donelaičio g. 73, 44249 Kaunas
Spausdino leidyklos „Technologija“ spaustuvė, Studentų g. 54, 51424 Kaunas